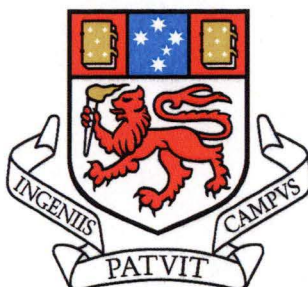# STUDY OF THE INTERACTIONS LEADING TO WOOD RESIN DEPOSITION

UNIVERSITY OF TASMANIA

David Vercoe

BTech (Forensic & Analytical Chem.), BSc (Hons)

Submitted in fulfilment of the requirements
for the Degree of

Doctor of Philosophy

School of Chemistry
University of Tasmania
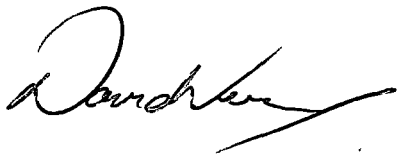Hobart, Tasmania
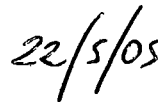Australia

January 2005

Declaration of originality

This thesis contains no material which has been accepted for the award of any other higher degree or graduate diploma in any other tertiary institution, and to the best of my knowledge, this thesis contains no material previously published or written by another person, except where due reference is made in the text of the thesis.

Statement of authority of access

This thesis may be made available for loan and limited copying in accordance with the Australian Copyright Act of 1968.

David Vercoe   22/5/05

David Vercoe   Date

ABSTRACT

In the production of mechanical pulp for paper manufacture, resinous material is released from the wood which can form colloidal dispersions that agglomerate and deposit onto surfaces. These deposits are known as pitch. It is known and cited in literature that the three major components of pitch formed from *Pinus radiata* extractives are fatty acids (namely those of chain length (C12-C20), resin acids and triglycerides.

The major aim of this thesis is to study the interaction between the three major components of wood pitch in order to gain a better understanding of the chemical interactions at a molecular level that cause pitch deposition. The interactions between the main components of the wood extractives; resin acids, fatty acids and triglycerides, have been studied using model compounds in order to investigate the effect of chemical structure on the interactions and deposition tendency.

Initially the interaction of just two components interacting with each other was investigated and showed that the difference in chemical structure and properties influenced the interaction and also the propensity to deposit. This difference in the formation of the hydrogen bond and also the stability, or strength, of the hydrogen bond can be used to explain the differences in deposition of fatty acid/resin acid mixtures. Studies undertaken to investigate a three-component system where all three hydrophobic extractives are present resulted in an extension of Qin's[1] model of the structure of a three-component pitch colloid. In this model the hydrophobic extractives, such as triglycerides, form a hydrophobic core and the more hydrophilic extractives, such as resin acids and fatty acids, interact with each other to form a hydrophilic outer layer with their hydrophilic groups extending into the aqueous surroundings. The amount of colloidal pitch deposited was found to be related to the solubility of the hydrophobic core and to the stabilisation energy of the hydrophilic outer layer.

The interaction between hemicelluloses and three of the major hydrophobic extractives of *Pinus radiata*, fatty acids, resin acids and triglycerides was also studied. Hemicelluloses belong to a group of heterogenous polysaccharides and due to their branched hydrophilic nature it is believed that they help to stabilise the colloidal pitch in its aqueous surroundings helping to prevent it from depositing onto surfaces. Through

the theoretical calculations of the individual sugar groups and different hemicellulose monomers, predictions were also made concerning the hemicellulose structure that will have the greatest stabilising properties against colloidal pitch.

ACKNOWLEDGEMENTS

Firstly I would like to acknowledge and thank my supervisors Dr. Karen Stack, Dr Adrian Blackman and Dr. Desmond Richardson for the opportunity to work under their supervision and for their constant guidance, support and ideas, which have made these past three years a truly enjoyable and rewarding experience.

Many thanks also go to all the other academic staff at both the University of Tasmania and the Flinders University of South Australia for their coursework and discussion over the years, which have provided the foundation for my understanding of chemistry.

I would also like to take this opportunity to thank Douglas McLean whose assistance and guidance throughout these years was invaluable and very much appreciated.

Many thanks to all my friends in the school and at the Norske Skog Boyer mill for all their assistance. Thanks also to my life-long friends, Peter and Kate, for their support and friendship throughout my life.

To my family, it is suffice to say I would not be where I am today without your continual love and support during the course of my studies. I cannot thank you enough.

And to Sarah... you were always around when I needed you – I am forever indebted to you for your encouragement and motivation over the past few years. My thanks and love to you always.

Falling into the deepest valley is nothing to fear.
It just means that you are in the perfect position
to climb the world's highest mountain.

Carl F. Hughes.

CONTENTS

GLOSSARY

- ∞ — infinity
- AM1® — (Austin model 1) a semiempirical method
- AMBER® — Assiste Model Building with Energy Refinement (Molecular Mechanics)
- *t*BME — *tertiary* butyl methyl ether
- BSA — N,O-bis(trimethylsilyl)-acetamide
- cmc — critical micelle concentration
- DOG — 1,3-dipalmitoyl-2-oleoyl-glycerol
- FAP — fatty acid present (mg/L)
- FID — flame ionisation detector
- GC — gas chromatography
- GCMS — gas chromatography/mass spectrometry
- GLP — triglyceride present (mg/L)
- GTO — Gaussian-type orbitals
- ΔH_f — heat of formation
- HF — Hartree-Fock
- HPLC — high performance liquid chromatography
- HPSEC — high performance size exclusion chromatography
- ID — internal diameter
- IR — infra-red spectroscopy
- IS — internal standard
- MM2® — Allingers 2nd Molecular Mechanics force field.
- MM3® — Allingers 3rd Molecular Mechanics force field.
- MNDO® — (modified neglect of diatomic overlap) a semi-empirical method
- PE — polyethylene

- pK_a — negative log of the acid ionisation constant

- PM3[®] — (parameterisation method 3) a semi-empirical method

- PVT-HTGC-FID — programmed injection temperature on-column high temperature gas chromatography with a flame ionisation detector

- RAP — resin acid present (mg/L)

- rpm — revolutions per minute

- SE — stabilisation energy

- TMP — thermomechanical pulp

- %TPD — percent total pitch deposited

- vdw — van der Waals

- Δv_s — stretching frequency

1. <u>INTRODUCTION</u>

To understand how pitch is formed and explain its deposition on different surfaces we first need to break down the problem and begin at the foundations, as the wet end of papermaking is an area of extremely complex chemistry[2]. A multitude of organic and inorganic dissolved or colloidal substances and ions interact in aqueous suspensions with each other and with fibres, fines, fillers, and other particles, and furthermore with added process chemicals[2]. Interactions also occur with surfaces of papermaking equipment, commonly leading to deposits. These interactions occur in highly turbulent conditions, varying temperatures and pH levels with chemical equilibria often not being reached. This work has focused on the wood resins in *Pinus radiata* and how they interact with each other at pH 5.5 and at 50 degrees Celsius, as these are the conditions that are used to make newsprint in an acidic environment.

1.1 Wood Resin

Wood resin is a broad term which encompasses a large number of individual chemical compounds found in wood plants. In a given species, the amount and composition of wood resin may vary significantly between trees. It is known that quantity and proportions of extractives can vary over season, genus, geographic location and age of the tree[3-5].

Figure 1.1 shows the structural polymeric constituents of wood, i.e. cellulose, hemicellulose, and lignin, which are much the same in various pulpwoods.

The extractive material however does vary quite considerably between hardwoods and softwoods, differing among tree families and even the genus. Extractives are also known to vary, often systematically, within a single stem section from the base to the top and from the pith to the bark of the tree[6]. Distribution of extractives in radiata pine and their variation in amount with tree age is illustrated in Figure 1.2, which shows the relatively high content of extractives in inner heartwood at the base of the tree.

Heartwood contains more resin acids than sapwood and only small quantities of fatty acid esters. Thus heartwood extractives contain about 70% resin acids, 10% fatty acid esters and 10% unsaponifiable neutral materials, whereas in sapwood the corresponding

values are approximately 40% resin acids, 40% fatty acid esters and 15% unsaponifiable neutral materials[7].
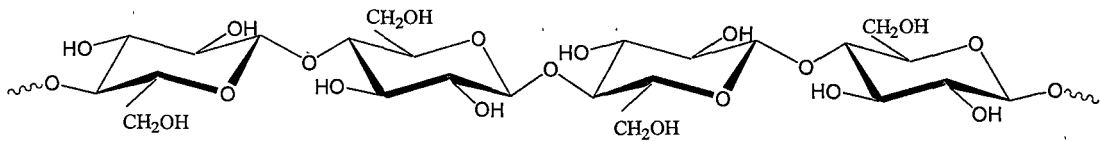
Cellulose
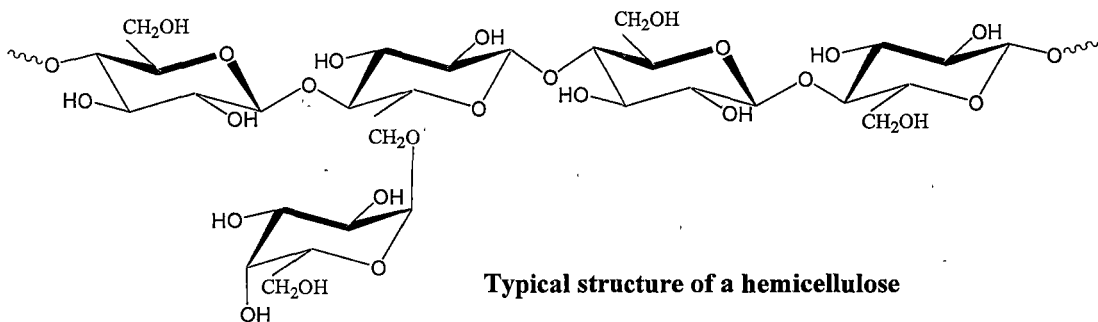
Typical structure of a hemicellulose
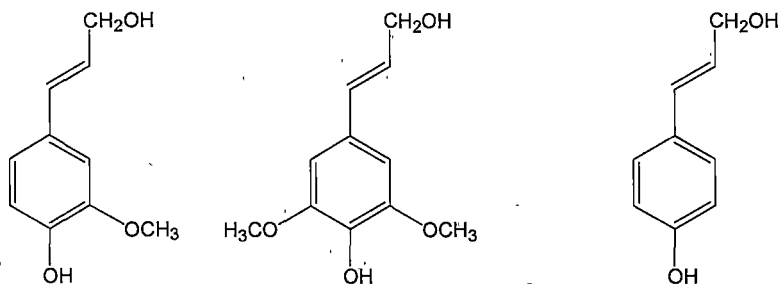
The building units (C_6C_3 precursors) of lignin

Figure 1.1. The major structural constituents of wood.
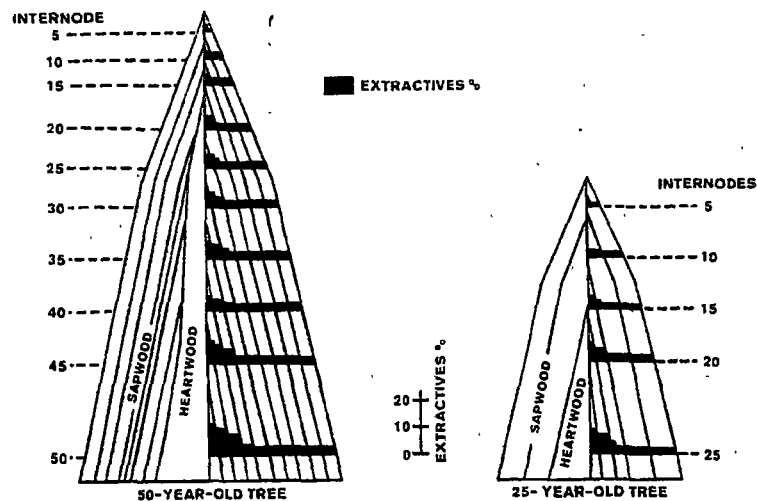
Figure 1.2. Variation in extractive distribution of radiata pine and the effects of heartwood.[5,7].

This difference in extractive content is partially due to the role of the extractives in the tree which vary from protection from insects, fungi and bacteria to repair and protection from wounding. Heartwood is the inner zone of wood which contains no living cells and in *Pinus radiata* it develops from a tree age of 12-14 years and upwards and is much drier than sapwood. Sapwood is the outer zone of wood which takes part in the conduction of water and storage of nutrients[8] and is lighter in colour than the corresponding heartwood. As it can be seen in Figure 1.2 heartwood always contains more extractives than sapwood. This difference in extractive content is due to the fact that the heartwood contains no living cells. The dying parenchyma cells produce the organic deposits such as resin, phenolic substances, pigments etc[9]. Figure 1.3 shows the cross section of a pine stem. Wood extractives are found throughout the tree however the parenchyma and secretory tissue (i.e. resin canals) are where the majority of extractive compounds can be found[10].
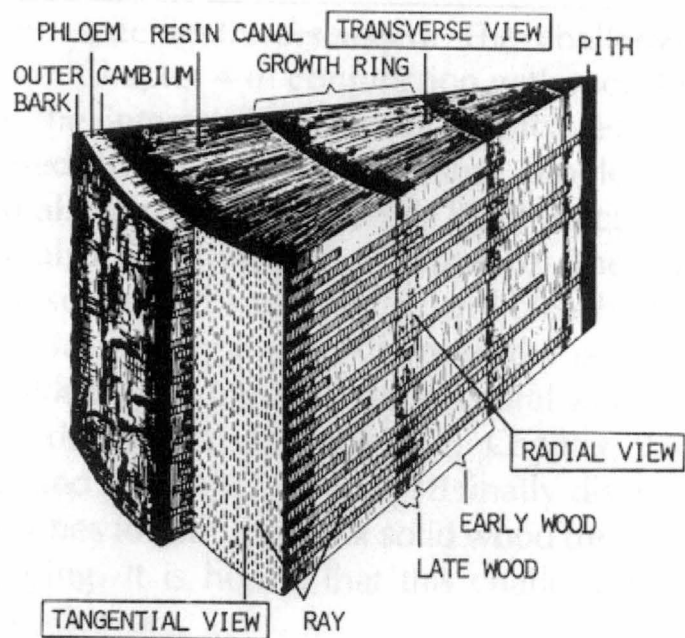
Figure 1.3. Sections of a four-year-old pine stem[9]

This extractive material is a heterogenous group of substances with variable chemical behaviour. In principle, the components can be grouped into two main classes: lipophilic (fatty) and hydrophilic substances[11, 12] (Table 1.1).

Table 1.1. Lipophilic and hydrophilic extractives[11, 12]

Lipophilic	Hydrophilic
Resin acids	Phenols
Free fatty acids	Lignans
Triglycerides	Flavonoids
Steryl esters	Tannins
Free sterols	Sugars
Monoterpenes	Salts

Hydrophilic compounds have a strong affinity for water and are generally therefore not a problem for pitch deposits.

Phenolic compounds are found throughout the tree. Lignans in particular can represent up to twenty-four percent of the extractive content of Norway spruce knots[13]. Tannins are quite common in eucalypts[14]. Examples of these and other major phenolic compounds are shown in Figure 1.4.

Stilbenes

Lignans

.Pinosylvin

Hydroxymatairesinol
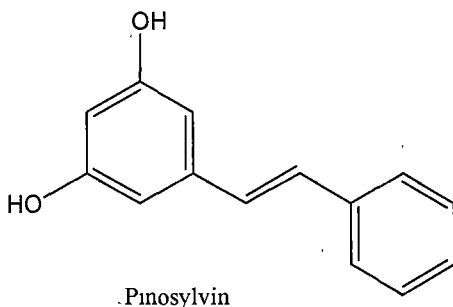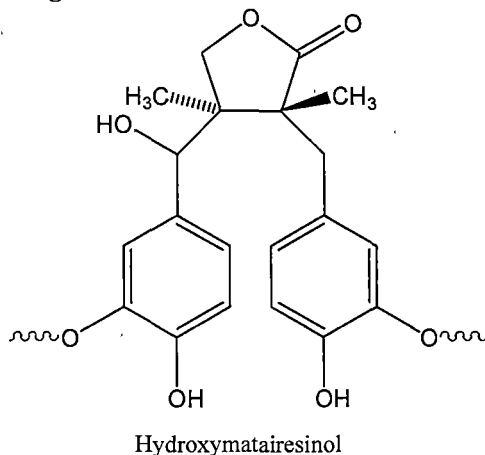
Tannins

Flavanoids

Ellagic acid

Genistein
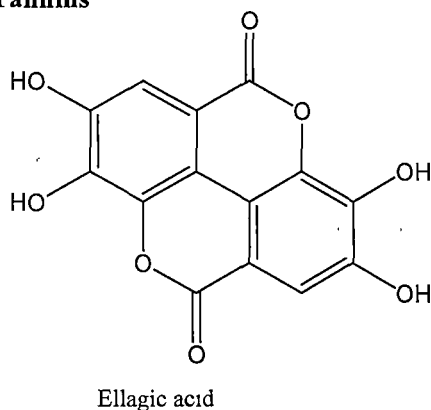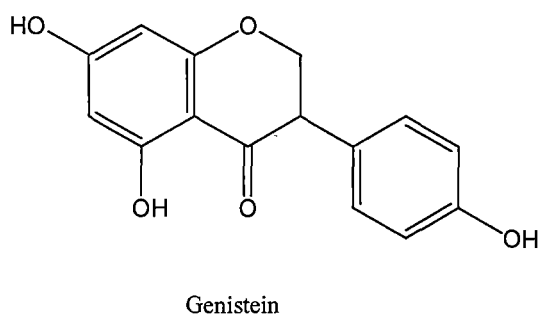
Figure 1.4. Examples of typical phenolic compounds.

By nature, lipophilic substances are hydrophobic and tend to build insoluble aggregates that often have a tacky consistency. The nature of the major proportion of extractives in pitch is lipophilic[11].

Resin acids are tricyclic diterpenoids and can be separated into three separate classes (Figure 1.5); the aromatic class (dehydroabietic acid), conjugated diene class (abietic acid, levopimaric acid, palustric acid and neoabietic acid) and alkene class (isopimaric acid, pimaric acid and sandaracopimaric acid). The main function of resin acids is to

seal the trees' wounds from fungal and bacterial attacks[15] as resin acids are toxic to most fungi and bacteria[16]. The tricyclic carbon ring system of the resin acid is obviously very stable since they have been found in fossil wood, soil, lignite, and amber[17-19].
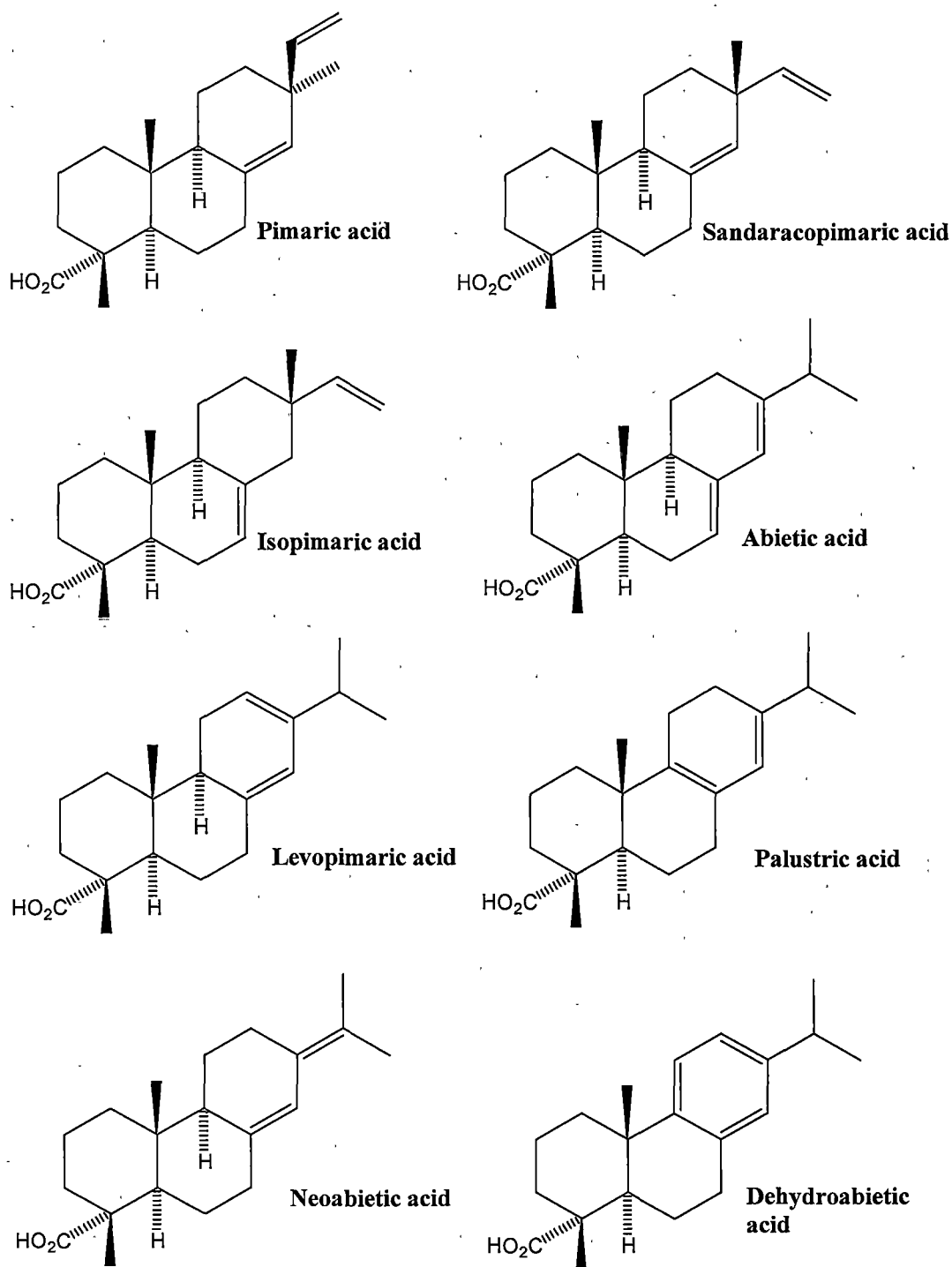
Figure 1.5. Eight common resin acids.

More than thirty saturated and unsaturated[20] fatty acids, of chain lengths typically between twelve and twenty-four carbons[21], are found in wood extractives. Straight chain saturated and unsaturated fatty acids with 16 to 24 carbon atoms (Table 1.2) are the most common fatty acids in wood plants with C18 mono-, di-, and tri-unsaturated acids dominating[22]. Like most organic extractives from organisms the cis isomers dominate in the unsaturated fatty acids. These fatty acids are often stored as triglycerides (i.e. fats) within the tree. The structure of these triglycerides is often depicted in a linear arrangement but it has been found that they are at their lowest energy when in a non-linear form (Figure 1.6)

Table 1.2. Most important fatty acids found in wood plants.

Fatty Acid	Common Name
C12:0	Lauric acid
C14:0	Myristic acid
C16:0	Palmitic acid
C18:0	Stearic acid
C18:1	Oleic acid
C18:2	Linoleic acid
C18:3	Linolenic acid
C20:0	Arachidic acid

COOH

Palmitic acid (C16:0)

COOH

Oleic acid (9-C18:1)

COOH

Linoleic acid (9,12-C18:2)

COOH

Linolenic acid (9,12,15-C18:3)

CO-O-CH$_2$

CO-O-CH$_2$

CO-O-CH$_3$

Tristearin

CO-O-CH$_2$

CO-O-CH

CO-O-CH$_2$

Trilinolenin

Cyclic structure
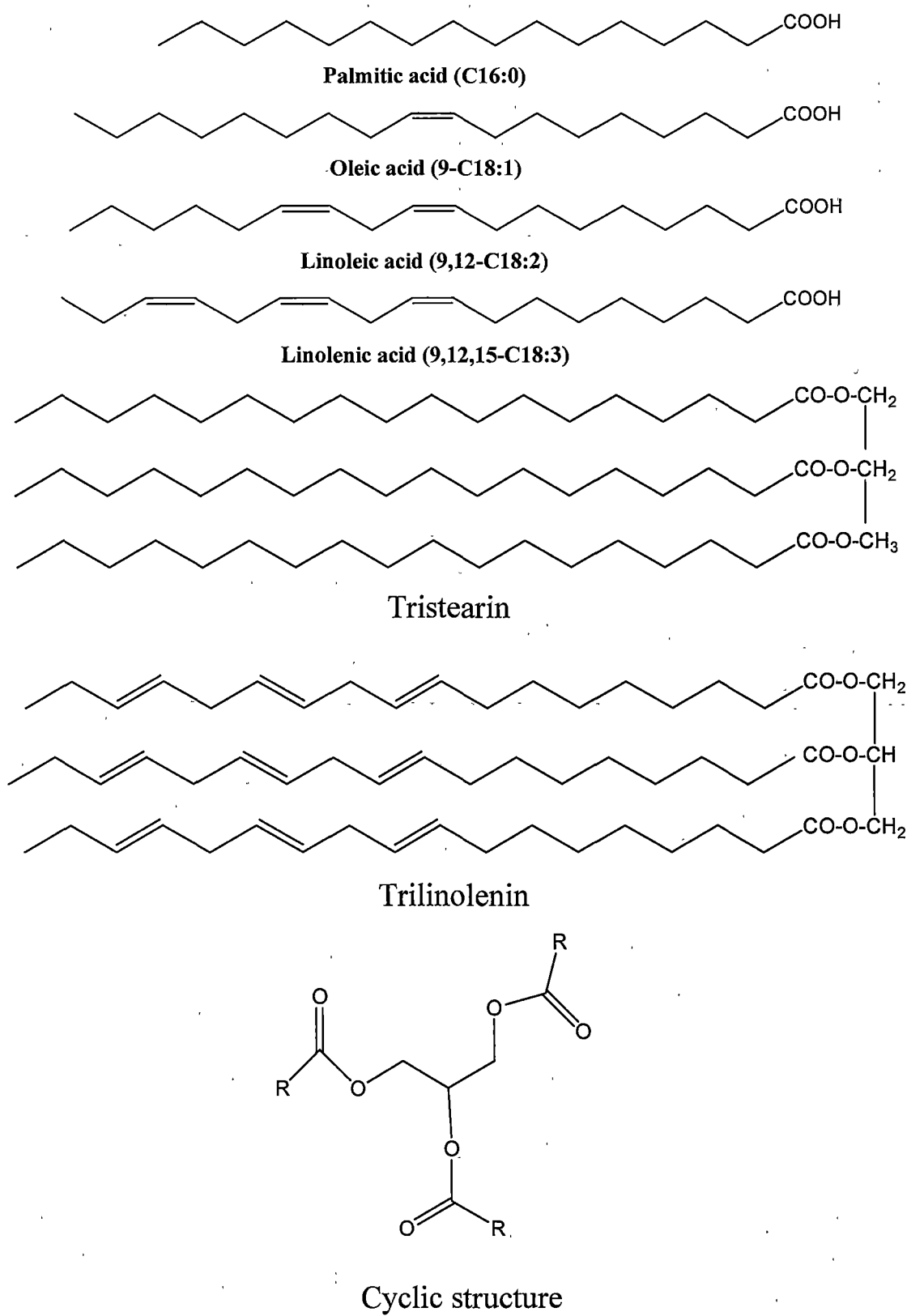
Figure 1.6. Major fatty acids and triglycerides.

Sterols (Figure 1.7) are strongly hydrophobic[20] and represent a large portion of the extractives that remain in some hardwood pulps. The most common sterol in wood plants is sitosterol[20]. Campesterol is a structurally similar monoenoic sterol but is less abundant than sitosterol. Sitostanol is the saturated analogue of sitosterol. Sterols occur mainly as fatty acid esters (waxes) and as glycosides, but also in the free form. Being sparingly soluble hydrophobic components they can cause problems in pulping and papermaking processes. However, sterols, especially sitosterol, are potential raw materials for making wood derived chemicals (e.g. hormones).
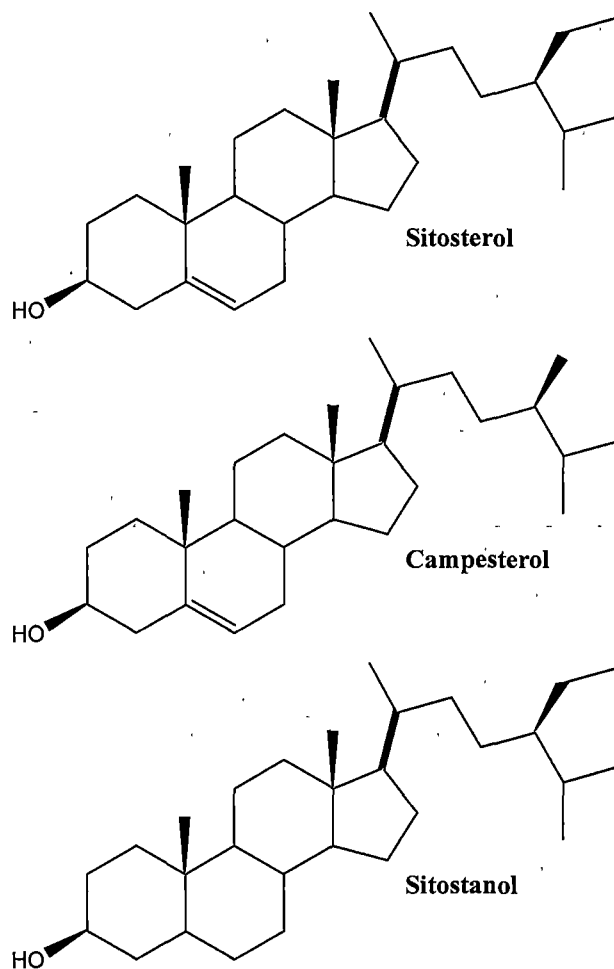
Figure 1.7. Major sterols.

Monoterpenes are volatile compounds and contribute substantially to the odour of wood[23]. The compounds in this group are dominant in turpentine and can be divided into acyclic, monocyclic, bicyclic, and the rare tricyclic structural types (Figure 1.8).

(-)-Limonene   α-Pinene   3-Carene   Camphene   Borneol
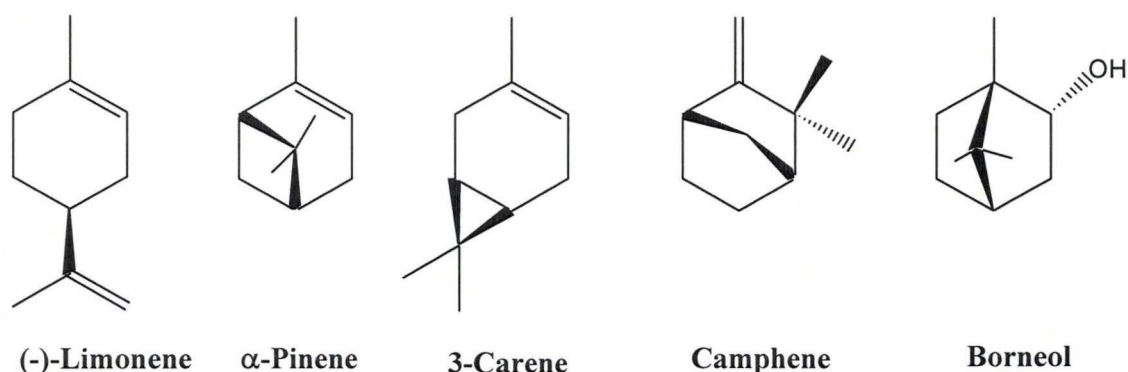
Figure 1.8. Major monoterpenes[23].

Wood resin composition in *Pinus radiata*

Pinus radiata is grown in large scale plantations in Australia, Chile and New Zealand, where it is the basis of substantial pulp and paper industries[24]. State Governments developed most of Australia's softwood plantations in the 1960s and 1970s, and were initially funded by Federal government loans. By 2002, there were 990 000 hectares of softwood (effectively all *Pinus radiata*) plantations established in Australia with a majority of these plantations in New South Wales and Victoria (Figure 1.9). Most would be considered mature or close to mature in terms of harvest potential.
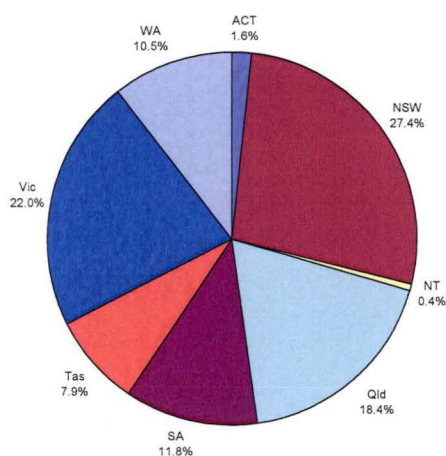
Figure 1.9. Percentage of each state contributing to the 990 000 hectares of softwood plantations in Australia[25].

Pinus radiata is used for the manufacture of a wide range of pulp and paper products in addition to sawn timber, posts, poles and reconstituted products such as plywood and medium density fibreboard. It has proved to be an excellent raw material. The papermaking properties of mechanical, semi chemical and chemical pulps made from *Pinus radiata* compare favourably with those from other species used commercially for pulp production[24].

Due to the importance of *Pinus radiata* to the pulp and paper industry in Australia our experimental work was based on its extractive composition. The extractive composition has been measured by many different methods including GC[26, 27] and HPLC[28]. Although there are many different methods for analysing the composition of extractive material each method gives varying results on different classes of extractives and by observing all of the different methods it is possible to gain an overall picture of the extractives composition of *Pinus radiata*. McDonald and Porter[26] analysed the acetone extracts of green *Pinus radiata* logs using GC, their results are shown in Table 1.3.

Table 1.3. Extractives from *Pinus radiata* by GC[26]

Extractive	% Total Composition
Resin acids	58.8
Fatty acids	11.2
Esters as Triolein	7.6
Phenolics	5.2
Unsaponifiables (i.e. sterols)	16.3
Essential Oils	0.8

McDonald and Porter[26] also analysed *Pinus radiata* tall oil using GC. Tall oil is the concentrated non-volatile portion of the extractives. Through observing the composition of tall oil it is possible to gain a better understanding of the composition of the overall wood extractives. Their results are shown in Table 1.4 with the compositions of fatty acids being a combination of the free fatty acids and the hydrolysed triglycerides.

Table 1.4. Fatty acid and resin acid extractive composition from *Pinus radiata* tall oil[26].

Extractive	% Total Composition
C16:0	0.7
C16:1	1.2
C17 Br (anteiso)	0.2
C18:0	0.8
C18:1 (oleic)	4.3
C18:2 (9,12) (linoleic)	1.1
C18:3 (9,12,15) (linolenic)	17.1
C20:1	6.6
C20:2 (11,14)	2.1
C20:3 (5,11,14)	not detected
C22:0	2.9
Pimaric	4.5
Sandaracopimaric	4.2
Palustric/levopimaric	0.7
Isopimaric	5.9
Abietic	39.9
Neoabietic	7.9
Dehydroabietic	not detected
Total fatty acids	36.9
Total resin acids	63.1

Suckling *et al*[28] examined the extractives of *Pinus radiata* through HPLC. Their results are shown in Table 1.5 however it should be noted that although Suckling *et al*[28] did detect sterols they were not reported quantitatively.

Table 1.5. Extractives from *Pinus radiata* by HPLC[28]

Extractive	% Total Composition
Dehydroabietic acid	5.7
Other resin acids	21.8
C18:2 (9,12) (Linoleic acid)	2.9
C18:1 and C16:0 (oleic and palmitic acids)	4.3
triglycerides	35.0

Wallis and Wearne[27] examined dichloromethane extractives of fresh *Pinus radiata* wood chips by HPSEC and GCMS. Their results are shown below in Tables 1.6 and 1.7.

Table 1.6. Extractives of *Pinus radiata* by HPSEC[27]

Extractive	% Total Composition
Triglycerides	21.8
Steryl esters	5.2
Fatty acids/sterols	0.9
Resin acids	72.0

Table 1.7. Extractives of *Pinus radiata* by GCMS[27]

Extractive	% Total Composition
Resin acids	96.0
Fatty acids	3.2
Sterols	0.8

Sim, Croucher and Wiseman[29] also investigated how the age of the wood affected the extractive composition in *Pinus radiata*. Table 1.8 describes the wood type used and Table 1.9 shows the composition of the extractives in the headbox at the groundwood mill at Norske Skog Tasman.

Table 1.8. Wood types used during trial[29].

Period	% young thinnings	% old thinnings	% top logs (clear fell tops)
1	22	46	32
2	100	-	-
3	-	59	41

Young thinnings: from stands up to 13 years old.

Old thinnings: 14-22 year old thinning stands.

Clearfell tops: 20-40+ year old clearfelling stands (tops only).

Table 1.9. Concentration and composition of dichloromethane extractives[29].

Period	Total extractives %	% of total extractives			
		Triglycerides	Waxes	Fatty Acids	Resin Acids
1	2.8	38	12	6	38
2	3.4	47	11	4	26
3	2.7	40	11	4	31

This information showing the difference in extractive level with the different methods is not included to criticise any method nor the results but to indicate the variance of these extractives in different conditions of analysis. Many attempts have been made to determine the seasonal variation in extractives but conflicting results have been reported. The very high natural variation in the extractives composition within the tree population, has no doubt, produced the variable results as a very large number of trees need to be sampled in order to obtain a statistically true representative sample.

Mutton[21, 30] reviewed early attempts to determine the seasonal variation in extractives. Scandinavian spruce and birch have been the species that have received the most attention however numerous other hardwood species have also been studied.

Arrhenius[31] investigated the variation in ether extractable substances in spruce and pine trees during a single year and found that the amount of resin decreased during spring and

early summer. Swan[32] examined the extractives in two spruce trees each month for one year and found that the resin acid content decreased during early summer while the total amount of fatty acids in the tree was constant throughout the year. The fatty acid composition did, however, change, with there being more low molecular weight acids present during the early summer and more of the C18-acid with three double bonds present during the winter. Pensar[33-35] has examined the extractives in earlywood and latewood from Scandinavian pine and spruce. Dahn[36] in a study of the youngest annual rings of spruce, concluded that because of the large variation between and within trees a possible seasonal variation of the petroleum ether soluble extractives could not be established, however he did show that the polar material was most abundant in winter and diminished during the spring. Ekman *et al*[37] published a comprehensive study of the distribution and seasonal variation of extractives in Norway spruce. He found only a small variation in lipophilic extractives throughout the year and slightly lower resin acid contents in the summer months. Polar extractives such as the sugars fructose, glucose and sucrose showed great seasonal variation. There was a large decrease in the amount of these extractives in the wood during spring and correspondingly a large increase in their abundance in late autumn. Lloyd[38] studied the seasonal variation in *Pinus radiata* extractives with different solvents. The dichloromethane and methanol soluble extractive content of the heartwood and sapwood cores are shown in Figure 1.10.

O METHANOL SOLUBLES - SAPWOOD
★ DICHLOROMETHANE SOLUBLES - SAPWOOD
● DICHLOROMETHANE SOLUBLES - HEARTWOOD
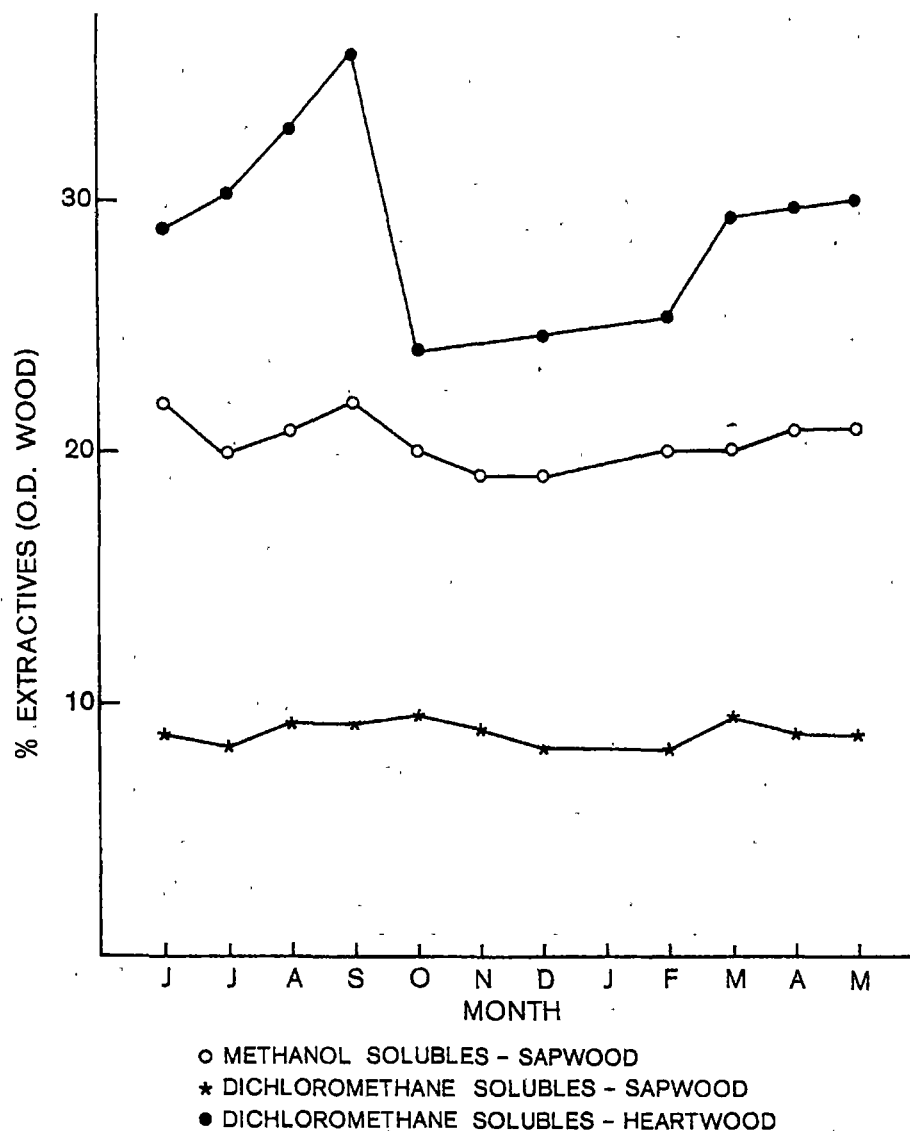
Figure 1.10. Seasonal change in extractives content of *Pinus radiata*[38].

The seasonal variation in the amount of dichloromethane-soluble extractives in sapwood cores was very small. There was found to be marginally more of these extractives in the wood during spring and autumn whereas the heartwood dichloromethane-soluble extractives showed significant seasonal variation. Methanol-soluble extractives in the sapwood cores did not show any distinct trends. Stack *et al.*[3, 39] observed an accumulation of glycerides in chips from *Pinus radiata* over the winter period. They monitored the glyceride content over a two year period (1995-1997) and showed a

minimum occurring from November through to March, with a maximum occurring from June to September (Figure 1.11).
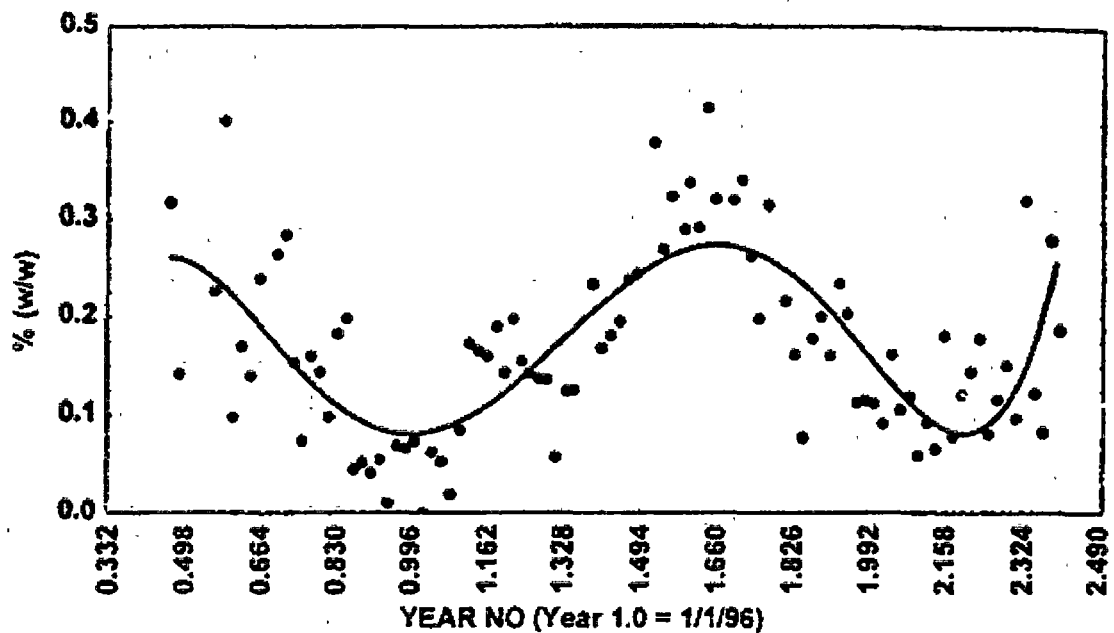
Figure 1.11. Seasonal variation of glycerides in *Pinus radiata* chips[3].

This known evidence of variance of extractive level is important when observing data as it must be taken into consideration when analysing the extractive content of any sample. The three hydrophobic extractives considered in this project are triglycerides, fatty acids and resin acids as they are three of the major extractives found in *Pinus radiata*. They constitute some 85-90% of the hydrophobic extractives in *Pinus radiata*.

1.2 Pitch Deposition

In the papermaking process, pitch and precipitates occur under certain circumstances that can give rise to a number of problems. The precipitates often have a negative impact on paper machine runnability and the quality of the paper produced. For example[11], the effects can appear as:

  ➢ Dirt particles in paper or on the paper machine (Figure 1.12)[40]

  ➢ Foam

  ➢ Impaired strength properties

  ➢ Changes in chemical paper properties, eg. hydrophobicity/hydrophilicity

  ➢ Picking on press rolls and dryer cylinders

  ➢ Odour and taste problems

  ➢ Toxicity in effluent

The terms 'precipitate' and 'pitch' are widespread among papermakers though not very well defined. Table 1.10[41] presents one proposal for classification of precipitates.
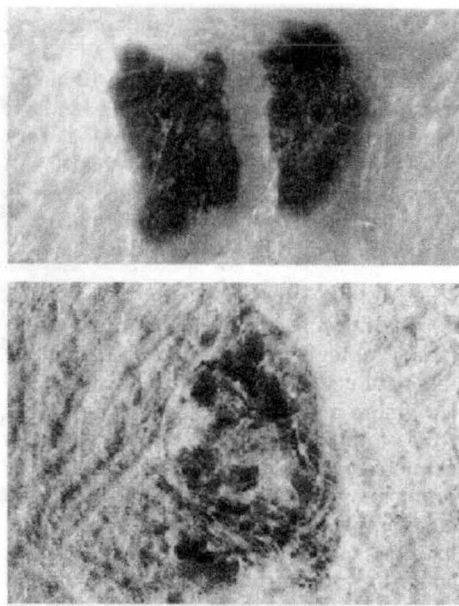
Figure 1.12. Visible pitch dirt specks in kraft pulp, 2-4 mm across as seen at low magnification[40].

Table 1.10. Classification of precipitates.[41]

Term	Example or Origin
Pitch	Agglomerates of extractives from chemical or mechanical pulp.
Stickies	Tacky material from waste paper, for example hot-melt, glue, bitumen, waxes, etc.
Dirt particles	Particles from waste paper not disintegrated.
White pitch	Synthetic binder from coated broke.
Coated broke deposits	Insufficiently disintegrated coated broke.

Pitch can also exist in several physiochemical forms during wood processing[42]. The different forms of pitch can shift from one form to another if under suitable kinetic conditions (i.e. temperature, pH, concentration and time). Many of these forms (Table 1.11) can be dealt with by a papermaking chemist, however deposited pitch is the most challenging.

Table 1.11. Different forms of wood pitch.

Type of pitch	Physiochemical form
Encapsulated pitch	The wood resin is trapped inside the cellular structure of the wood fibre.
Attached pitch	The wood resin is attached to the outside of the wood fibre.
Entrapped in sheet[43]	The wood resin is entrapped in the wood fibres as the fibre mat is being formed.
Soluble pitch	The wood resin is soluble in its aqueous surroundings.
Colloidal pitch	A mixture of wood resin components that are arranged as a stable colloid to remain homogenous in the aqueous surroundings. This colloidal structure is often referred to as a pitch particle and has an average size of one micrometer in diameter (Figure 1.13)[44,45].
Agglomerated pitch	A composite of resin molecules, which are neither in the colloidal or attached form but still in solution. These molecules are usually larger than the colloidal pitch.
Coated talc[46,47]	Talc is attached to the wood resin to prevent the tackiness and help prevent deposition and the problems caused by this.
Deposited pitch	Agglomerated pitch, which has ceased being in solution and has deposited onto a surface. This is the most challenging form of wood pitch and causes the papermaker the most difficulties.
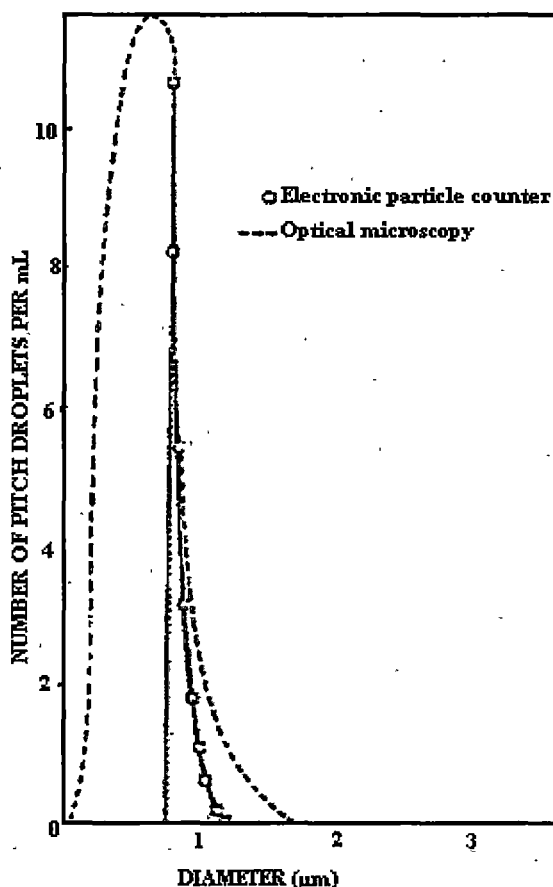
Figure 1.13. Suspended pitch particle size as determined with a Coulter Counter (solid line) and by optical microscopy (dashed line)[44].

Although *Pinus radiata* is not as resinous as some other pine species (e.g. Southern Pine) it can cause pitch problems for papermakers. Figure 1.14 depicts a common Fourdrinier paper machine[48] and the amount of pitch deposits and problems associated with them can vary quite considerably along the machine. Pitch can deposit along the slice lip in the headbox, which in turn destroys sheet uniformity and increases the variation in cross machine directional basis weight. If the deposits occur on the wire table and press section, water removal cannot occur at its maximum performance resulting in a wet sheet. Press section deposits can also occur in the dryer section which adds insulation to the dryers, again resulting in wet sheet. The most common manifestation of pitch is sheet breaks due to pitch either in the sheet or on the various machine components (e.g. centre roll, machine clothing or couch rolls).
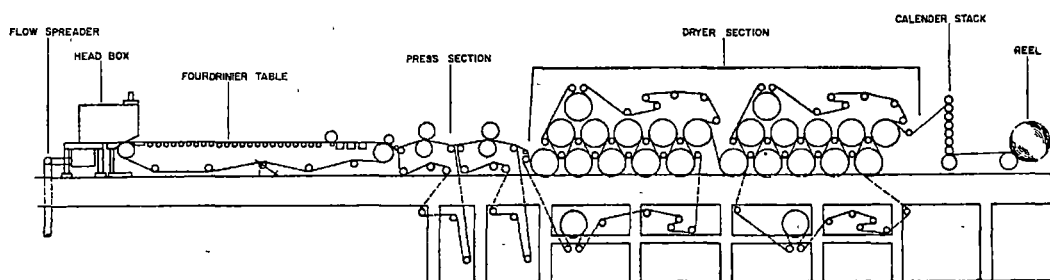
Figure 1.14. Fourdrinier paper machine[48]

It is known that different surfaces[49,50], shear forces[49] and viscosity[51] as well as the chemical composition of pitch[52] can effect pitch deposition in the papermill. Back has shown[49] that different surfaces affect the amount of pitch deposited as shown in Table 1.12. He showed this by using a deposition experiment similar to the one employed in this research and was able to show that there was an increase in pitch deposition when a copper propeller was used opposed to a plastic one.

Table 1.12. Pitch accumulated on a variety of surface[49].

Material	% Resin deposited[†]	% Resin deposited with copper propeller[†]
Glass	0	31.9
Natural rubber	5.2	25.3
Regenerated cellulose film	8.3	31.9
Aluminium	12.2	25.3
Copper	19.7	22.7
Phospor bronze wire	18.3	22.7
Polytetrafluoroethylene	19.2	30.1
Woollen felt	100	12.7

†Assuming 229 mg of extractive were present.

Ohtani[50] also showed that an activated (+50 Volt) carbon cloth could absorb 10 to 15 times the amount of extractives than steel. Pitch deposits vary significantly in their viscosity and stickiness. Many people[3, 49, 51, 53] have used the surface energy and viscosity, or stickiness, of pitch to help explain its deposition.

1.3   Recent Research Concerning Wood Pitch

Recent work by McLean *et al* has shown that chemical composition as well as different temperatures and pH conditions can affect pitch deposition[52]. McLean also focussed his study on pitch deposition with a similar composition as this study using a fatty acid, resin acid and triglyceride. This thesis studies the interactions of different fatty acids, resin acids and triglycerides. The work, outlined below, varied the amount of an individual fatty acid (FAP), resin acid (RAP) and triglyceride (GLP) present keeping the structure of each component constant. In his study McLean studied two pH values, namely pH 5.5 and pH 7.0, at two different temperatures, 20°C and 50°C. The results of this work showed very different deposition behaviour for the four conditions of pH and temperature investigated as the composition of the pitch changed. (Figure 1.15).

McLean presented his results as a four dimensional system using two dimensional triangular coordinate plots. There are two major steps in analysing these plots. The first step is to properly identify the concentration of each of the three components, leading to deposition, at any point within the triangular coordinate plot. All three sides of the triangle in Figure 1.15 are labelled according to the extractive they represent (RAP, FAP or GLP). In reading the coordinates for any point within the triangular plot, one draws a line perpendicular to the plane of increasing component concentration to the label axis. The example given in Figure 1.16 is the point that represents 35mg/L of FAP, 20mg/L of GLP and 5mg/L of RAP

a) pH 5.5, 50°C

b) pH 5.5, 20°C

c) pH 7.0, 50°C

d) pH 7.0, 20°C

Figure 1.15. McLean's model surface plots for each of the temperature and pH conditions[52,54].

Figure 1.16. Diagram explaining triangular coordinate systems. Illustrating a point of 35mg/L FAP, 20mg/L GLP and 5mg/L RAP[54, 55].

The second step is determining component interactions by the examination of the shape of the contour lines within a triangular coordinate plot. The amount of total pitch deposited (TPD in mg/L) at any given combination of resin acid, fatty acid and triglyceride is recorded on the actual contour lines within the triangular plot. The shapes of these contour lines express the influences, and interactions between components, that the three variables (FAP, RAP and GLP) have on TPD.

If only one component is responsible for deposition (TPD) (i.e. no interaction between components) then the contour lines will be linear and perpendicular to the concentration plane of the component responsible for deposition. Two way interactions between components can be identified through contour lines that are parabolic in shape whereas when the interaction of all three components is responsible for deposition (TPD) the contour lines will be circular.

Table 1.13 summarizes the findings of M°Lean's study. The results showed that an interaction between the three components, resin acid, fatty acid and triglyceride, occurred and that the interaction was dependent on the pH and temperature of the sample. It could also be observed that these changes in interactions influenced the deposition behaviour.

Table 1.13. Summary of the different behaviour of pitch deposition with different conditions[52].

Condition	Result
pH 5.5 at 20°C	The interaction between resin acid and fatty acids are primarily responsible for depositions at these conditions of temperature and pH.
pH 7.0 at 20°C	Triglycerides and resin acids interact under these conditions, the result of which is pitch deposition.
pH 5.5 at 50°C	Deposition under these temperature and pH conditions is proportional to resin acid concentration.
pH 7.0 at 50°C	Resin acids, fatty acids and triglycerides interact and form pitch deposition at these modern papermaking conditions. Although fatty acids play a role in this interaction it is the interaction between the resin acids and triglycerides that is the predominant cause of this deposition. Of the resin acid and triglyceride the resin acid levels are more responsible for pitch deposition.

Although the work did indicate that an interaction might be occurring between the three components it gave no insight into how or where these interactions were occurring. Other work by Qin *et al*[1] has measured viscosity, tackiness and surface energy of model resin mixtures to obtain a better understanding of resin properties and the possible relationship between the deposition tendency and the chemical composition of resin. In view of interactions, Qin *et al* were able to report that colloidal resin droplets form a two layered structure in process waters, with an interior domain, and an outer surface layer. The most hydrophobic steryl esters and triglycerides form the core and the main part of

the resin droplets, while the resin acids, fatty acids and sterols, which have a higher acid-base component of the work of adhesion, are enriched at the outer surface with their carboxyl and hydroxyl groups extending into the water. As this group is based in Finland they were working with TMP from spruce, *Picea abies*, instead of *Pinus radiata*. However they found that for an average sized colloidal droplet the diameter of the interior domain is about 0.24 μm, and the thickness of outer film is less than 0.01 μm. Because of high viscosity of resin acids and sterols, the outer part of the colloid may be a viscous and rigid film. Although the exterior part of the colloid is much thinner than the interior, the outer layer probably plays a much greater role in determining colloidal properties, such as chemical reactivity, charge, colloidal stability and pitch deposition tendency[1].

1.4 Project Aims

This project aimed to investigate the interactions between three of the major lipophilic extractives of *Pinus radiata*, namely the resin acids, fatty acids and triglycerides. The interactions between these components were studied as simple two component systems and as more complex three component systems. Deposition studies and theoretical computer modelling were undertaken to gain a better understanding of how these interactions between the components occur, how strong these interactions are and how much pitch is deposited due to these interactions. Model compounds of the main lipophilic wood extractive components were used to study the effect of varying chemical structure, chain length and degree of saturation on the interactions between the components and the deposition tendency of the components.

To gain an insight into a more 'realistic' model of what is happening in the paper machine when wood fibres are present, the interaction between the wood extractives and hemicelluloses was included in a separate study. Hemicelluloses can act as a natural stabiliser as they contain many hydrophilic functional groups that can interact with the pitch colloid and help stabilise the colloidal pitch. Although some research into interactions between hemicellulose from spruce[56] has been reported by overseas researchers this study aimed to investigate the effect that the addition of a model hemicellulose, guar gum, has on the deposition of both the individual components and of

a three-component system. Theoretical computer modelling was also been used to gain a better understanding of the nature of the chemical interaction and the effect of the chemical structure of the hemicellulose of the interaction and stabilisation of model pitch colloids. To the best knowledge of the author it is the first time that computer modelling has been employed to study the interactions between the components of the wood extractives.

2. <u>GENERAL EXPERIMENTAL</u>

This chapter describes the instrumentation, chemicals and procedures used throughout this work, unless specified otherwise in a particular chapter.

2.1 Instrumentation-Gas Chromatography

All samples were analysed using a programmed injection temperature on-column high temperature gas chromatograph with a flame ionisation detector (PVT-HTGC-FID). Samples were analysed using a Varian 3800 GC equipped with a Varian 8400 autosampler. The 1μL samples were injected onto a 15 metre Phenomenex® 100% polydimethylsiloxane (ZB-1, 15m x 0.53 mm ID x 0.15μm FT) Zebron™ capillary GC column. The injector temperature was held at 90°C for the first 30 seconds after injection and then increased to 325°C at a rate of 200°C/min. The oven/column temperature was held at 90°C for the first 1.5 minutes after injection and then increased to 320°C at a rate of 12°C/min. The FID temperature was held at 360°C for the entire duration of the ~33 minute program. This temperature program is graphically depicted in Figure 2.1. Ultra high purity helium was used as the carrier gas and the column was held at a constant pressure of 3.0 psi with a corresponding linear velocity of 54.8 cm/s. The detailed software output of Varian GC analysis method is included in Appendix A.
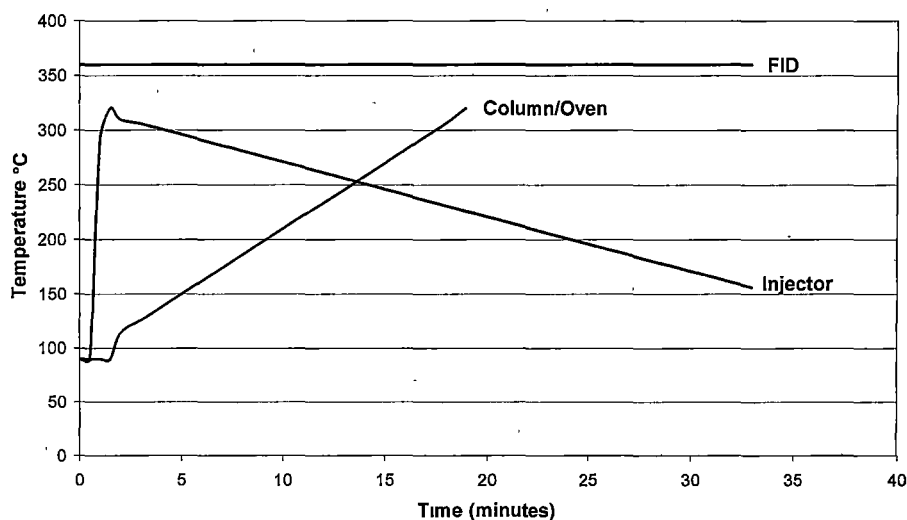
Figure 2.1. GC component temperatures during analysis.

2.2 Reagents

Unless specified otherwise all chemicals were of analytical reagent grade and are listed in Table 2.1-Table 2.5. All the samples' purity was checked by GC.

Table 2.1. Resin Acids. All resin acids were purchased from Helix Biotech.

CAS #	Compound	Molecular Formula	% Purity
1740-19-8	Dehydroabietic acid	$C_{20}H_{28}O_2$	99+
514-10-3	Abietic acid	$C_{20}H_{30}O_2$	90-95
5835-26-7	Isopimaric acid	$C_{20}H_{30}O_2$	99+

Table 2.2. Fatty Acids. All fatty acids were purchased from Sigma Aldrich.

CAS #	Compound	Molecular Formula	% Purity
143-07-7	Lauric acid	$C_{12}H_{24}O_2$	99+
544-63-8	Myristic acid	$C_{14}H_{28}O_2$	99+
57-10-9	Palmitic acid	$C_{16}H_{32}O_2$	99+
57-11-4	Stearic acid	$C_{18}H_{36}O_2$	99+
112-80-1	Oleic acid	$C_{18}H_{34}O_2$	99+
60-33-3	Linoleic acid	$C_{18}H_{30}O_2$	99+
463-40-1	Linolenic acid	$CH_{30}O_2$	99+
506-30-9	Arachidic acid	$C_{20}H_{40}O_2$	99+
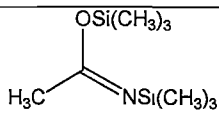
Table 2.3. Triglycerides. All triglycerides were purchased from Sigma Aldrich.

CAS #	Compound	Molecular Formula	% Purity
538-24-9	Trilaurin	$C_{39}H_{74}O_6$	98+
555-43-1	Tristearin	$C_{57}H_{110}O_6$	99+
14465-68-0	Trilinolenin	$C_{57}H_{92}O_6$	98+
122-32-7	Triolein	$C_{57}H_{104}O_6$	99+

Table 2.4. Internal Standards and spikes for the GC method. All compounds were purchased from Sigma Aldrich.

CAS #	Compound	Molecular Formula	% Purity
1002-84-2	Pentadecanoic acid	$C_{15}H_{30}O_2$	99+
506-12-7	Heptadecanoic acid	$C_{17}H_{34}O_2$	99
2190-25-2	DOG	$C_{53}H_{100}O_6$	~99
35602-69-8	Cholesteryl stearate	$C_{45}H_{80}O_2$	98
593-39-5	Petroselenic acid	$C_{18}H_{34}O_2$	99

Table 2.5. Other chemicals used in this work. All chemicals purchased through Sigma Aldrich unless specified otherwise.

CAS #	Compound	Molecular Formula	% Purity
7447-40-7	Potassium chloride[†]	KCl	99.5
7647-01-0	Hydrochloric acid	HCl	32%
7757-79-1	Potassium nitrate[†]	KNO_3	99.5
108-88-3	Toluene	C_7H_8	98+
110-86-1	Pyridine	C_5H_5N	99+
10416-59-8	BSA	$C_8H_{21}NOSi_2$	90
67-64-1	Acetone	C_3H_6O	98+
75-36-5	Acetyl chloride	C_2H_3ClO	99+
67-56-1	Anhydrous ethanol	C_2H_6O	99.8
9000-30-0	Guar	hemicellulose	95+
2123-19-15	13-pentacosanone[‡]	$C_{25}H_{52}O$	99+
693-67-4	1-bromoundecane	$C_{11}H_{23}Br$	98
1634-04-4	*t*BME	$C_5H_{12}O$	99.8
10416-59-8	BSA	$\underset{H_3C}{\overset{OSi(CH_3)_3}{\diagup \diagdown}}NSi(CH_3)_3$	95+

† supplied by BDH

‡ supplied by Lancaster Chemicals

2.3 Procedures

cmc measurements

The critical micelle concentrations were calculated by observing a pronounced discontinuity in the surface tension of solutions with varying concentrations of the surfactant (Figure 2.2). The surface tension measurements were conducted using an Analite™ surface tension meter. Solutions of varying concentrations were placed in the sample dish and placed on the platform. This platform was then raised until the plate just immersed into the test solution and the height control was rotated back ½ turn. The surface tension was measured in milliNewtons/metre.
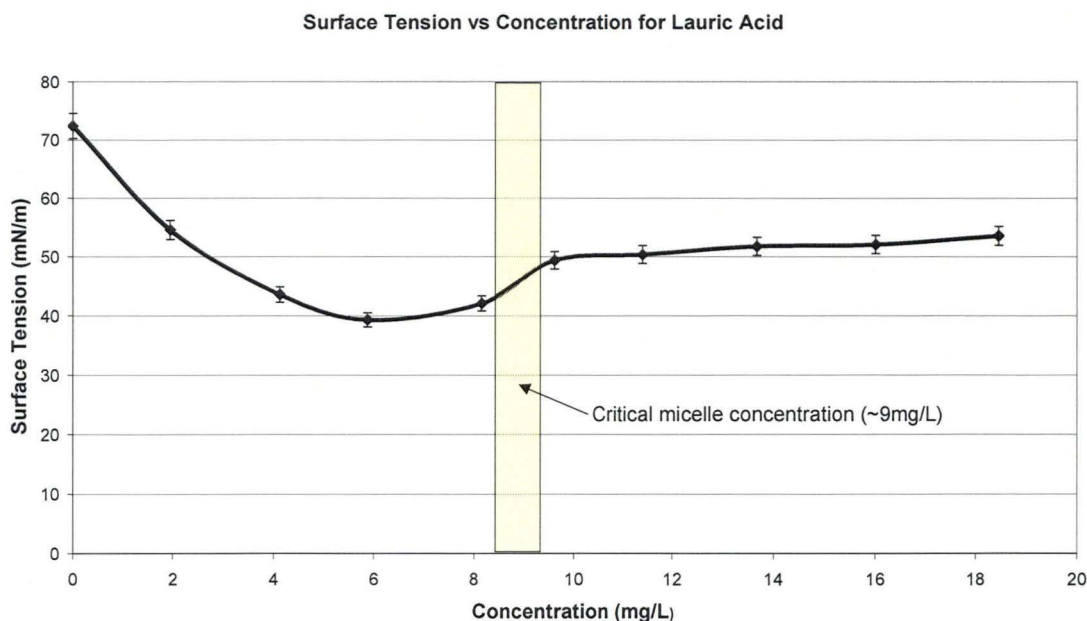
Figure 2.2. The typical variation of surface tension of an aqueous solution of lauric acid close to the cmc.

pK_a method

This procedure and discussed results are based on the work by McLean *et al*[57] which was based on the work of others[58, 59].

The majority of the substances examined are insoluble in water. As a result, the potassium salts of the acids were first prepared using 10% molar excess of potassium hydroxide, the minimum amount of distilled water and heated at 90°C for 20 minutes. At all times the amount of acid used was above its cmc. The salt solution was then filtered through a 0.2 μm filter.

The potassium salts were then titrated using a weak solution (0.005 to 0.0005M) of hydrochloric acid in order to determine the colloidal pK_a value. An average of three colloidal pK_a values are reported. All measurements were conducted in a thermostatically controlled oil bath.

Maintenance of a pH probe in wood extractive solutions[54, 60]

The pH of the deposition solutions was measured using an ORION Triode^{TM} pH electrode (model: 91-57BN). Special care and use of the probe was required to ensure

accurate and reproducible pH readings of the deposition solution. These procedures are based on the electrode maintenance procedures described in the pH probe manual[61]. Whilst not in use the pH probe was stored in a saturated potassium chloride (KCl, BDH 99.8% purity) solution, the pH probe reference chamber was also filled with the saturated KCl solution as well. Two days before using the probe it was stored in a 0.1M hydrochloric acid (HCl) solution. The day before use the pH probe was stored in a saturated KCl solution and the pH probe reference chamber was filled with Milli-Q® water. The morning that the pH probe was to be used the reference chamber was filled with fresh saturated KCl solution. This was a variation on electrode maintenance procedures described in the pH probe manual[61]. The pH was calibrated using pH 4, pH 7 and pH 10 buffer solutions supplied from BDH. The temperature adjusted buffer concentrations were used to establish the pH measurement reference slope. A series of "quick rinses", based on electrode maintenance procedures described in the pH probe manual[61], were also used in between the measuring of deposition solutions. The first "quick rinse" contained laboratory grade methanol to remove the fatty acids and triglycerides. The second "quick rinse" contained laboratory grade acetone to try to further dissolve any extractives that had agglomerated on the pH probe. The third "quick rinse" contained 0.1 M HCl for a general cleaning of the probe. The fourth and fifth "quick rinses" contained the standard dialysis wash solution comprised of distilled water, which had been brought to pH 5 using 0.16M HNO_3 and contained a slight electrolyte residual of 0.001M KNO_3. This rinsing method is depicted graphically in Figure 2.3.

used probe   clean probe

| Methanol | Acetone | 0.1M HCl | 1st Wash Solution | 2nd Wash Solution |
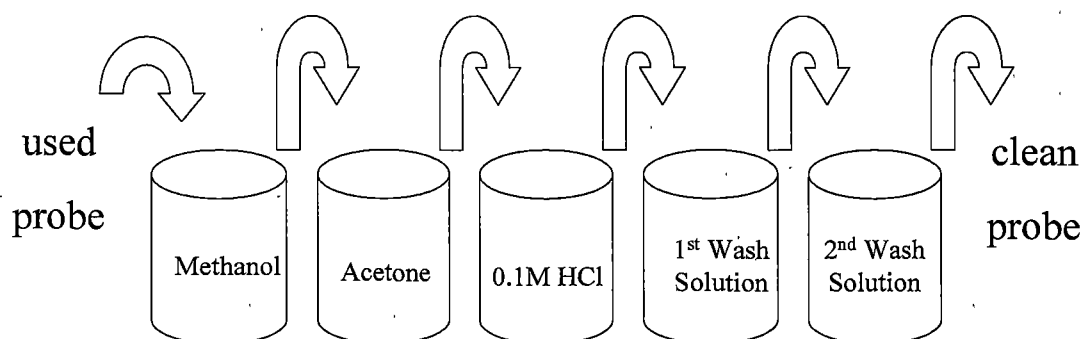
Figure 2.3. Rinsing method for pH probe between measurements[54].

When pH measurement began to drift the probe was placed in the third "quick rinse" (HCl) for 2-3 minutes and the deposition solution pH was tested using pH test strips (Sigma P-4411 pH 7.0-14.0 and P-4661 pH 0.0-6.0) to verify whether the pH probe had been reading properly.

Theoretical Calculations

Initial generation of structures

The structures were first drawn in Spartan®. The Spartan® structures were saved in 'mol2' format and converted to MM3 format through the chemical filetype conversion software BABEL.

Conformational search of structures

A new force-field parameter that encouraged hydrogen bonding was added to the MM3 external file, extra.para, according to the procedure listed in the MM3(1992) documentation. The stochastic search was performed using a maximum push length of 1.5Å and 300 pushes. These results were then converted to 'MM3' format using the selectcon script. The conformational search information was saved by default in MM3's SORT.LIS file and viewed using a Unix editor to determine the energies of the located conformers. The MM3 structure files were then converted to 'mol2' format using BABEL and viewed in Spartan® to check structural validity.

Selection of conformers for re-optimisation

Modelled conformers within an energy window of ~3.5kcal/mol (~15kJ/mol) from the global minimum were selected and the conformers within this window were converted to 'mol2' format.

Re-optimisation of structures

The modelled conformers were re-optimised using MOPAC a molecular orbital. The conformers with the lowest global minimum were again selected and converted to 'mol2' format.

3. PHYSICAL AND CHEMICAL CHARACTERISTICS OF HYDROPHOBIC EXTRACTIVES

3.1 Introduction

The hydrophobic extractives found in wood plants have very different physiochemical characteristics. Three of these characteristics include the critical micelle concentration (cmc), the pK_a and the solubility of the extractives. All of these factors can affect the strength and/or the occurrence of any interaction between the extractives and therefore the amount of pitch that is deposited. Without an understanding of these three characteristics it is impossible to know how much of the extractives are present in solution, if the extractives are in a micellar form, whether or not the carboxylic acids are undissociated or not and hence impossible to interpret any interaction that may be occurring.

Physical forces between the extractives are of great importance. Van der Waals forces will affect the structure of any complex formed. The forces between the molecules affect the shape of the individual components. This difference in shape will differ depending on the environment the molecule is in and also the length and/or size of the extractive. The structure of the complex will therefore affect the stability of the complex and the amount of pitch deposited in the pulp and paper making process.

The aim of this chapter is to explain these physical and physiochemical characteristics and how they influence the individual hydrophobic extractive components. The cmc values for the extractives were measured and theoretical computer modelling was used to predict the shape of each extractive as well.

3.2 The Critical Micelle Concentration

Introduction

The concentration at which a micelle forms can be identified by observing a pronounced discontinuity in physical properties of the solution such as the surface tension. It can also be measured by observing other discontinuities in other methods such as osmotic pressure, turbidity, magnetic resonance and self diffusion but a general definition is[62]:

$$\left(\frac{d^3\phi}{dC_T^3}\right)_{C_T=\text{cmc}} = 0 \qquad\qquad\qquad (3.1)$$

Where ϕ is the surface tension and C_T is the total concentration of the surfactant.

There are many factors which affect the cmc. For surfactants with a single straight hydrocarbon chain, the cmc is related to the number of carbon atoms in the chain (m) by:

$$\log_{10}(\text{cmc}) = b_0 - b_1 m_c \qquad\qquad\qquad (3.2)$$

where b_0 and b_1 are constants[62].

Non-ionic surfactant molecules may cluster together in aggregates of 1000 or more. The micelle population is often polydispersed, and the shapes of the individual micelles varies with concentration. Spherical micelles do occur, but micelles are more commonly flattened spheres close to the cmc[63].

The cmc is obviously of concern with the hydrophobic extractives found in *Pinus radiata* as it is known that pitch forms in the micellular form before agglomerating and depositing onto surfaces[62, 63]. To gain an understanding of the interactions that occur in pitch deposition the components must be above the cmc in the deposition experiments. As lauric acid was the most soluble of the extractives studied it had the highest cmc (7-9 mg/L). All experimental work was therefore carried out above that concentration.

cmc of major extractives.

The cmc of the major lipophilic extractives of *Pinus radiata* at 20°C were measured as described in Chapter 2.3 and are listed in Table 3.1. It can be observed that as the solubility of the extractive increases so does the cmc.

Table 3.1. cmc of the common lipophilic extractives of *Pinus radiata*.

Extractive	cmc (mg/L) (±2%)
Lauric acid C12:0	9.0
Myristic acid (C14:0)	7.0
Palmitic acid (C16:0)	5.5
Stearic acid (C18:0)	4.0
Oleic acid (C18:1)	4.5
Linoleic acid (C18:2)	5.5
Linolenic acid (C18:3)	6.5
Arachidic acid (C20:0)	3.8
Dehydroabietic acid	4.0
Isopimaric acid	2.5
Abietic acid	3.0
Tristearin	2.5
Trilinolenin	6.0

3.3 pK_a

Introduction

The pK_a of acidic extractives such as fatty acids and resin acids is of importance as it affects the strength and occurrence of any interactions. pK_a is the negative logarithm of the acidity constant, K_a.

$$pK_a = -\log K_a \tag{3.3}$$

where the K_a is:

$$K_a = \frac{\left[H_3O^+\right]\left[A^-\right]}{\left[HA\right]} \tag{3.4}$$

It is defined as the pH at which 50% of the acid is ionised, or dissociated. The amount of dissociated acid will affect the amount or strength of interaction as it is through the acidic proton that interactions occur through hydrogen bonding.

It can be seen that there is an inverse relationship between the magnitude of the pK_a and the strength of the acid. The larger the pK_a, the weaker the acid.

When a carboxylic acid (RCOOH) is placed in water it undergoes dissociation to form the hydronium ion (H_3O^+) and its conjugate base (RCOO⁻). This reaction can be written as:

$$RCOOH + H_2O \rightleftharpoons H_3O^+ + RCOO^- \qquad (3.5)$$

The above equation is usually represented as an equilibrium constant (K), which is defined as:

$$K = \frac{[H_3O^+][RCOO^-]}{[RCOOH][H_2O]} \qquad (3.6)$$

In most instances the concentration of water, $[H_2O]$, is constant. Thus the equilibrium constant can be redefined as the acidity constant (K_a). This is written as follows:

$$K_a = \frac{[H_3O^+][RCOO^-]}{[RCOOH]} \qquad (3.7)$$

The negative logarithm of each side of the Equation 3.7 yields Equation 3.8.

$$-\log K_a = -\log[H_3O^+] - \log\left(\frac{[RCOO^-]}{[RCOOH]}\right) \text{ or } pK_a = pH - \log\left(\frac{[RCOO^-]}{[RCOOH]}\right) \qquad (3.8)$$

When 50% of the acid is ionised (or dissociated):

$$[RCOO^-] = [RCOOH] \qquad (3.9)$$

Equation 2.10 thus becomes:

$$pK_a = pH \qquad (3.10)$$

pK_a of major extractives

As already stated, the pK_a of the extractive is important as it can affect the strength or occurrence of an interaction. Increasing pH decreases the likelihood of hydrogen bonding through the dissociation of the acid proton. When the pH is less than the pK_a there exists a large amount of undissociated acid and hence the possibility of any hydrogen bonding occurring increases.

As pK_a has an inverse relationship to temperature as seen in equation 3.11 we expect the pK_a to decrease with increasing temperature.

$$pK_a = \frac{\Delta G_{aq}}{\ln 10 RT}$$ (3.11)

Work was undertaken[57], in conjunction with fellow researcher Douglas McLean, to investigate the pK_a of various extractives at both 20°C and 50°C to gain an insight into the relationship between the different temperatures. The pK_a of these extractives can be seen in Table 3.2. The table also compares pK_a results reported in literature. The variance in pK_a values reported by others[64, 65, 66, 67, 68, 69] vary due to different experimental methods, purity of sample and concentration of sample measured.

Table 3.2. The pK$_a$ values of lipophilic extractives commonly found in *Pinus radiata*[57].

Saturated fatty acids

	pK$_a$ @ 25°C	pK$_a$ @ 50°C
Lauric (C12:0)	7.07[57] 5.30[64] ~7.50[65]	6.48[57]
Myristic (C14:0)	7.88[57] ~6.30[64] 8.10-8.20[65] 7.90[66]	7.25[57]
Palmitic (C16:0)	8.34[57] 5.06[67] 8.60-8.80[65] 9.70[66]	8.63[57]
Stearic (C18:0)	9.89[57] 10.15[68] 9.00[69]	9.28[57]
Arachidic (C20:0)	9.82[57]	9.28[57]
Behenic (C22:0)	9.89[57]	9.53[57]
Lignoceric (C24:0)	10.21[57]	9.81[57]
Cerotic (C26:0)	10.21[57]	9.83[57]

Unsaturated fatty acids

	pKa @ 25°C	pKa @ 50°C
Elaidic **(18:1;(*trans*)9)**	8.31[57] 9.95[68] 8.30[66]	7.65[57]
Oleic **(18:1;(*cis*)9)**	8.22[57] 5.02[67] 9.85[68]	8.29[57]
Linoleic **(18:2;(*cis*)9,12)**	7.43[57] 9.24[68] 8.00[66]	7.79[57]
Linolenic **(18:3;(*cis*)9,12,15)**	6.83[57] 8.28[68]	6.26[57]

Resin acids

	pKa @ 25°C	pKa @ 50°C
Abietic	7.26[57] 7.60[58] 6.39[70] 7.15[71]	6.18[57]
Dehydroabietic	6.77[57] 5.84[72] 5.71[70] 7.25[71]	6.18[57]
Isopimaric	7.08[57]	6.23[57]
Neoabietic	7.07[57]	6.23[57]

The values reported through the work undertaken in conjunction with Douglas McLean were conducted above the critical micelle concentration of each sample. This concentration leads to a measurement of the pK_a of the colloid formed rather than of the

carboxylic acid where you would expect a value between 4-5. Figure 3.1 shows that as fatty acid chain length increases so does pK_a[59]. The shorter chain length (C1:0 to C9:0) fatty acids have a pK_a values between 4-5. There is a critical chain length somewhere between 9 and 12 carbons where the pK_a starts to trend upwards on a steeper slope with increasing chain length. The increase in pK_a values starts to taper off when the fatty acids have 18 or more carbon atoms in their straight chain. This lower pK_a of the short chain fatty acids is because they are for the carboxylic acid, rather than that of the colloidal acid.
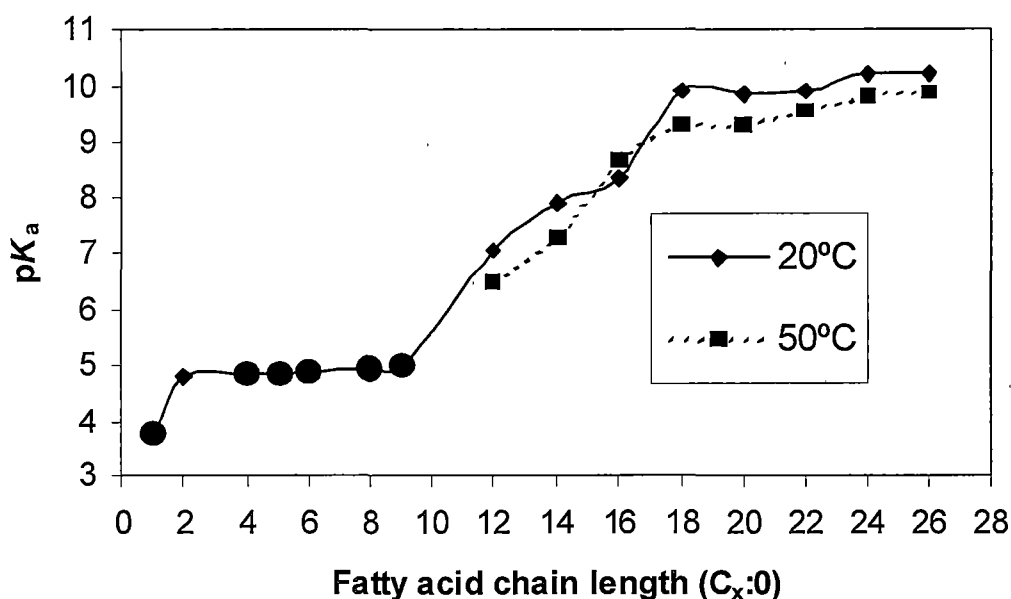
Figure 3.1. Fatty acid chain length versus pK_a. (Circles (●) denote values from CRC handbook[73], diamonds (♦) and squares (■) denote experimental data.)[57]

The effect of degree of saturation of the fatty acid in relation to the pK_a of the components' colloid (colloidal pK_a) shows that, as degree of unsaturation increases, the colloidal pK_a decreases at 20°C. A similar result was observed by Kanicky and Shah[68]. The effect is less clearly demonstrated at 50°C due to experimental errors.

The colloidal pK_a of resin acids was found to be between 6 and 7. The trends would appear to be driven by the electron-withdrawing groups present in the various resin acid structures. Of the four resin acid structures shown in Figure 1.5, dehydroabietic acid's aromatic ring is the strongest electron-withdrawing group. Consequently dehydroabietic

acid has the lowest colloidal pK_a value at 20°C. The double bonds in neoabietic and isopimaric acids are further away from the acidic proton than the double bonds of abietic acid. Due to this greater withdrawal distance the colloidal pK_a values for neoabietic and isopimaric acids are lower than the colloidal pK_a value for abietic acid at 20°C. It is unclear why abietic acid does not follow the electron-withdrawing group interpretation at 50°C.

Taking standard deviation and experimental error into account the colloidal pK_a values are slightly lower at 50°C than at 20°C. These temperature biased colloidal pK_a values are expected given the inverse relationship between pK_a and temperature in the thermodynamic definition of pK_a, shown in Equation 3.12.

$$pK_a = \frac{\Delta G_{aq}}{\ln 10 \cdot RT}$$ (3.12)

Where: R is the gas constant

                T is temperature in Kelvin

                ΔG_{aq} is the Gibbs energy of the acid in an aqueous solution.

This result of the colloidal pK_a values being lower at 50°C than at 20°C is important for papermakers in predicting the type of species present at a particular pH and hence the colloidal behaviour and deposition tendency of the extractives.

3.4 Solubility

Introduction

The solubility of the extractives in water is of great importance when considering the interactions that may be occurring between different molecules. The solubility is the quantity of solute that dissolves in a given quantity of solvent to form a saturated solution[74]. The papermaking process is mostly conducted in aqueous conditions so the solubility of the individual extractives will affect how much of these extractives are in solution and hence how much is available to interact with surrounding molecules. Many variables in the papermaking process have an effect on the solubility of the variables studied in this project with the two major variables being pH and temperature.

Solubility of extractives

Fatty Acids

It is a well known and documented fact that as the chain length of a fatty acid increases its solubility in water decreases. The solubility of the fatty acids with varying chain lengths that are present in wood plants[73] are depicted graphically in Figure 3.2. The solubility in water decreases quite considerably with the higher chain lengths being virtually insoluble in aqueous conditions.

Fatty Acid Chain Length vs Solubility (mg/L)
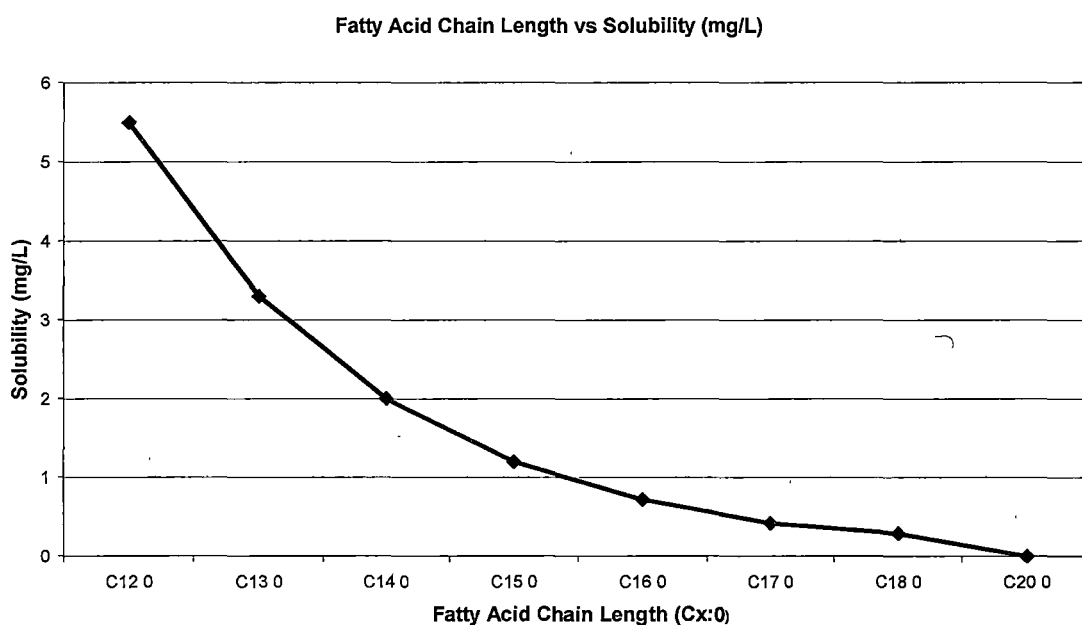
Figure 3.2. Solubility of fatty acids (C12-C18) in water[73].

Resin acids

Table 3.3 shows the solubility of the separate resin acids under aqueous conditions[75]. It can be seen that isopimaric acid has the lowest solubility (1.70mg/L) with dehydroabietic acid having the highest solubility (5.11mg/L). The other resin acid used in the study, abietic acid, has a solubility of similar order to isopimaric acid (2.75mg/L).

Table 5.2. Solubility of resin acids in water[75].

Resin Acid	Solubility (mg/L)
Isopimaric acid	1.70
Sandaracopimaric acid	1.82
Pimaric acid	2.17
Palustric acid	2.41
Neoabietic acid	2.31
Levopimaric acid	2.54
Abietic acid	2.75
Dehydroabietic acid	5.11

This significantly larger solubility for dehydroabietic acid is due to its aromaticity. This is explained in greater detail in Chapter 6 but it is due to the methods of hydrogen bonding between the individual dehydroabietic acid molecules and with the surrounding water molecules.

3.5 van der Waals Forces and Ion-Ion Interactions

Introduction

Van der Waals forces are essential in adsorption and are therefore crucial in papermaking. These forces interact between uncharged molecules, and their strengths are typically weaker than other forms of chemical bonds such as ionic, covalent and hydrogen bonding. Van der Waals attractive forces are the sum of the following terms:

➢ Dipole-dipole interactions

➢ Dipole induced-dipole interactions

➢ London or Dispersion forces

The potential energy of all these terms is proportional to r^{-6}, where r is the distance between molecules (or atoms). Thus the attractive energy is 64 times greater when the distance between two neighbouring molecules is halved. The short-range repulsive potential energy, which is due to the overlapping of outer electrons, for many molecules is proportional to r^{-12}, and the intermolecular potential energy (Lennard-Jones 6-12 potential) can be written as the sum of the attractive and repulsive potentials:

$$E_p = \left(\frac{A}{r^{12}}\right) - \left(\frac{B}{r^6}\right)$$ (3.12)

Equation 3.12 corresponds to the curve shown in Figure 3.3a. The Lennard-Jones potential (Figure3.2b), however, is not very accurate in describing the interaction between molecules, even for noble gas atoms.
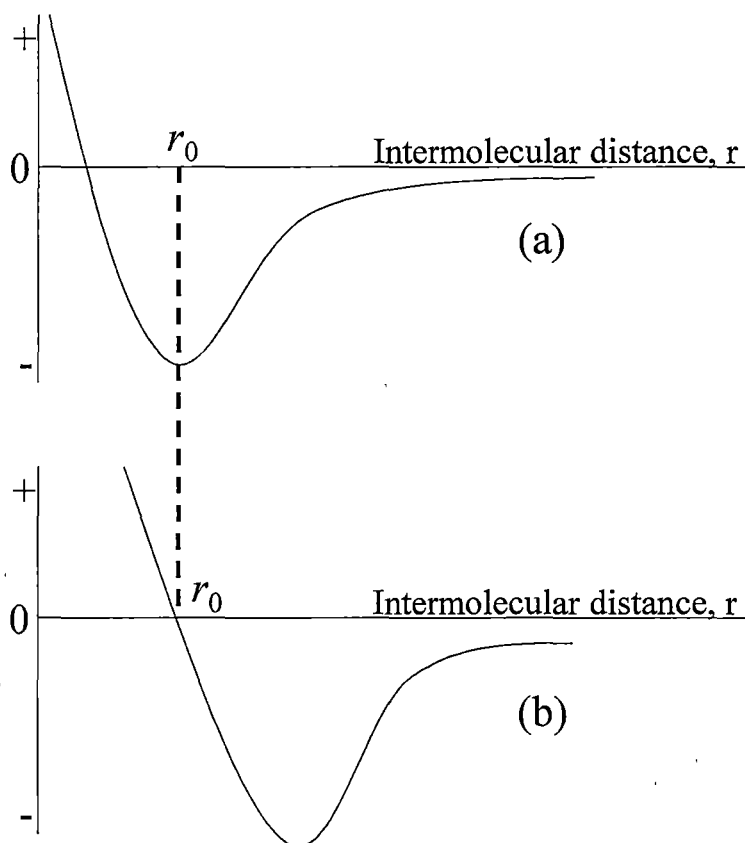
Figure 3.3. The shape of (a) the Lennard-Jones 6-12 potential curve and (b) the corresponding force, as a function of intermolecular distance[63]

Dipole-dipole interactions arise when a positive end of a polar molecule is directed toward the negative end of another polar molecule. This induces a dipole moment in a second molecule and results in a dipole induced-dipole interaction. Dipole-dipole forces are typically only less than 1% as strong as covalent or ionic bonds and they rapidly become weaker as the distance between the dipoles increases. Even molecules without dipole moments exert forces on each other. These rather weak forces are called London

dispersion forces. Although it is assumed that the electrons of an atom are uniformly distributed about the nucleus, a momentary nonsymmetrical electron distribution can develop and produce a dipolar charge arrangement which can affect the electron distribution of a neighbouring atom. The resulting interatomic attraction is relatively weak and short lived, but can be very significant for large atoms. Between macroscopic bodies London interactions become more long-range, because of additivity of these interactions. In short, London dispersion forces arise from interactions between fluctuating dipoles whose time-average value is zero.

Ion-ion interaction is evident in electrolyte solutions, ionic solids, and molten salts. The potential energy is proportional to r^{-1}. Ionic-dipole interaction occurs in electrolyte solutions, and its potential is proportional to r^{-2}. Table 3.3 shows a comparison between these different kinds of interaction energies.

Table 3.3. Comparisons of different types of intermolecular forces[63, 76]

Force	Dependence on force	Distance of energy	Typical potential energy values[†]	
			$\dfrac{E_p \text{ per molecule}}{J}$	$\dfrac{E_p \text{ per molecule}}{\text{kJmol}^{-1}}$
Ion-ion	r^{-2}	r^{-1}	-1.16×10^{-18}	-680
Ion-dipole	r^{-3}	r^{-2}	-1.20×10^{-19}	-72
Ion-induced dipole	r^{-5}	r^{-4}	-1.08×10^{-19}	-65
Dipole-dipole	r^{-7}	r^{-6}	-2.54×10^{-20}	-15.3
Dipole-induced dipole	r^{-7}	r^{-6}	-1.56×10^{-21}	-0.9
Dispersion	r^{-7}	r^{-6}	-7.34×10^{-20}	-44.2
Repulsion	r^{-13}	r^{-12}	-	-

[†]Calculated for the following values: electronic charge (1.602×10^{-19}C); dipole moment of 1D (3.338×10^{-30}); polarisability of 1.5×10^{-30}m^3; intermolecular distance 2.00×10^{-10}m. The dispersion energy values are for water molecules.

van der Waals forces on extractives

It is well known, documented[77, 78] and understood that fatty acid chain lengths are linear chains. Intermolecular forces are the attractive forces between molecules or between ions and molecules. Without such interactions, all substances would be ideal gases. Intermolecular forces, particularly those not involving ions, are collectively known as van der Waals forces. At a certain point in a fatty acid these van der Waals forces in the fatty acid chain length overcome the other forces surrounding the molecule and the fatty acid chain bends into a non-linear conformer. Little work has been done to investigate the critical chain length where non-linear behaviour occurs. Goodman[79] has done some studies using different calculation methods and found varying results(Table 3.4).

Table 3.4. Results from Goodman's study showing the shortest chains known to have nonlinear global minima.[57]

Class	Model	Shortest chain
Isolated molecules	MM2	$C_{18}H_{38}$
	MM3	$C_{25}H_{52}$
	AMBER	$C_{26}H_{54}$
Solvent effects	AMBER/water	$C_{22}H_{46}$
	AMBER/chloroform	$C_{143}H_{288}$
Semiempirical	PM3	$C_{12}H_{26}$
Molecular orbital theory	AM1	$C_{60}H_{122}$
	MNDO	No limit

The effects of van der Waals forces on the three extractives were investigated using exhaustive conformational searching using the MM3 force field as described in Chapter 2.3. This method was time consuming with often over 300 structures being found within $50kJmol^{-1}$ of the global minimum energy structure. Investigations were undertaken using molecular mechanics with the fatty acid in varying environments. A minimum carbon chain of eleven carbons was found for fatty acids with no surrounding molecules in the gas phase. The reason that the folded conformations are preferred for longer alkanes is that the attractive van der Waals forces outweigh the energetic cost of twisting

the carbon chain away from the preferred extended conformation[79]. Obviously in a pulp and paper mill process environment the fatty acids have varying surroundings. When the fatty acids were modelled with a resin acid present very different results were found. It was also found that the type of resin acid affected what the minimum chain length for a bending chain is (Table 3.5).

Table 3.5. Effect of resin acid structure on minimum fatty acid chain length for a bending chain[*].

Resin Acid	Minimum Chain Length
Abietic Acid	C_{22}
Isopimaric Acid	C_{22}
Dehydroabietic Acid	C_6

[*]Calculations done in gas phase.

If the fatty acid is interacting with a non-aromatic resin acid (abietic acid and isopimaric acid) the fatty acid chain length is stabilised by the van der Waals interactions between the fatty acid and the resin acid and the fatty acid chain does not bend unless the chain length is greater than 22 carbons. The aromatic resin acid (dehydroabietic acid) however has a totally different effect on the structure of the fatty acid chain. Due to the different form of hydrogen bond between the aromatic resin acid and fatty acid (see Chapter 4) the fatty acid bends to surround the rest of the molecule and to position itself over the aromatic ring. In this instance the chain length is straight until the chain length reaches six or more. This difference in structure due to the van der Waals forces will affect the overall structure of the pitch colloid. This difference in colloidal structure will lead to a difference in the propensity for a colloidal pitch molecule to deposit.

3.6 Conclusions

The physiochemical characteristics are very important when investigating the interactions between organic compounds. Without knowledge of these characteristics it is impossible to know what state the extractive is in and how it may behave. If compounds are interacting via hydrogen bonding with each other leading to pitch deposition they must be above the critical micelle concentration and undissociated.

These two factors will lead to a stronger interaction between the components and must be kept in consideration when trying to understand their behaviour. While interacting with each other the van der Waals forces affect the structure of the interacting complex and therefore the shape and stability of the complex itself.

All of the studies were conducted at pH 5.5 and above the cmc of lauric acid. In doing this the conditions in a paper mill are being imitated, ensuring that there is a large amount of undissociated carboxylic acid and that the components are interacting in a micellar environment. The van der Waals interactions between the molecules lead to the structure of the complex which affects the structure and stability of the resin droplet or colloid.

There are major differences in both the chemical structure and physiochemical properties between each class of extractive (i.e. resin acid, fatty acid, triglyceride) but also variation between many of the compounds in each individual class. This fact is important when trying to understand any interactions occurring between the components, compounds in each extractive class must be investigated rather than just investigating a representative from each extractive class. By observing the interactions between individual compounds rather that representatives of each class an overall understanding of the interactions between hydrophobic extractives leading to wood pitch deposition can be gained.

4.   COMPUTATIONAL CALCULATIONS. MOLECULAR MECHANICS OR SEMI EMPIRICAL THEORY?

4.1   Introduction.

More and more chemists are turning to computational methods for confirmation of experimental results, assistance in analysing experimental data, and guidance in designing new experiments.

It was envisaged that molecular modelling could be used in this research project to gain an insight into the type of interactions occurring and the strength of these interactions between the individual components and the surrounding water molecules. The structures of the individual extractives present in *Pinus radiata* are fairly large complex carboxylic acids (fatty acids and resin acids) and large ester linkages (triglycerides) which lead to van der Waals interactions and hydrogen bonding interactions. Many different methods of different theoretical levels were available to this study but the size of the systems investigated limited the practicality of these methods to two computational methods of different theoretical levels; molecular mechanics which is a simpler and faster calculation and semi-empirical methods which involves a higher level of theory.

Before any computational calculations could be conducted the level of theory at which calculations are performed must be chosen. Two levels of theory were available. These were MM3, a molecular mechanics method, and PM3, a higher level of theory which uses molecular orbital calculations. In choosing which theoretical method to use there are a few points that have to be considered:

> **What do you want to calculate?** In this case the stable conformers of individual components and of any complexes formed between them are of interest. A comparison of the stabilisation energies of the complex and the most stable energies of the individual components not interacting will be undertaken.

> **How big (number of atoms) is the size of your calculations?** With the three component studies it is necessary to conduct calculations with up to 500 atoms. Due to this large number of atoms, time and program capabilities must be considered.

> ➤ **What is the nature of the interactions?** Lower level of theory may not be
> capable of accurate analysis of certain interactions between molecules. In this
> case simple carboxylic acids and triglycerides are being studied. The main
> interactions of interest are hydrophobic interactions, van der Waals interactions
> and hydrogen bonding. Both levels of theory will be able to calculate these with
> certain parameters being used.

The aim of this chapter is to discuss the differences between the two different levels of
theory. It will also provide background theory into the calculations used in the two
methods and conclude as to which level of theory will be used for the interaction studies.

4.2 Molecular Mechanics

The 1960s witnessed an explosion in the application of quantum mechanical methods.
The origin of these methods lies in vibrational spectroscopy, where the information
derived from detailed analysis of vibrational spectra required the development of
potential functions to describe the overall molecular behaviour.

The theoretical basis of the molecular mechanics method can be derived by taking an
alternative approach to the Born-Oppenheimer approximation to that considered in
molecular orbital methods: in this case the nuclear motion is considered while implying
a fixed electron distribution associated with each atom. To this end a model has been
developed whereby a molecule is represented as a collection of spheres (possibly
deformable) joined by springs. The motions of these atoms can be described by the laws
of classical physics and simple energy functions can be used[76]. This allows much larger
chemical systems (of the order of thousands of atoms) to be investigated.

The energy of a molecule is calculated as a sum of the steric and non-bonded
interactions present (Equation 4.1). Therefore, each bond length, angle and dihedral is
treated individually while non-bonded interactions represent the influence of non-
covalent forces[76, 80-82].

$$E_{tot} = E_l + E_\theta + E_\omega + E_{nb_1} + E_{nb_2} \qquad\qquad (4.1)$$

Here $E_l + E_\vartheta + E_\omega + E_{nb_1}$ and E_{nb_2} are respectively the total bond, angle, dihedral and two forms of non-bonded energies (vdw and electrostatic) as represented in Figure 4.1.

$$E = \sum_l$$

$$+ \sum_\theta$$

$$+ \sum_\omega$$

$$+ \sum_{nb1}$$

$$+ \sum_{nb2}$$
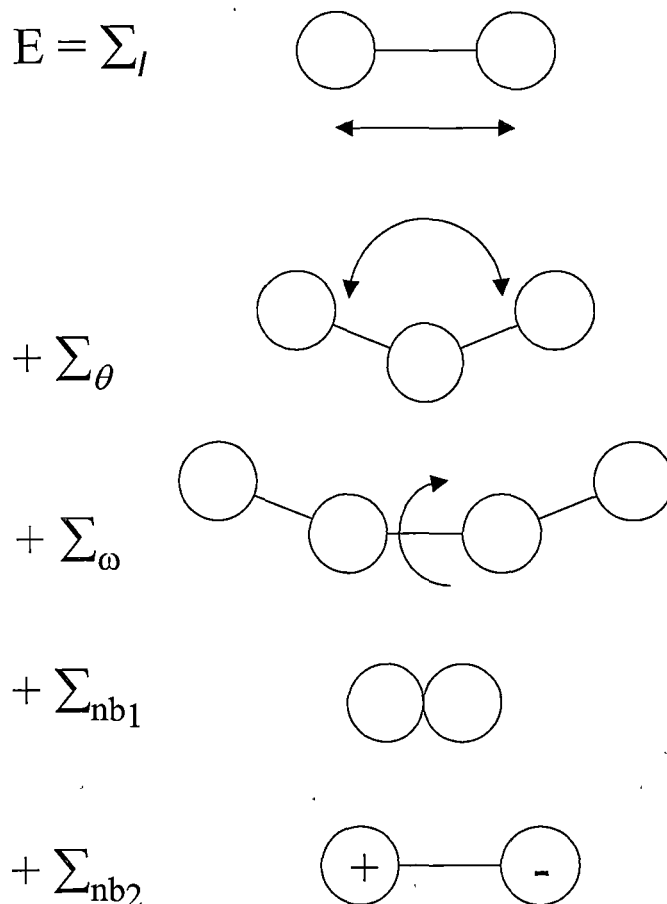
Figure 4.1. Pictorial representation of the terms included in a molecular mechanics force field[76, 80].

Bond Stretch

The typical vibrational behaviour of a bond is near harmonic close to its equilibrium value but shows dissociation at longer bond lengths (Figure 4.2). The most accurate description is the Morse function[76, 82]

$$E_1 = \sum D_e \left[1 - \exp\{-\alpha (l - l_0)\} \right]^2 \tag{4.2}$$

Where l_0 is the equilibrium bond length, D_e the dissociation energy, and α a force constant. However, the exponential calculation is computationally expensive therefore most force fields have adopted a simple harmonic function

$$E_1 = \sum k_l (l - l_0)^2 \qquad\qquad\qquad (4.3)$$

k_l being the stretching force constant describing the deformation. The bond stretch is treated in the same fashion as a stretching spring. This equation has obvious limitations in that it only approximately describes the actual behaviour of the bond. Furthermore, at extended bond lengths it is much too steep (Figure 4.2), and provides no representation of dissociation at very large deformations. Other variations have been used to accommodate more accurate long distance behaviour. Most commonly this takes the form of an additional cubic term

$$E_1 = \sum k_1 (l - l_0)^2 + k_1' (l - l_0)^3 \qquad\qquad (4.4)$$

but this suffers from the problem of inversion at long distances. Attempts have been made to remedy this by adding a quartic term which reverses the inversion[76, 82].
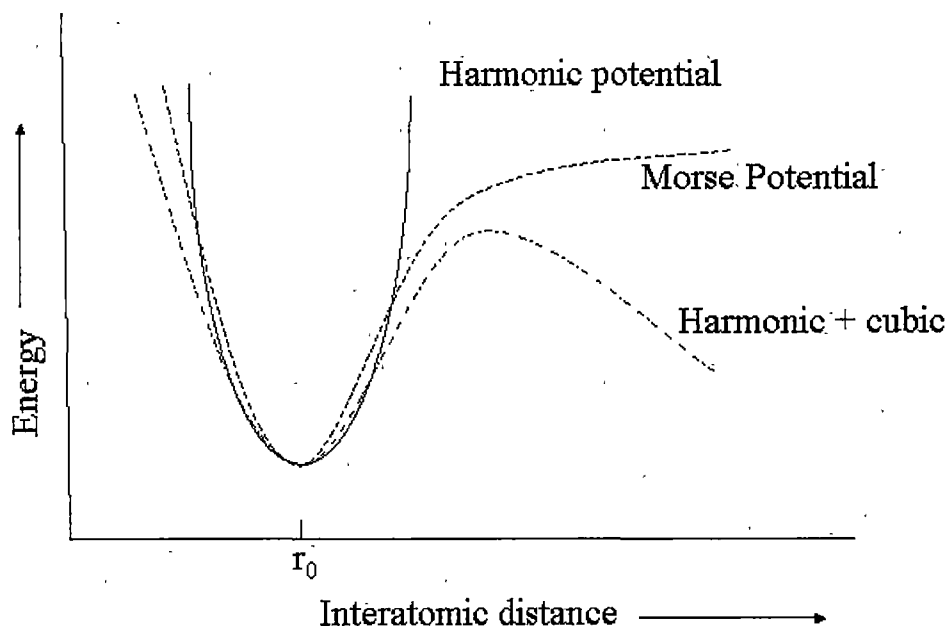
Figure 4.2. Curves showing the variation of bond stretch energy with distance[76, 82].

Bond Angles

Historically, bond angles have been treated in the same way as bond lengths and are usually described by a harmonic function.

$$E_\theta = \sum k_\theta (\theta - \theta_o)^2 \tag{4.5}$$

As before, k_θ is a force constant and θ_0 the equilibrium value for the bond angle. Again, this term is not ideal for the full range of values observed so higher order terms must be added. In very strained ring systems, however, it is usually not possible to use the constants derived for unstrained and acyclic molecules so separate three- and four-membered ring constants have been developed.

Dihedral angles

With initial force fields it was thought that this term could be omitted; gauche-trans energy differences would then result from non-bonded interactions. This soon proved to be an impossible task and dihedral angle terms were explicitly included. The functional form of this term is a Fourier series

$$E_{\omega} = \sum V_{n}(1 + s \cos n\omega) \tag{4.6}$$

Where V_n is the rotational barrier height, n the periodicity of rotation (e.g. in ethane n=3; in ethene n=2) and s = 1 for staggered minima and −1 for eclipsed minima. Figure 4.3 shows the n = 1, 2 and 3 curves.
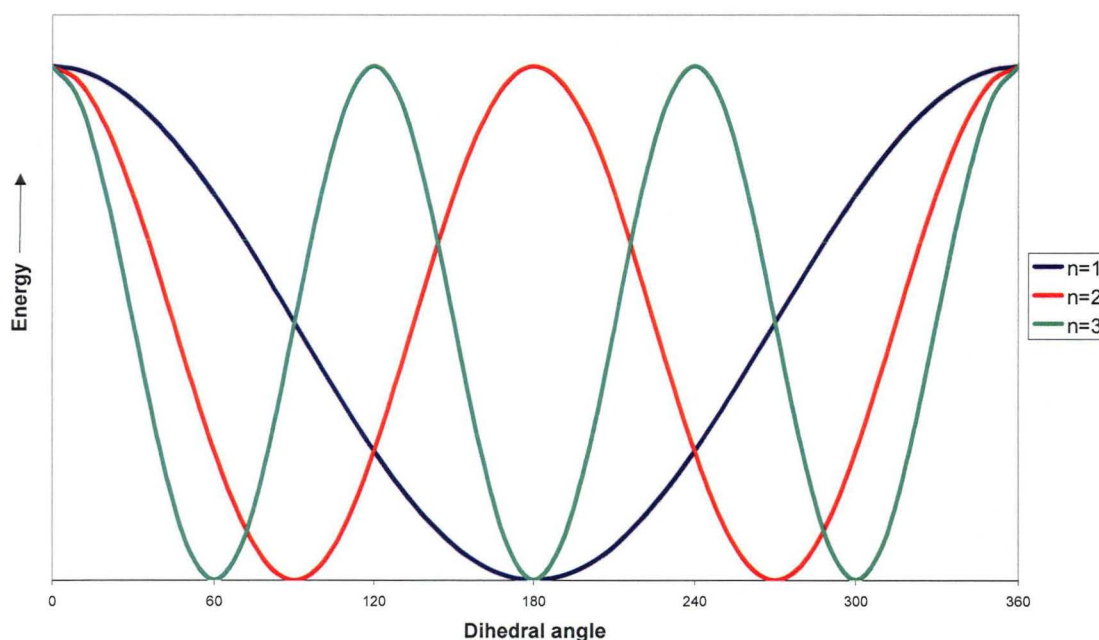
Figure 4.3. Variation of energy with dihedral angle for one, two and threefold barriers[76, 82].

In the simple molecules above, a single term, summed over all interactions, would suffice, but as the symmetry across the rotatable bond breaks down, the complexity of the energy profile increases. These can be corrected by the inclusion of other Fourier terms. If we consider butane as 1,2-dimethylethane the eclipsing interaction of the two methyl substituents will be higher in energy than that between one methyl and one

hydrogen, or between two hydrogens. Increasing the size of the C-C-C-C three fold barrier (V_3) would artificially modify the energy of the other eclipsing interactions. Modifying the interaction by the inclusion of a one-fold term (since the methyl-methyl eclipse occurs only once per 360° rotation) is the only option available. By way of warning, it should also be noted that the V_n parameters do not represent the complete rotational barrier but that van der Waals interactions must also be taken into account[76, 82].

Non bonded interactions

The interactions discussed in the previous sections can also be grouped together as the bonded interactions, in the sense that they are defined by the connectivity of the molecule. The non-bonded interactions, on the other hand, are distance dependent and are calculated as the sum over all the atoms with a 1,4 or greater separation. It is usual to consider these interactions as having two components: van der Waals and electrostatic. The former can be considered as both a size parameter and representative of electron correlation (resulting from instantaneous dipole interactions), while the latter provides a quantitative measurement of the influence of polarity on the energy and structure.

Many different functional forms have been used for van der Waals interactions but the most common is the 6-12, or Lennard-Jones potential[76, 82]

$$E_{vdw} = \sum \varepsilon \left[\left(\frac{r_m}{r} \right)^{12} - 2 \left(\frac{r_m}{r} \right)^6 \right]$$

(4.7)

where ε is the well depth and r_m is the minimum energy interaction distance (Figure 4.4). Short-range repulsions are accounted for by the r^{-12} term whereas London dispersion-attraction forces are mediated by the r^{-6} component. At short distances the repulsive term dominates.
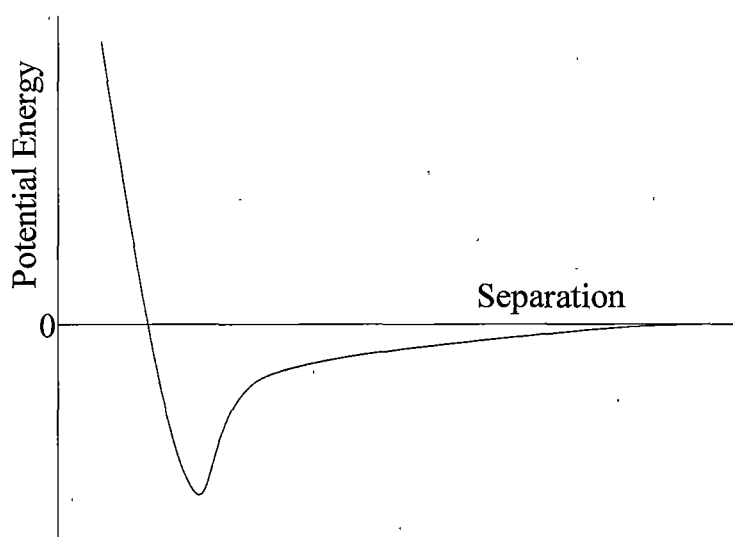
Figure 4.4. A typical van der Waals curve[76, 82].

Other forms have been proposed for the van der Waals interaction, principally because the r^{-12} term can be too steep at just less than optimal distances; these short contacts can be important when investigating sterically crowded structures. In the Buckingham potential

$$E_{vdw} = A\exp(-Br) - Cr^{-6} \qquad\qquad (4.8)$$

an exponential replaces the repulsive r^{-12} term. In most circumstances this function behaves similarly to the Lennard-Jones equation but at very short interatomic distances the function inverts and goes to -∞, an obvious danger in poorly constructed model structures[76, 82].

The choice of function has tended to be driven by computing requirements. For a small molecule the number of interactions is relatively small and the close range behaviour is crucial. In this situation the cost in calculating r, as opposed to r^2, and the exponential is not particularly high. For a protein, the number of interactions is considerably higher, but the contacts are likely to be close to equilibrium values. Using the Lennard-Jones function avoids the calculation of large numbers of square roots and exponentials (r^{-6} can be calculated from r^2). The 6-12 function also has the added advantage of requiring fewer parameters.

The second component of the non-bonded potential is the electrostatic term. This is usually calculated using partial charges (q) on the atom centres with the energy calculated using Coulomb's law

$$E_{el} = \sum \frac{q_i q_j}{D r_{ij}}$$ (4.9)

The dielectric constant D takes a value appropriate to a given solvent or is made proportional to the distance r_{ij} between the charges i and j.

Although this method of calculation sounds ideal, the following caveats must be kept in mind. First, as the method neglects explicit representation of electrons, it is restricted principally to the discussion of molecular ground states. This disallows the investigations of reactions. Secondly, the results obtained will only be as good as the potential functions and parameters used. Much of the potential surface defined by the force field has little validity as, typically, only extrema (stable conformers, rotational barriers, etc.) are used in the parameterisation procedure.

4.3 Quantum Mechanical and Semi-Empirical Methods

Quantum mechanics is the correct mathematical description of the behaviour of electrons and thus of chemistry. In theory, quantum mechanics can predict any property of an individual atom or molecule exactly. In practice, the quantum mechanics equations have only been solved exactly for systems with one electron in the outer shell. Two equivalent formulations of quantum mechanics were devised by Schrödinger and Heisenberg[83, 84]. Only the Schrödinger form is presented here since it is the basis for nearly all computational chemistry methods. The Schrödinger equation is

$$\hat{H}\psi = E\psi$$ (4.10)

where $\hat{H}$ is the Hamiltonian operator, ψ a wave function, and E the energy. In the language of mathematics, an equation of this form is called an Eigen equation, ψ is then called the eigenfunction and E an eigenvalue.

The wave function (ψ) is a function of the electron and nuclear positions. As the name implies, this is a description of an electron as a wave. This is a probabilistic description of electron behaviour which means that it can describe the probability of electrons being in certain locations but not exactly where the electrons are located.

The Hamiltonian operator $\hat{H}$ is, in general,

$$\hat{H} = - \sum_{i}^{\text{particles}} \frac{\nabla_i^2}{2m_i} + \sum_{i<j}^{\text{particles}} \sum \frac{q_i q_j}{r_{ij}} \tag{4.11}$$

$$\nabla_i^2 = \frac{\partial^2}{\partial x_i^2} + \frac{\partial^2}{\partial y_i^2} + \frac{\partial^2}{\partial z_i^2} \tag{4.12}$$

where ∇ is the Laplacian operator acting on particle i. Particles can be both electrons and nuclei. The symbols m_i and q_i are the mass and charge of particle i, and r_{ij} is the distance between particles. In currently available software, the Hamiltonian above is rarely used. Separating the nuclear and electron motions can simplify the problem. This is called the Born-Oppenheimer approximation. The Hamiltonian for a molecule with stationary nuclei is

$$\hat{H} = - \sum_{i}^{\text{electrons}} \frac{\nabla_i^2}{2} - \sum_{i}^{\text{nuclei}} \sum_{J}^{\text{electrons}} \frac{Z_i}{r_{ij}} + \sum_{i<j}^{\text{electrons}} \sum \frac{1}{r_{ij}} \tag{4.13}$$

Here, the first term is the kinetic energy of the electrons only. The second term is the attraction of electrons to nuclei. The third term is the repulsion between electrons. The repulsion between nuclei is added onto the energy at the end of the calculation.

Once a wave function has been determined, any property of the individual molecule can be determined. This is done by taking the expectation value of the operator for that property, denoted with angled brackets $\langle \; \rangle$, for example, the energy is the expectation value of the Hamiltonian operator given by

$$\langle E \rangle = \int \psi * \hat{H} \psi \tag{4.14}$$

Computations that are derived directly for theoretical principles with no inclusion of experimental data are called *ab initio* calculations. The term *ab initio* is Latin for "from the beginning". This type of calculation is an approximate quantum mechanical calculation. The approximations made are usually mathematical approximations, such as using a simpler functional form for a function or finding an approximate solution to a differential equation.

Hartee-Fock Approximation

The most common type of *ab initio* calculation is called a Hartree-Fock calculation[61], in which the primary approximation is the central field approximation. This means that the Coulombic electron-electron repulsion is taken into account by integrating the repulsion term. This gives the average effect of the repulsion, but not the explicit repulsion interaction. This is a variational calculation, meaning that the approximate energies calculated are all equal to or greater than the exact energy with the energies calculated in units called Hartrees (1 Hartee = 27.2116 eV = 4.36 x 10^{-18}J). Because of the central field approximation, the energies from Hartree-Fock (HF) calculations are always higher than the exact energy and tend to a limiting value called the Hartree-Fock limit as the basis set is improved.

One of the advantages of this method[82] is that it breaks the many electron Schrödinger equation into many simpler one electron equations. Each one-electron equation is solved to yield a single electron wave function, called an orbital, and an energy, called an orbital energy. The orbital describes the behaviour of an electron in the net field of all the other electrons.

The second approximation in the HF calculations is due to the fact that the wave function must be described by some mathematical function, which is known exactly for only a few one-electron systems. The functions used most often are linear combinations of Gaussian-type orbitals exp $(-ar^2)$, abbreviated GTO. The wave function is formed from linear combinations of atomic orbitals or, stated more correctly, from linear combinations of basis functions. Because of this approximation, most HF calculations calculate energies are greater than the Hartree-Fock limit, that is, you require an infinite basis set to achieve the HF limit[81].

The Gaussian functions are multiplied by an angular function in order to give the orbital symmetry of a s, p, d orbital and so on. A constant angular term yields s symmetry. Angular terms of x, y, z give p symmetry. Angular terms of xy, xz, yz, x^2-y^2, $4z^2-2x^2-2y^2$ yield d symmetry. This pattern can be continued for the other orbitals.

These orbitals are then combined into a determinant. This is done to satisfy two requirements of quantum mechanics. One is that the electrons must be indistinguishable. By having a linear combination of orbitals in which each electron appears in each orbital, it is only possible to say that an electron was put in a particular orbital but not which electron it is. The second requirement is that the wave function for electrons must be antisymmetric with respect to interchanging two particles. Thus, if electron 1 and electron 2 are switched, the sign of the total wave function must change and only the sign can change.

The functions put into the determinant do not need to be individual GTO functions, called Gaussian primitives. They can be a weighted sum of basis functions on the same atom or different atoms. Sums of functions on the same atom are often used to make the calculation run faster whereas sums of basis functions on different atoms are used to give the orbital a particular symmetry. For example, a water molecule with C_{2v} symmetry will have orbitals that transform as A_1, A_2, B_1, B_2, which are the irreducible representations of the C_{2v} point group. The resulting orbitals that use functions from multiple atoms are called molecular orbitals. This is done to make the calculation run much faster[84].

Semiempirical Methods

Semiempirical calculations are set up with the same general structure as a HF calculation in that they have a Hamiltonian and a wave function[84]. Within this framework, certain pieces of information are approximated or completely omitted. Usually the core electrons are not included in the calculation and only a minimal basis set is used. Also, some of the two electron integrals are omitted. In order to correct for the errors introduced by omitting part of the calculation, the method is parametised. Parameters to estimate the omitted values are obtained by fitting results to experimental data or *ab initio* calculations. Often these parameters replace some of the integrals that are excluded[80].

The advantage of semiempirical calculations is that they are much faster than *ab initio* calculations[84]. The disadvantage of semiempirical calculations is that the results can be erratic and fewer properties can be reliably predicted. If the molecule being computed is similar to molecules in the database used to parameterise the method, then the results may be very good. However, if the molecule being computed is significantly different from anything in the parameterisation set, the answers may be very poor. However, semiempirical methods are not as sensitive to the parameterisation set as molecular mechanics calculations.

Semiempirical methods are parameterised to reproduce various results. Most often, geometry and energy (usually the heat of formation) are used[83]. Parameterisation method 3 (PM3) was the method available to our research. PM3 uses nearly the same equations as other semiemperical methods but has an improved set of parameters with it currently being extremely popular for organic chemists. PM3 is more accurate than other semi-empirical methods for hydrogen bond angles and energies[81] and is also more popular than other semiempirical methods due to the availability of algorithms for including solvation effects in the calculations. There are also some known strengths and limitations of PM3. Overall heats of formation are more accurate than other semiempirical methods. Hydrogen bonds are usually too short by 0.1Å, but the orientation is usually correct[82]. On average, PM3 predicts energies and bond lengths more accurately than other semiemperical methods[81].

4.4 Comparisons of Methods

When using computational chemistry to answer a chemical question, the obvious problem is that the researcher needs to know how to use the software. The difficulty sometimes overlooked is that one must estimate how accurate the answer will be in advance. Table 4.1 indicates the accuracies of both the molecular mechanics method MM3 and the semiemperical method PM3 relative to experimental results[81].

Table 4.1. Accuracies[†] of two methods used relative to experimental results[81]

	ΔH_f	Bond Length	Bond Angle	Dipole	Cost
MM3	2.51kJ/mol	0.01 Å	1.0°	0.07 D	Very low
PM3	3.47kJ/mol	0.04 Å	3.9°	0.60 D	Low

† all accuracies are std. dev.

The information that was required from the computational data was mainly the ΔH_f of each component and of the complex formed. Initial studies were conducted using both methods of calculation. The differences between the two methods was found to be minimal and the same trends were observed for each method (Table 4.2). The procedure used to undertake the calculations is described in Chapter 2.3.

Table 4.2. ΔH_f values for single components using MM3 and PM3 calculations.

	ΔH_f (kJ/mol)	
	MM3	**PM3**
C12:0	-654.5	-644.6
C14:0	-704.0	-690.3
C16:0	-722.0	-750.3
C18:0	-789.9	-778.6
C18:1	-628.8	-689.5
C18:2	-568.8	-577.2
C18:3	-538.4	-497.4
C20:0	-842.8	-819.8
Abietic Acid	-359.4	-477.0
Isopimaric Acid	-377.3	-476.4
Dehydroabietic Acid	-435.1	-484.7
Tristearin	-542.4	-538.1
Trilinolenin	-493.3	-486.4

In observing the data in Table 4.2 calculated and the information given in Table 4.1, showing that the error in ΔH_f calculations using MM3 is significantly smaller, it was decided that molecular mechanics would be used in all further studies of the interactions. After the conformers were found using MM3 they were re-optimised using PM3 as this method is best for theoretical work that involves hydrogen bonding.

This research was interested in looking at how the three major lipophilic extractives of *Pinus radiata*, namely the resin acids, fatty acids and triglycerides, interacted with each other through hydrogen bonding and van der Waals interactions but also how stable these interactions were compared to the extractives behaving independently in an aqueous environment. To gain an understanding of how stable these complexes were, the stabilisation energy (SE) of the complexes were considered. SE is calculated from the ΔH_f of the single components and the complex formed from the individual components. Considering the reaction pathway of the two components in the aqueous solution the ΔH_f varies for the complex and for the single components in solution. Figure 4.5 shows the reaction pathway for two components A and B and two different complexes between them (AB_1 and AB_2). The difference in energy between the complex and the two single components is the SE. A lower complex energy leads to an increase in SE which in turn leads to a more stable complex and hence an increased probability in its occurrence. From Figure 4.5 it can be seen that complex AB_2 is more stable than AB_1 and also more stable than the two components A and B behaving independently, indicating that it has a higher probability of occurring.
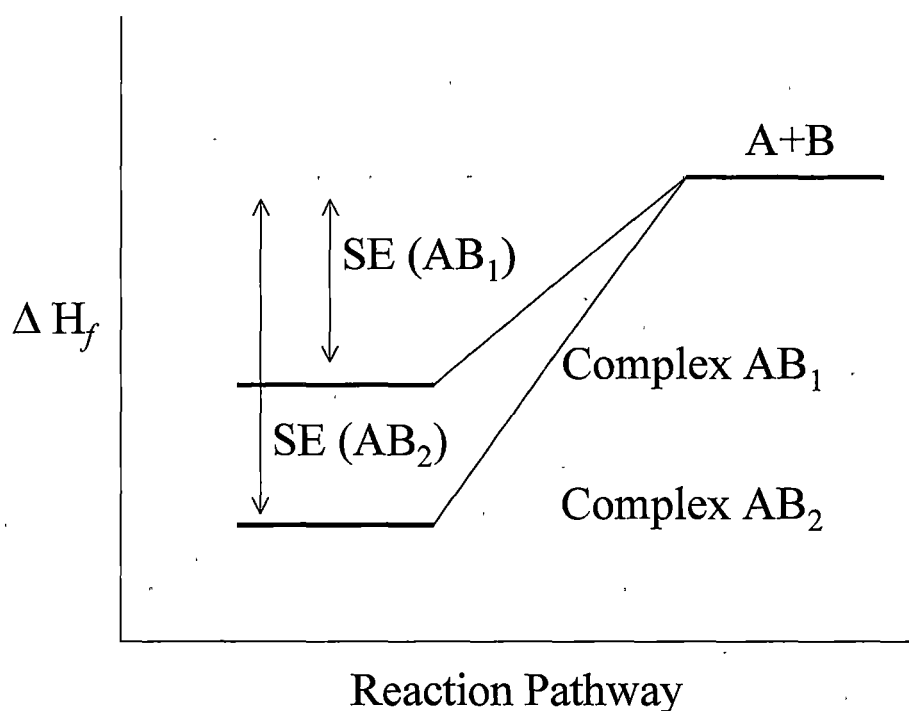
Reaction Pathway

Figure 4.5. Reaction pathway for components A and B with formation of two complexes for AB.

In order to ensure that SE could be used to study the effects on hydrogen bonding between wood extractives a simple modelling experiment was conducted with a molecule that is widely known to stabilise through hydrogen bonding, namely water. It is well documented and known that water molecules hydrogen bond to themselves and stabilise their structure with an increasing number of molecules[74]. Figure 4.6 shows the minimised structure of a water molecule and how multiple water molecules aggregate through hydrogen bonding.
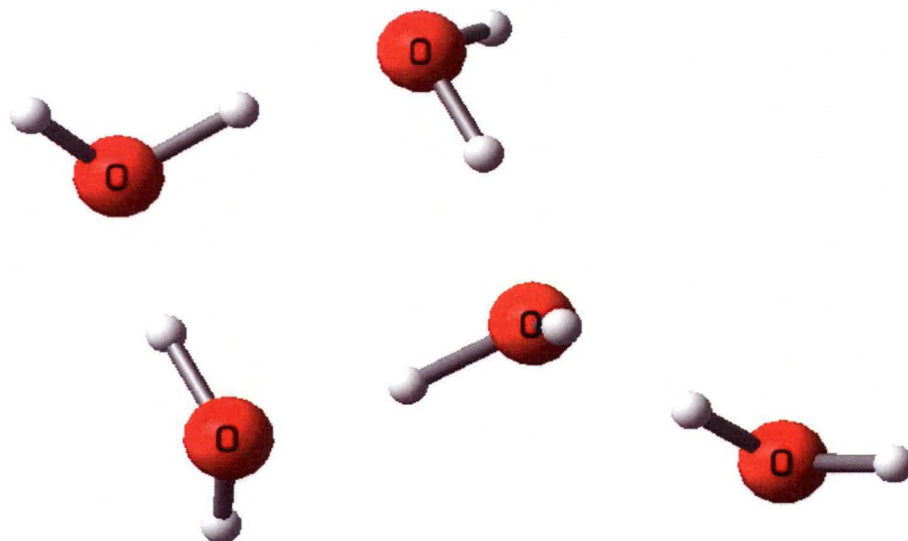
Figure 4.6. The structure of five agglomerated water molecules.

Water has a ΔH_f value[63] of –285.83kJmol^{-1}. Table 4.3 shows the calculated SE of aggregates of increasing numbers of water molecules. This data indicates that SE does increase and hence demonstrates that SE can be used to investigate the stabilisation effects of hydrogen bonding between wood extractives.

Table 4.3. Stabilisation energies of water agglomerates with increasing number of molecules.

Number of Water Molecules	A+B kJmol^{-1}	Stabilisation Energy [(A+B)-complex] kJmol^{-1}
1	-285.8	0.0
2	-571.7	25.2
3	-857.5	47.2
4	-1143.3	77.9
5	-1429.2	111.1

This evidence for SE allows it to be used for the interactions between wood extractive components in any sized system with any amount of molecules involved in the interaction. When investigating a three-component system of a resin acid, fatty acid and triglyceride, consideration needs to be given to the effect that the different molecules will have on the strength and type of hydrogen bond present in the complex. To investigate if the strength of the hydrogen bond was represented correctly with the SE the acetic acid dimer was compared with the interaction between acetic acid and its respective salt. In this second instance only one hydrogen bond is available between the two components and therefore a lower stabilization energy is expected (Figure 4.7).
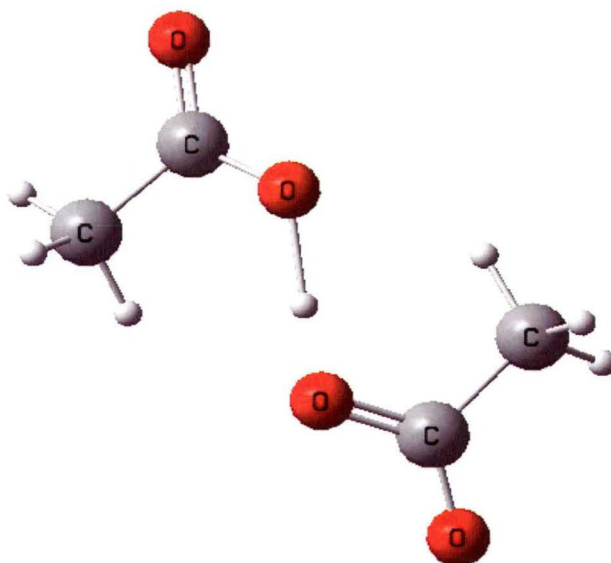
Figure 4.7. Interactions between acetic acid and its respective salt.

Table 4.4 presents the SE for the homogenous and heterogenous dimers between acetic acid and its respective salt. It indicates, as expected, the strongest interaction is between the acetic acid dimer and the weakest between the acetic salt dimer.

Table 4.4. Stabilisation energies of interactions with varying hydrogen bond strengths.

Complex	A+B	Stabilisation Energy [(A+B)-complex]
Acetic acid : Acetic acid	-205.2	88.7
Acid acid : Acetic salt	-231.0	40.3
Acetic salt : Acetic salt	-256.8	0.0

ΔH_f Acetic acid = -102.57kJmol^{-1}

ΔH_f Acetic salt = -128.40kJmol^{-1}

These two tests give confidence to the idea of using SE to study and predict the differences in stability by pitch components.

4.5 Conclusions

Two methods of computational chemistry were investigated for the study of interactions between the wood extractives of *Pinus radiata*. These two methods were two different levels of theory and molecular mechanics was decided to be the most suitable method for the global minimum search while PM3 was used for the re-optimisation. The stability of the interactions was calculated through the stabilisation energy and this was proven to be a correct observation through the modelling of some simple known examples. Through this knowledge of stabilisation energies we can successfully model the extractive components and understand the strength and probability of any interactions occurring.

5 COMPUTATIONAL CALCULATIONS OF THE HYDROGEN BOND

5.1 Introduction

The hydrogen bond often presents an uncertain footing to the chemist as it is the borderland between chemical bonds and the weaker and less specific interactions that cause every known substance to liquefy if the temperature is sufficiently high. Amazingly, one of the first descriptions of the hydrogen bond was given almost four decades ago and remains acceptable in the context of chemical knowledge today;

> *Water...shows tendencies both to add and give up hydrogen, which are nearly balanced. Then...a free pair of electrons on one water molecule might be able to exert sufficient force on a hydrogen held by a pair of electrons on another water molecule to bind the two molecules together....Indeed the liquid may be made up of large aggregates of molecules, continually breaking up and reforming under the influence of thermal agitation.*
>
> *Such an explanation amounts to saying that the hydrogen nucleus held between two octets constitutes a weak 'bond'*[85].

Very strong dipole-dipole attractions occur between hydrogen atoms bonded to small, strongly electronegative atoms and nonbonding electron pairs on other such electronegative atoms. This type of intermolecular force is called a hydrogen bond, and with a bond dissociation energy of 1-9 kcalmol[-1], is weaker than an ordinary covalent bond but much stronger than the dipole-dipole interactions that occur in such molecules as acetone[85]. Broadly, a hydrogen bond is said to exist when there is evidence of a bond and that this bond specifically involves a hydrogen atom already bonded to another atom.

Classes of Hydrogen Bonding

With the above definition of the hydrogen bond it can be seen there are two possible classes of hydrogen bond. This is to say that the interaction involves two functional groups in the same or different molecules with one of these groups serving as the proton

donor and the other as the proton acceptor. These two classes are the intermolecular hydrogen bond and the intramolecular bond.

Intermolecular Hydrogen Bonds

The widest general class of hydrogen bonding involves the association of two molecules of the same or different substances. The resulting hydrogen bonded complexes are not limited to dimeric linkages, although these are the most common. Intermolecular hydrogen bonds may occur in chains, rings, or three-dimensional networks[86].
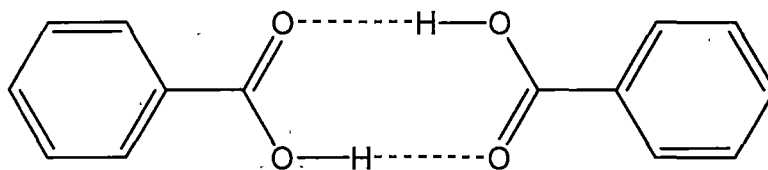
Intermolecular Hydrogen Bonding

Intramolecular Hydrogen Bonds

The other broad class contains those substances in which the hydrogen bonds are formed between groups within a single molecule.

The formation of a hydrogen bond in a solution or compound modifies a great many physical and a few chemical properties. Usually the properties are changed sufficiently to require special treatment for associated materials in any correlation of behaviour. These changes are not in light of the fact that hydrogen bonding may alter the size, shape, and arrangement of atoms, as well as the electronic structure of the functional groups.
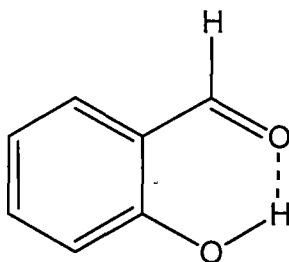
Intramolecular Hydrogen Bonding

5.2 Different Types of Intermolecular Hydrogen Bonds

If we consider the intermolecular means of hydrogen bonding there are four possible mechanisms for the occurrence of hydrogen bonding. All of these four possibilities follow the definition of a hydrogen bond and have been well documented in the literature. They are;

The Dimer

This is the most common and documented form of hydrogen bond[78, 85, 86]. It is exemplified by the carboxylic acids involving the formation of dimers with zero dipole moment and resulting in a non-polar liquid.
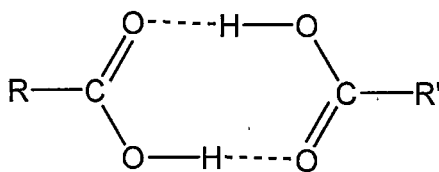
Dimer with the α proton.

This is similar to the well-documented dimer but instead of hydrogen bonding to the acidic proton the carbonyl group hydrogen bonds to the α proton. This form of hydrogen bonding is most common with smaller carboxylic acids, those not of much greater size than butanoic acid[85-87].
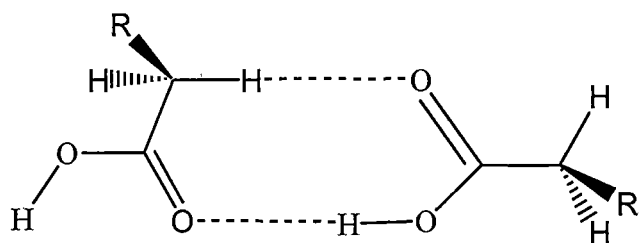
Catemer motif.

On the other hand, water, alcohols and some amides can form polymers which are chain-like in their arrangement. The polymers form a liquid phase of high dielectric constant[87, 88]. This form of hydrogen bonding is again mainly common with smaller molecules.
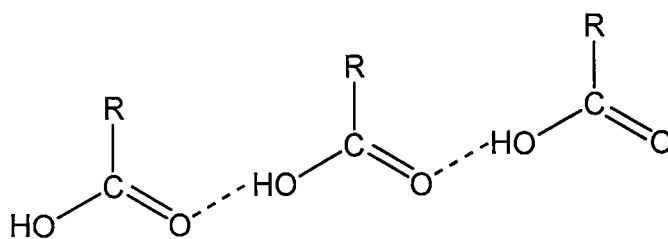
Hydrogen Bonding and Aromatic Systems.

Whether aromatics can act as hydrogen bonding bases has great practical as well as theoretical interest[85, 87]. There have been many experimental studies of hydrogen bonding substances dissolved in benzene with the apparent implication that the solvent is considered inert. The theoretical interest stems from the proposal that the hydrogen bonding base need not be a highly electronegative atom.

The evidence relative to hydrogen bonding obtained from IR and Raman studies is voluminous[85]. The correlation of base strength with stretching frequency(Δv_s) as shown in Table 5.1 typifies the evidence.
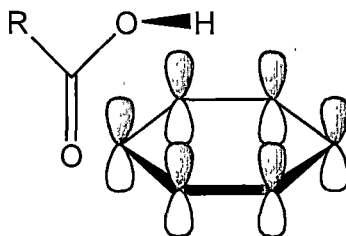
Table 5.1. Δv_s as a measure of base strength

Solvent	Δv_s in cm^{-1}		
	CH$_3$OD	Pyrrole	HCl
Aromatics			
Chlorobenzene	21[89]	-	52[90]
Benzene	24[89,90]	39[91-93]	81[90]
Toluene	26[89]	49[92]	87[90]
m-Xylene	29[89]	52[92]	108[90]
Nitrobenzene	52[90]	48[92]	113[94]
Mesitylene	34[89]	58[92]	119[90]
Esters			
Ethyl acetate	51[95]	-	254[96]
Nitriles			
Acetonitrile	87[90]	-	-
Ethers			
Anisole	94[97]	-	250[98]
Diethyl ether	96[99]	141[91]	438[90,98]
n-Butyl ether	101[99]	100[100]	447[90]
p-Dioxane	111[99]	-	362[96]
Ketones			
Acetophenone	101[101]	92[92]	-
Acetone	121[101]	107[92]	-
Amides			
N,N-Dimethylacetamide	147[97]	-	-
Amines			
Pyridine	213[101,102]	265[92,103,104]	-
Triethylamine	289[102]	295[91]	-

Of course, hydrogen bonding affects band intensities and bandwidths as well as frequencies. The measurements of the IR spectral properties of a variety of hydrogen bonding systems by Huggins and Pimentel[91] are informative and show that benzene, though quite a weak base, has behaviour which correlates very well with the criteria for well recognized hydrogen bonding systems. Additional data provided by CDCl$_3$-aromatic systems[105] shows that the characteristic intensification of v_s results from interaction with the aromatics.

Proton NMR studies offer ambiguous support for hydrogen bonding[106]. At first consideration, the data seems to oppose the hydrogen bond postulate, because the interaction with aromatics shifts the proton resonance of CHCl$_3$ and H$_2$O to higher fields. The hydrogen bond interaction usually shifts the resonance to lower fields. However, it seems quite definite that the anomalous shift has been correctly interpreted in terms of the unique diamagnetic anisotropy of the aromatic π-electrons. This interpretation inherently involves a specific orientation of the proton relative to the π-electrons. In addition, then, to explaining the unexpected direction of the NMR shift, this interpretation offers evidence that the proton position in the complex is appropriate for hydrogen bonding.

There are numerous types of data indicating association of some type which could be hydrogen bonding. Solubility data for HCl in aromatics and H$_2$O in benzene reveal association, as do freezing point diagrams of HCl with aromatics and of CHCl$_3$ with aromatics. The distribution coefficients listed in Table 5.2 suggest that benzene has greater base strength than CCl$_4$, as do IR studies of the association of *N*-ethylacetamide in various solvents[107]. Heats of mixing of CHCl$_3$ and aromatics are consistent with hydrogen bonding association. Tuomikoski has interpreted dipole measurements of pyrrole in benzene as indicating hydrogen bonding[108].

Table 5.2. Partition coefficients (k) of acetic acid in various organic solvent-water systems[85].

No.	Organic solvent				
of carbon atoms	Phenols	Alcohols	Esters	Ethers	Other
4	-	Butanol (26°C) **0.91**	Ethyl Acetate (18°C) **1.1**	Diethyl ether **2.0**	-
6	Phenol **0.71**	Cyclohexanol **1.12**	Butyl acetate **2.8**	Di*iso*propyl ether (23°C) **3.8**	Benzene (25°C) **25**
7	Cresol **1.04**	-	-	-	Toluene (25°C) **25**
8	-	Octanol (20°C) **2.04**	Hexyl acetate **2.8**	di-*n*-Butyl ether (23°C) **10**	CCl$_4$ **50**

$$k = \left(\frac{acid\ conc.\ (in\ water)}{acid\ conc.\ (in\ organic\ solvent)} \right)$$

t = 15°C, unless noted.

In conclusion, the data strongly supports the existence of complex formation between acids and aromatics acting as bases. Since there is ample evidence that the proton of the acid is specifically involved in the interaction, it can properly be called a hydrogen bond. An important implication of the conclusion that the base can be aromatic is that the base must be a good electron donor but not necessarily a highly electronegative group.

5.3 Modelling the Hydrogen Bond

To say that solvation plays an enormous role in determining properties of molecules is self-evident. In physical-organic chemistry the effect of varying the solvent on reaction rates and behaviour is well known[109]. In the terms of wood pitch, the problem is how and why the extractives adopt a particular interaction or conformation based simply on their aqueous surroundings and differential solvation effects between hydrophilic and

hydrophobic sidechains. Clearly the environment surrounding a molecule is very important. But can it be represented?

The five terms outlined in Chapter 4.2 describing molecular mechanics constitute the core of almost all molecular mechanics force fields; in some cases the entire energy function. In many situations, however, it is necessary for additional terms to be included.

For systems where hydrogen bonding is vital for stability, e.g. biological molecules, it has been common to include an additional, explicit hydrogen bond energy function to ensure correct geometries. In certain large molecule force fields this takes the form

$$E_{hb} = \sum \left(\frac{C_{ij}}{r_{ij}^{12}} \right) - \left(\frac{E_{ij}}{r_{ij}^{10}} \right) \qquad\qquad (5.1)$$

Other force fields attempt to simulate hydrogen bonds using just the van der Waals and electrostatic terms without the inclusion of a special attractive potential. This latter method could well be the more valid as, in an attempt to retain optimum hydrogen bonding geometries, the explicit function might give correct configurations at the expense of creating strain elsewhere.

The simplest way to take into account the influence of the solvent is to make the assumption that its major effect is to screen the electrostatic interactions in the solute. This can be accomplished by including the appropriate dielectric constant (water = 78.54 at 25°C) in the denominator of the electrostatic term in the molecular mechanics energy function. The calculation is then carried out on the isolated molecule. This method has clear limitations, the most obvious being that it takes no account of favourable solute-solute interactions. In aqueous solution there could be a number of hydrogen bonds. By neglecting the van der Waals component, contraction of molecular volume can result as the molecule seeks to maximize favourable interactions. In the presence of solvent this tendency is balanced by van der Waals interactions between solvent and solute.

5.4 Aims

The aims of this chapter are to confirm that the hydrogen bond can be successfully modelled using both molecular mechanics and semi empirical methods. The study is focussed on modelling intermolecular hydrogen bonds with aromatic systems. Dehydroabietic acid is the only aromatic extractive studied in this research and it has been observed that its characteristics such as interactive behaviour, solubility and pK_a are very different to the other non-aromatic extractives present including the other non-aromatic resin acids which are similar in structure without the aromaticity. Through this work we intend to show that dehydroabietic acid does interact differently through its electron rich aromatic ring rather than forming the dimer through the carboxylic head groups like the other extractives previously mentioned.

5.5 Experimental.

Summary of calculations

MM3 was used to undertake conformational searches of structures of each component as described in Chapter 2.3. Modelled conformers within a given energy window of the global minimum were selected and re-optimised using a molecular orbital calculation.

Calculation of electron density plots

A HF/STO-3G single point calculation was conducted on the MOPAC re-optimised conformers. Cube files for density and electrostatic potential (ESP) were generated from the SCF density using a Gaussian 03 utility program. The surface represents the electron density at an isovalue of 0.01 electrons while the colours are representative of the ESP at that point of the surface.

5.6   What is the Strength and Probability of a Hydrogen Bond Over an Aromatic With This Extractive System?

'Building blocks' trial

As the major hydrogen bonding components of the wood extractives are large carboxylic acids with more than 12 carbon atoms present it would be an understandable prediction that the only form of hydrogen bonding present would be that of the dimer form. When computational studies were undertaken to confirm this we found that this was true for all systems investigated except those involving the aromatic resin acid dehydroabietic acid. These results were unexpected and initially introduced some doubt into the modelling methods of the components interacting.

For reassurance of the modelling method and to confirm that the aromatic resin acid did interact differently to the non aromatic systems several model systems were studied as building blocks to prove, or disprove, the possibility of a hydrogen bond over aromatic systems where the dimer form of hydrogen bonding is also possible.

Four systems, or building blocks, were chosen for this study and are outlined in Table 5.3. These systems were chosen as they are representative of the extractive components that we are investigating.

Table 5.3. The four systems studied to investigate aromatic hydrogen bonding.

	System
A	Formic acid and benzene
B	Formic acid and tricyclic hydrocarbon
C	Stearic acid and tricyclic hydrocarbon
D	Stearic acid and dehydroabietic acid

The first system studied was that of formic acid and benzene (Figure 5.1). In this instance there is only one means of hydrogen bonding possible over the aromatic ring. Molecular modelling calculations indicate that this does occur.
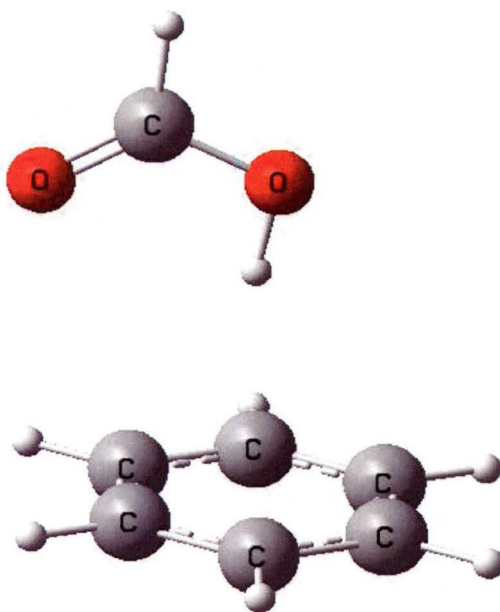
Figure 5.1. Interaction between formic acid and benzene (A)

This bond length was calculated using Pythagoras' theorem to find the bond length through the centre of the benzene ring (Figure 5.2). Where the bond length is equal to:

$$\left(\frac{1}{2}a\right)^2 + b^2 = c^2$$

$$\therefore\ b^2 = c^2 - \left(\frac{1}{2}a\right)^2 \tag{5.2}$$

$$\therefore\ b = \sqrt{c^2 - \left(\frac{1}{2}a\right)^2}$$
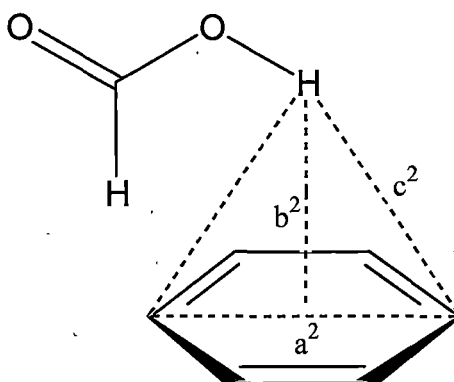
Figure 5.2. How the hydrogen bond length was calculated.

The lengths of the aromatic hydrogen bond lengths can be seen in Table 5.4. A shorter bond length indicates a stronger hydrogen bond and tighter complex. It is expected and observed that the hydrogen bond length will slightly increase when there is an increase in the complexity of the system. This is due to the increased steric hindrance and van der Waals forces between the increased number of atoms.

Table 5.4. Hydrogen bond length over aromatic ring for various systems.

System	Hydrogen bond length (Å)
A	2.158
B	2.763
C	3.108
D	3.276

After confirming that aromatic hydrogen bonding does occur over an aromatic system formic acid was modelled with a tricyclic system containing one aromatic ring, which is the backbone of dehydroabietic acid (Figure 5.3). The calculations confirmed that the addition of the two non aromatic rings had no effect on the position of the hydrogen bond and very little on the strength. This is due to formic acid being such a small molecule and not having many other atoms to interact with the protons of the tricyclic system.
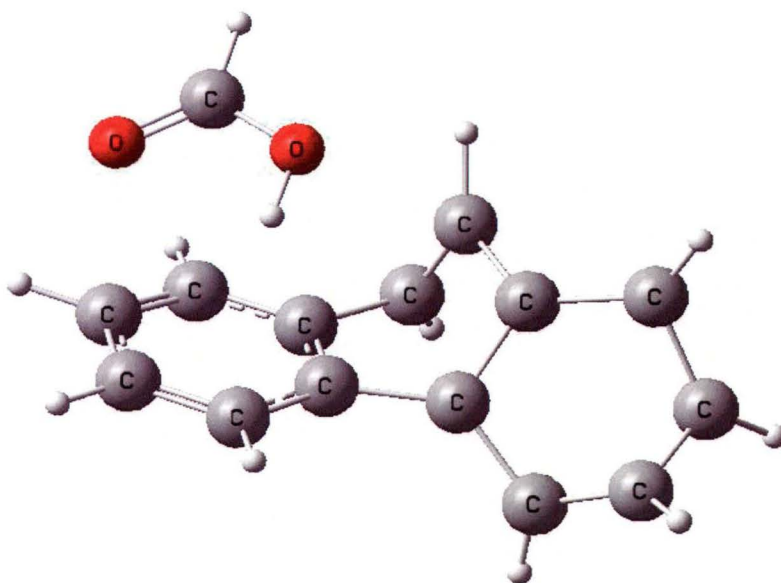
Figure 5.3. Interaction between formic acid and tricyclic system (B)

Increasing the length the alkyl chain of the formic acid to stearic acid did however have an effect on the length of the hydrogen bond (Figure 5.4). This is simply due to steric forces and the increased van der Waals forces present with the increased number of atoms.
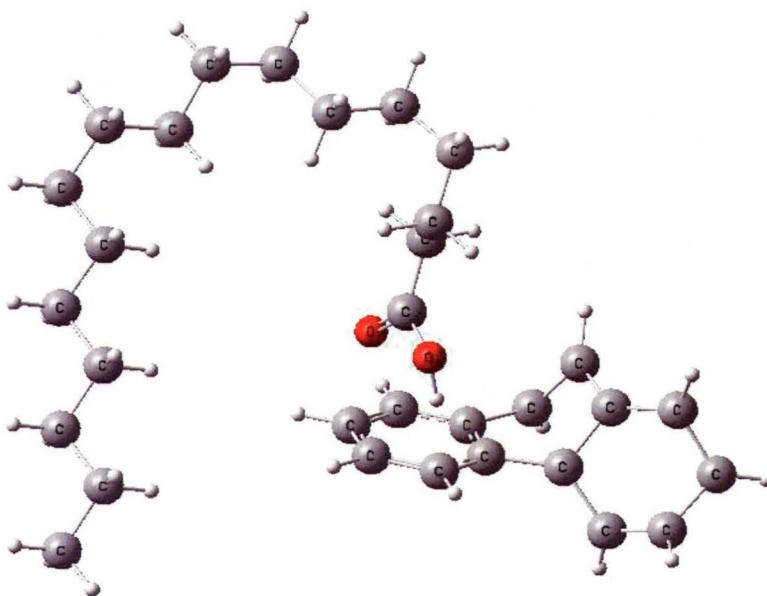
Figure 5.4. Interaction between stearic acid and tricyclic system (C) (N.B C3 is obstructed from view behind C4)

Conclusions from the first three trial complexes indicated that the bulk of the structures involved in the interactions did have an effect on the length, or strength, of the hydrogen bond but nevertheless there was still a hydrogen bond present in each system. However, the question still remains if the aromatic hydrogen bond would still prefer to form the dimer if a second carboxylic acid group was present on the tricyclic system. To investigate this the tricyclic skeleton of dehydroabietic acid including the acid group was modelled with formic acid again. The stabilization energy of the two different complexes, the dimer and the aromatic hydrogen bond, was observed (Table 5.5) and it was found that the aromatic hydrogen bond had a higher stabilisation energy with a relatively similar bond length to those present in the earlier studies.

Table 5.5. Stabilisation energies of the two different complexes possible with aromatic system (D).

System	Stabilisation Energy (kJ/mol)
Dimer	38.7
Aromatic hydrogen bond	53.2
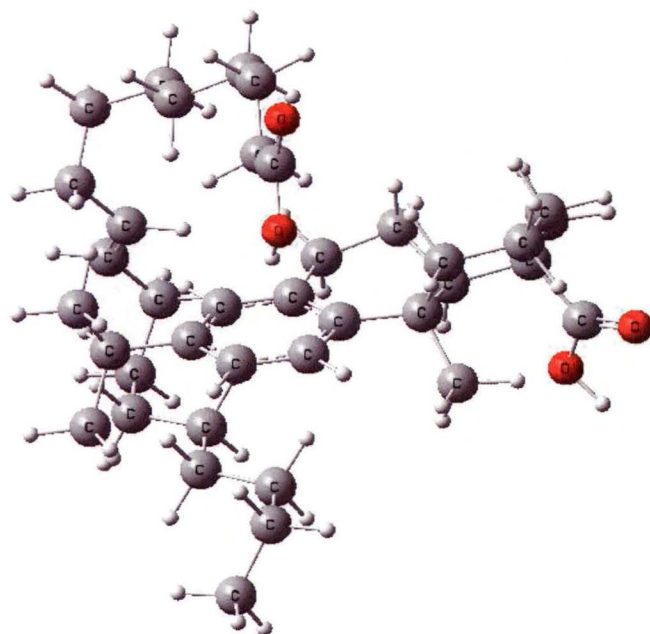
Aromatic hydrogen bond
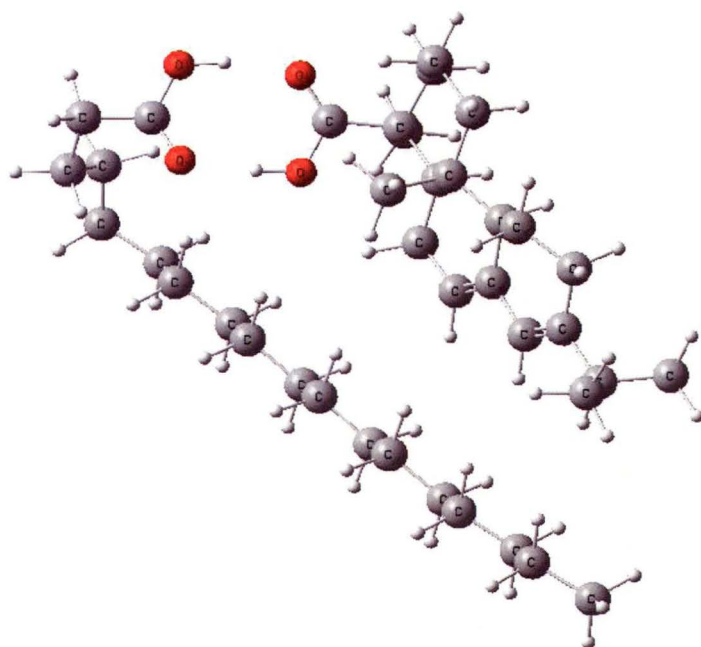
Dimer hydrogen bond

Figure 5.5. Two different complexes possible with the aromatic system. Fatty acid is stearic acid and resin acid is dehydroabietic acid. (D)

From these calculations of model systems we can be confident that a hydrogen bond does form over the aromatic ring in dehydroabietic acid in preference to the dimer form that is expected between two carboxylic acid head groups. As seen in Table 5.4 the length of the hydrogen bond does slightly increase with the increasing size of the complex but this is simply due to increased van der Waals forces present. This difference in interaction between the aromatic and non-aromatic resin acids may explain some difference in deposition of pitch molecules.

Electrostatic potential studies

Through using trial systems to understand the aromatic hydrogen bonding we were able to prove that this form of hydrogen bonding did exist but an improvement on this method would be if we could easily visualise the electrostatic potential of the individual molecules and also the electrostatic potentials of the complexes formed between the individual complexes. It has already been mentioned that a hydrogen bond requires a good electron donor or highly electronegative group present and these can be easily seen through electron density plots as bright red regions surrounding the molecules. Figure 5.6 shows the electron density map for dehydroabietic acid. It is clearly visible that there is a negative electrostatic potential surrounding both the carboxylic acid group and the aromatic ring supporting the fact that aromatics can form hydrogen bonds.
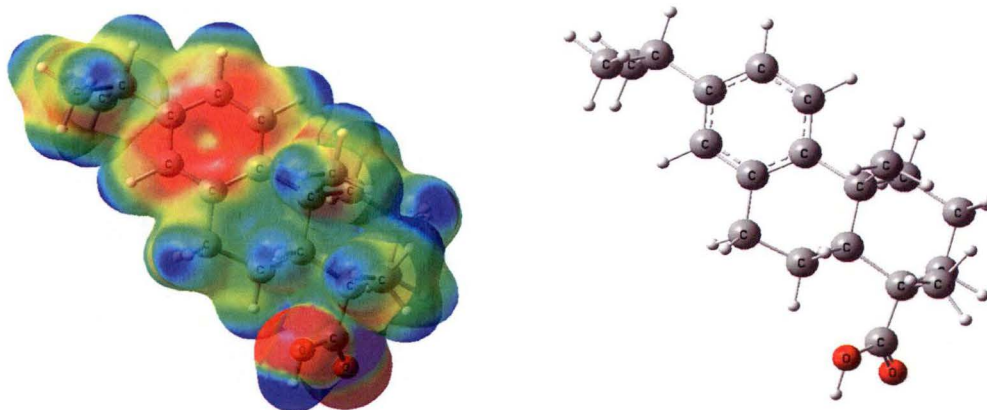
Figure 5.6. Electrostatic potential plot of dehydroabietic acid.

Figure 5.7 shows the electrostatic potential plot for oleic acid and as expected there are two regions with a negative electrostatic potential in the molecule, at the carboxylic acid head group and at the position of the double bond.
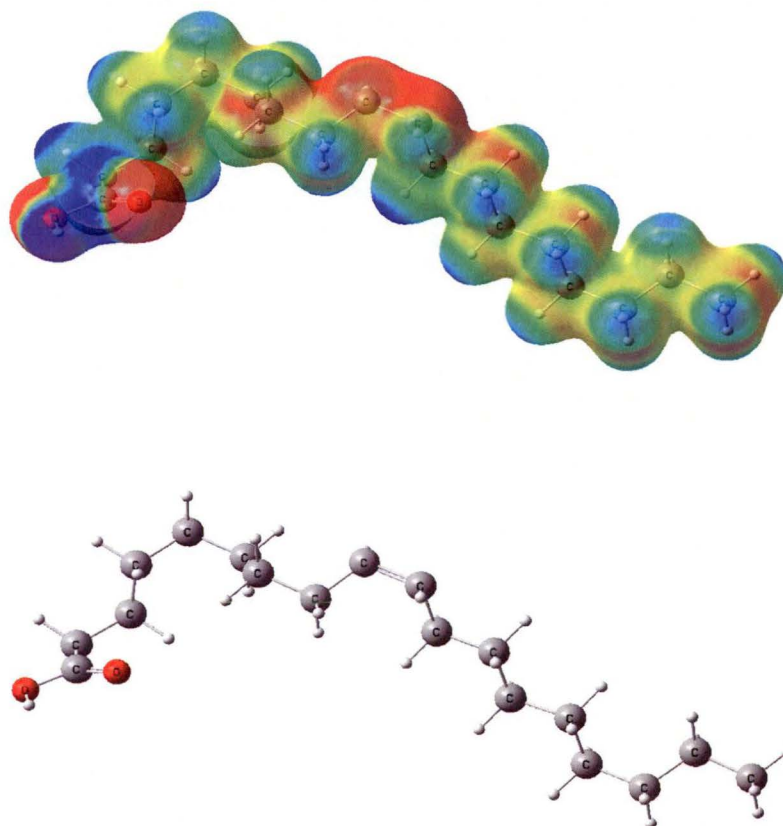
Figure 5.7. Electrostatic potential plot of oleic acid (C18:1).

When the two above extractives interact with each other there is a donation and acceptance of electrons over the aromatic ring where the hydrogen bonding is occurring (Figure 5.8). This can be seen through the loss of the red colour over the aromatic ring and the greater intensity of blue on the acidic proton of the stearic acid. The other region with a negative electrostatic potential is on the carboxylic acid group of the resin acid that is free to interact, hydrogen bond, with the surrounding water molecules of the aqueous atmosphere.
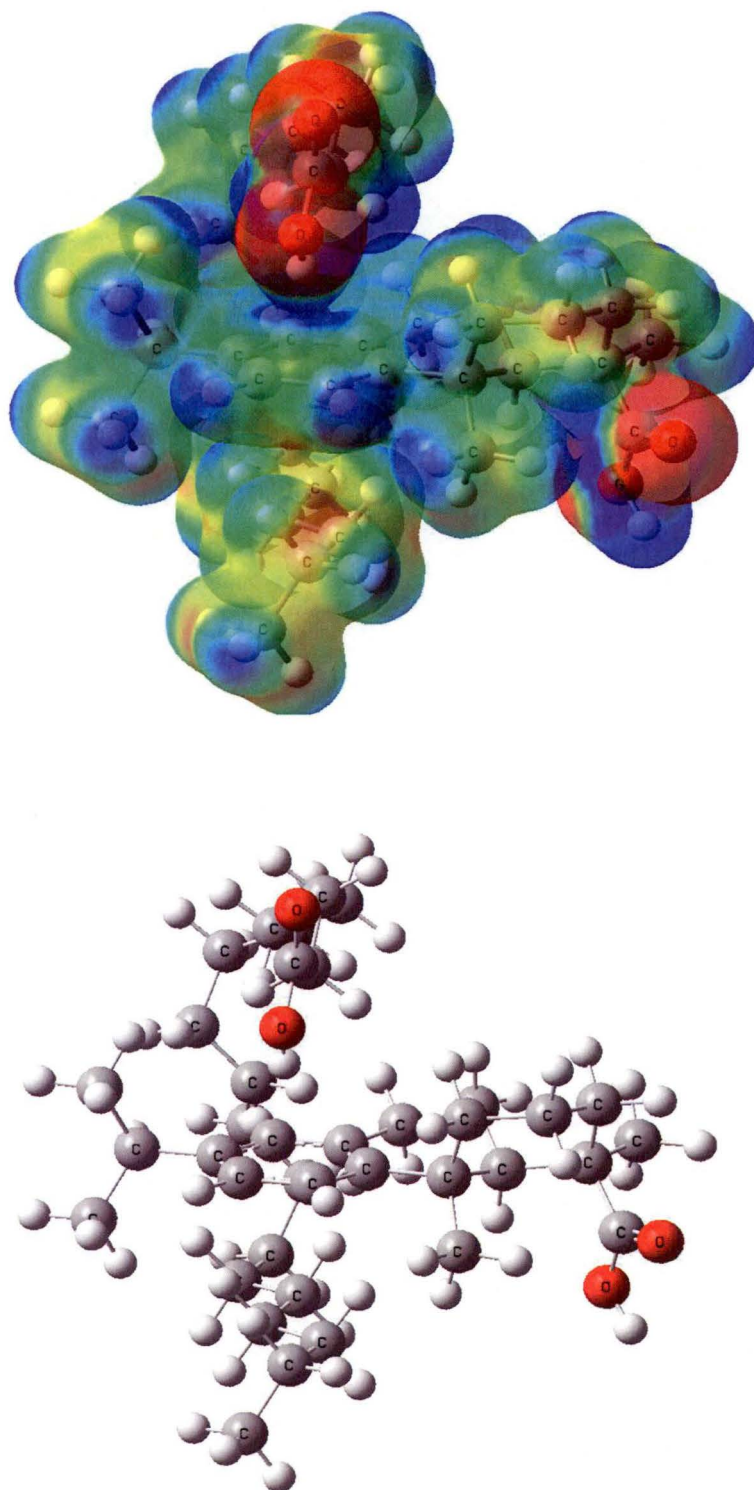
Figure 5.8. Electrostatic potential plot of the oleic acid/dehydroabietic acid complex.

5.7 Conclusions

Through the data presented in this chapter it can be concluded that the hydrogen bond can be modelled successfully with a molecular mechanics method. It was observed that there is an aromatic hydrogen bond involving dehydroabietic acid which explains its difference in characteristics and interactive behaviour between the aromatic and non-aromatic resin acids. Non-aromatic resin acids prefer to interact with other components through intermolecular dimer hydrogen bonding. It has also been shown that electron density plots are an informative method for observing hydrogen bonding between extractive components as it is visually informative.

6. INTERACTIONS OF COMPONENTS

6.1 Introduction and Aims

The three major lipophilic extractives in *Pinus radiata* are resin acids, fatty acids and triglycerides. To simplify the system, it was decided to focus the initial studies on a model composed of just two components. There are three possible binary combinations of these extractives;

> Resin acid and Fatty acid

> Resin acid and Triglyceride

> Fatty acid and Triglyceride

Within each extractive type there is a range of compounds of varying structure and size. To differentiate how the chemical structure may influence the interactions between each extractive type they were divided into sub-types. The fatty acids were divided into two groups, one involving the length of the alkyl chain and the second concerning the degrees of saturation. The saturation of the triglyceride was also investigated with two triglycerides of equal chain lengths of C18:0 and C18:3 being used. As previously mentioned there are three classes of resin acid and one resin acid was chosen from each of these classes.

Each combination was studied individually and gave surprising and informative results on the interactions that were occurring between the individual extractives. Deposition studies and molecular modelling experiments were carried out to investigate the interactions.

As well as the components studied in two-component systems they were combined in a three-component study with each of the three components interacting together. The methods employed in the two-component studies were also used in the three-component study.

6.2 Experimental

Deposition Studies

Colloidal Preparation - Dialysis

In order to study the deposition of pitch from its aqueous colloidal form to its agglomerated form additional laboratory steps were needed to be taken to ensure that the beginning, or pre-deposition, samples were of the aqueous colloidal form. Model pitch dispersions were prepared using a variation on methods developed by Sundberg[110] and Stack[3]. The model pitch dispersions were a mixture of a two of the three extractives found in *Pinus radiata*. The model solutions were prepared by quickly adding acetone mixtures of the fatty acid and resin acid, in a 1:1 molar ratio, to distilled water (250 mL) with stirring, which had been adjusted to pH 5 (HNO_3) and contained a slight electrolyte residual (0.001M KNO_3). The acetone was removed by dialysis using a cellulose membrane tubing (Sigma D-9402, 76mm wide, >12,000 MW) and a wash solution of distilled water, which had also been adjusted to pH 5 (HNO_3) and contained a slight electrolyte residual (0.001M KNO_3).

The model solutions were dialyzed for 24 hours, with the wash solution being changed every 30 minutes for the first 5 hours. The model solutions were then diluted to 400mL using fresh wash solution. The 400mL samples were then adjusted to pH 5.5 (KOH), which is representative of pH encountered in pulp mills, in order to study their depositional characteristics.

Deposition

Deposition was conducted by stirring 400mL of the dialyzed dispersions in PE jars using a paddle stirrer at 330 RPM (Cole Palmer, PE coated) as the shear force generator. All depositions were conducted over a two-hour period at a temperature of 50°C in a temperature bath.

Extraction

The model pitch components were extracted from the model pitch dispersions, before and after deposition, using the organic solvent, tertiary butyl methyl ether (*t*BME), Aldrich 99.8% purity HPLC grade [1634-04-4]). The pitch-containing *t*BME supernatant was pipetted off the top of centrifuged 5mL pitch dispersion aliquots to which 100μL of internal standard (pentadecanoic acid - Aldrich 99+% purity [1002-84-2], heptadecanoic acid (IS)– Sigma 99% purity [506-12-7], 1,3-dipalmitoyl-2-oleoyl-

glycerol – Sigma 99% purity [2190-25-2] and cholesteryl stearate – Sigma 99% purity [35602-69-8]) had been added. The pH was adjusted to 3.5 pH (HNO₃) as per Holmbom and Sjöström's procedure[111]. This was repeated in duplicate for each of the samples both before and after the deposition studies.

Derivatisation – Silylation

$$ R\!-\!OH \; + \; \underset{H_3C}{\overset{OSi(CH_3)_3}{\diagdown\diagup}}\!NSi(CH_3)_3 \quad \longrightarrow \quad R\!-\!OSi(CH_3)_3 \; + \; \underset{H_3C}{\overset{H}{\diagdown\diagup}}\!NSi(CH_3)_3 $$
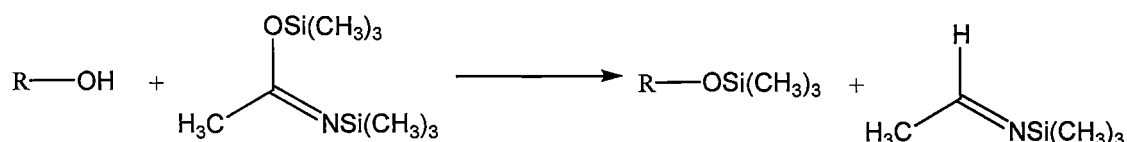
The samples were blown to dryness and silylated with 100µL of pyridine (Aldrich 99+% purity [110-86-1]) and 100µL of BSA (*N,O*-bis(trimethylsilyl)-acetamide, Sigma 95% purity GC grade [10416-59-8]) followed by heating at 20 minutes at 60°C. The GC vials were cooled to room temperature and then filled to 1mL with toluene (Aldrich 99.8% purity HPLC [108-88-3]).

GC analysis

The silylated samples were then analysed using programmed injection temperature on-column high temperature GC with a short column and a flame ionisation detector (PVT-HTGC-FID) as described in Chapter 2.1.

Data analysis

GC data was analysed using Varian Star 5.5 software package using heptadecanoic acid (Sigma 99% purity [506-12-7]) as the internal standard and 1,3-dipalmitoyl-2-oleoyl-glycerol – Sigma 99% purity [2190-25-2] as the recovery standard. FID correction factors were developed through the use of spikes (petroselinic acid – Sigma 99% purity [593-39-5], dehydroabietic acid - Helix Biotech [1740-19-8], Triolein – Sigma [122-32-7]) which were injected at various points throughout every sample run. Pentadecanoic acid (Aldrich 99+% [1002-84-2]) was used to verify that silylation did in fact occur. Each sample, pre and post deposition, was extracted, silylated and injected twice. The average of these values was used to calculate the concentrations of the solutions before and after deposition. The quantity of the individual components was determined by the difference between the pre and post deposition concentrations. The %TPD was equal to

the difference between the pre and post depositions total concentration (mg/L) divided
by the pre deposition and multiplied by 100%.

Experimental Error and Reproducibility of deposition and Analytical techniques

Each experimental data point reported through the deposition method was obtained from
the average of five experimental results obtained. This average value has been reported
in conjunction with the calculated standard deviation.

Theoretical Calculations

Summary of calculations

MM3 was used to undertake conformational searches of structures of each component as
described in Chapter 2.3. Modelled conformers within a given energy window of the
global minimum were selected and re-optimised using a molecular orbital calculation.

Synthesis of alkane for three-component synthesis

Grignard synthesis
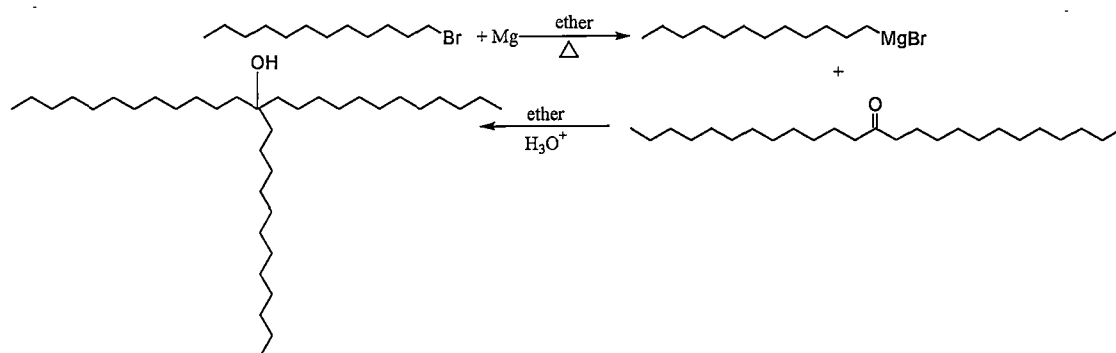
It was imperative that all equipment and reagents were absolutely dry. 1-
bromoundecane (4.7g, 20mmol) in dry diethyl ether under N_2 was added to a 5% molar
excess pre-washed magnesium (550mg, 21mmol) and gently heated for 10 minutes. The
reaction was then left to reflux for 24 hours to form the Grignard reagent.
13-pentacosanone (7.4g, 20mmol) was added dropwise to the Grignard reagent
(20mmol) dropwise maintaining a gentle reflux and allowed to stir for 24 hours. The
crude product was then quenched with hydrochloric acid (2mL, 1M) and extracted with
diethyl ether and evaporated to dryness to give the desired alcohol, 10.4g (97%).

υ_{max} = 3316.3(s), 2918.2(s), 2852.0(m), 2360.8(w), 1700.3(w), 1376.7(s), 1152.3(m), 720.5(w), 668.1(w).

Dehydration of alcohol
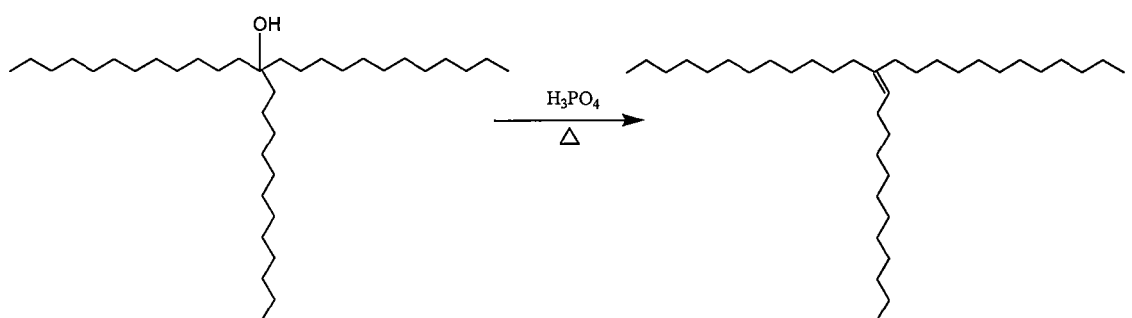
The crude alcohol (10.4g, 19.5mmol) in dry diethyl ether was refluxed with phosphoric acid (100mL) for 48 hours. The crude product was then quenched with cold water (5mL) and extracted with diethyl ether and evaporated to dryness to give the desired alkene, 10.0g (99%).

υ_{max} = 2917.6(s), 2852.9(m), 2358.5(w), 1709.6(w), 1647.4(s), 1378.5(s), 1148.2(m), 722.5(w), 666.1(w).

Reduction of alkene
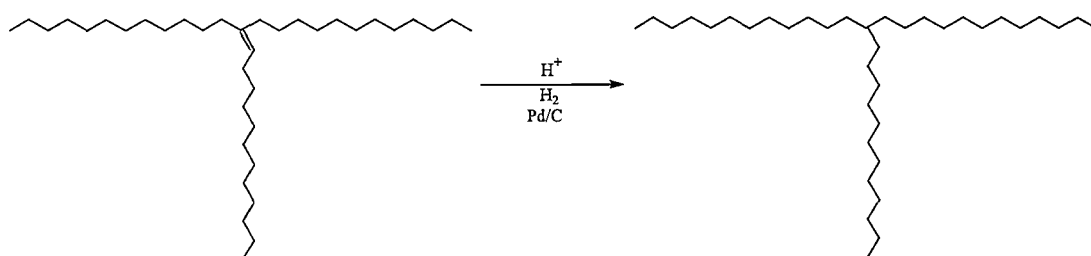
Hydrogen gas was allowed to pass over the crude alkene (10g, 19.4mmol) in diethyl ether with concentrated hydrochloric acid (10mL, 32%) and 5% palladium on carbon (10mg) as a catalyst. The crude product was then quenched with cold water (5mL) and extracted with diethyl ether and evaporated to dryness to give the desired alkane, 9.8g (98%).

υ_{max} = 2917.6(s), 2852.9(m), 2358.5(w), 1709.6(w), 1378.5(s), 1148.2(m), 722.5(w), 666.1(w).

6.3 Discussion of Methods.

Deposition Studies

To ensure that the concentration of the two components was high enough to guarantee interaction, it was decided to conduct these deposition studies above the cmc (see Chapter 3). It was found that the highest cmc for this study was that for lauric acid and was approximately 9 mg/L. All deposition work was therefore done above that concentration in the studies ranging from 12-15 mg/L. It was also questionable as to whether some of the fatty acids with a higher chain length such as arachidic acid (C20:0) would not form micelles but prefer to precipitate out of solution. It was found that although the less soluble fatty acids did precipitate out of solution at higher concentrations a cmc was found at approximately 3.5 mg/L.

Each experimental combination was dialysed to remove any solvent present and then placed in a sealed polyethylene (PE) jar in a 50°C water bath with constant agitation for two hours. The organic components were extracted before and after the agitation and concentrations were calculated using gas chromatography (GC). The amount of pitch deposited was then calculated using the difference between the two measurements (Figure 6.1). The above method was validated by extracting the deposit from the walls of the jar and running the sample on the GC and then comparing it to the amount calculated by difference (Table 6.1). The results in Table 6.1 indicate that the difference calculation was a valid method for determining the amount of pitch deposited.
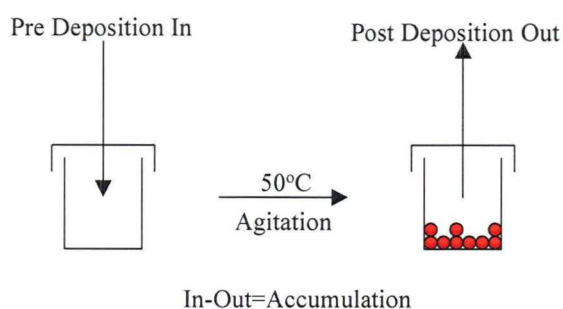
Figure 6.1. Schematic diagram of jar depositions.

Table 6.1. Method Validation Data. (Note: Resin acid used was dehydroabietic acid and Fatty acid was C18:0)

	Dispersion Concentration before Deposition (mg/L) (IN)	Dispersion Concentration after Deposition (mg/L) (OUT)	Accumulation (mg/L) (IN – OUT)	Concentration of Deposit on Walls (mg/L)
Resin Acid	19.6	15.5	4.1	4.1
	20.5	16.0	4.5	4.0
Fatty Acid	11.4	7.9	3.4	3.5
	13.3	9.4	3.9	3.2

Figure 6.2 shows the GC chromatogram of the model colloidal wood resin before deposition, after deposition and of the wall extracts. The results indicate that the pitch deposited is a result of physical interaction between the two components and that no other components were formed through chemical means.

Model colloidal wood resin before deposition
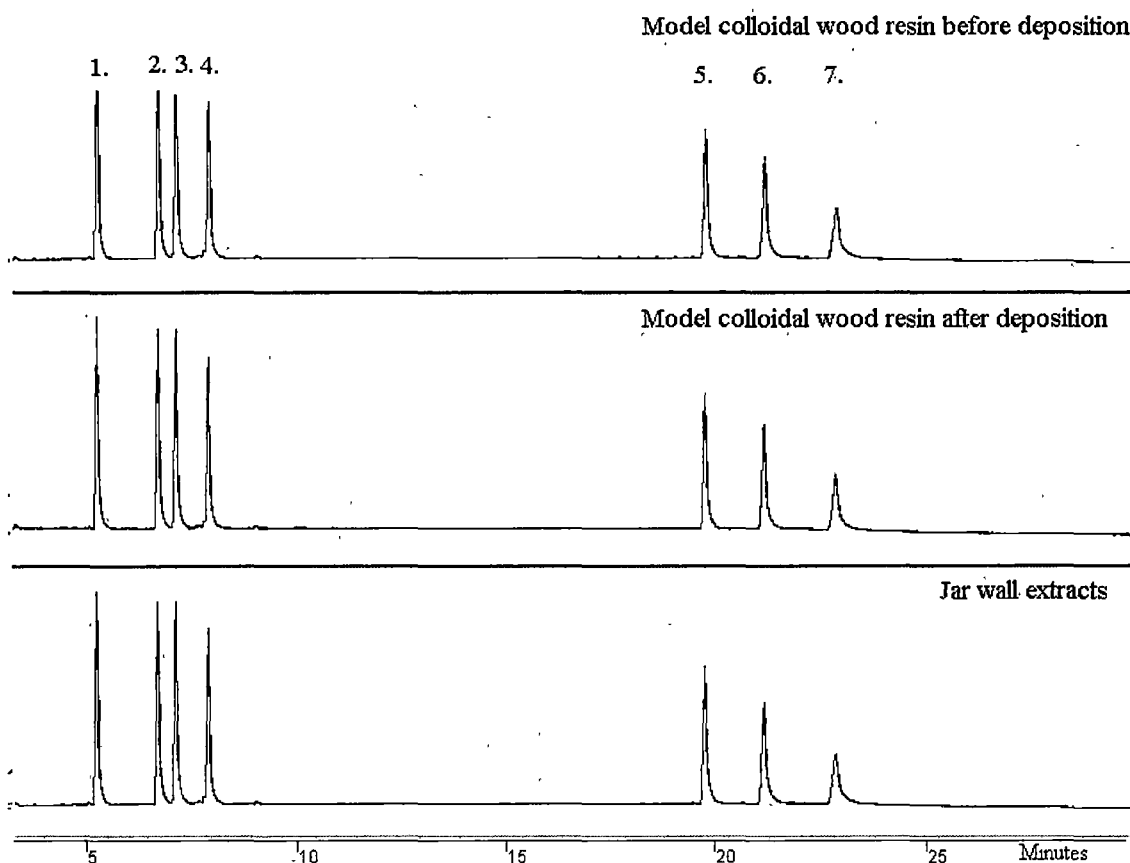
Figure 6.2. GC chromatogram of before deposition, after deposition and wall extracts.

1 *silyl ester of pentadecanoic acid (spike),* 2 *silyl ester of heptadecanoic acid (IS),* 3 *silyl ester of stearic acid,* 4 *silyl ester of dehydroabietic acid,* 5 *cholesteryl stearate (spike),* 6 *1,3-dipalmitoyl-2-oleoyl-glycerol (spike),* 7 *triolein (spike)*

Molecular Modelling

As explained in previous chapters, molecular modelling was used to investigate any interactions that were occurring and to gain a better understanding of any results obtained through the deposition studies. Molecular mechanics was used to investigate the stabilisation energies of the molecules and the method of hydrogen bonding. Many tests were conducted to test the reliability and confidence of the results obtained from the molecular modelling as mentioned previously (Chapters 4 and 5).

6.4 Two-Component Results

<u>Resin Acid and Fatty Acid Interactions</u>

The effects of the resin and fatty acids' chemical structure were investigated in order to determine how changing the chemical structure may affect pitch deposition and also the interaction between the components. Our initial hypothesis was that the deposition of pitch was related to the solubility (refer to Chapter 3) of the components but research soon indicated that this was simply not the case and that interactions were occurring between different molecular types. If the amount of pitch deposited was related to the solubility of the fatty acid, then an inverse relationship between solubility and deposition would be expected. To investigate if the above statement was correct a single component study was conducted with only the fatty acid placed into the jar. As expected an inverse relationship was seen (Figure 6.4) with the total pitch deposited (%TPD), or the precipitate, increasing with the increased chain length.
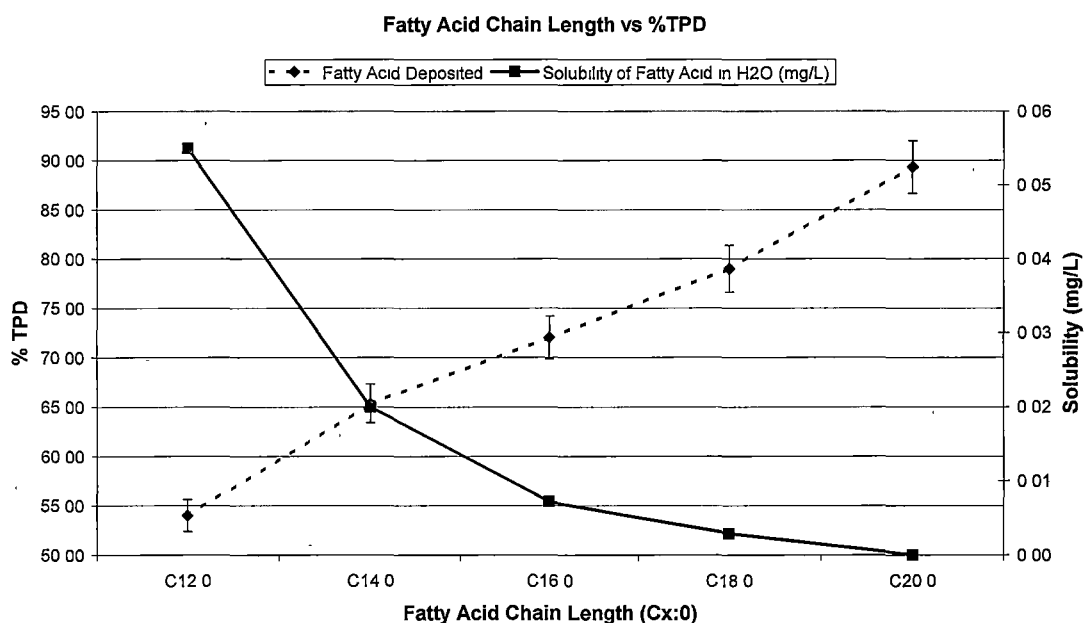
Figure 6.4. Effect of fatty acid chain length on amount fatty acid deposited. (Error bars indicate one standard deviation from the mean)

A two component system, namely that of a fatty acid and resin acid was then investigated. To help understand how each of these variables behaved with each class of resin acid, one was chosen from each class. The resin acid from each class was chosen based on purity, availability and cost and were dehydroabietic acid (*aromatic*), abietic

acid (*conjugated diene*) and isopimaric acid (*alkene*). When looking at the %TPD in a two-component system (Figure 6.5), it appeared to be directly proportional to the solubility of the fatty acid. The results indicate that deposition of the two-component system is not inversely related to the solubility of the fatty acids and that an interaction is occurring between the two components, affecting their stability in solution as well as their deposition. The results also show that the aromatic resin acid, dehydroabietic acid, had less deposition than the non-aromatic resin acids which may be either related to its solubility or suggesting that the aromatic resin acid may be interacting differently with the fatty acid. Molecular modelling will be able to give a better insight into how dehydroabietic acid interacts with fatty acids and will be explained later.
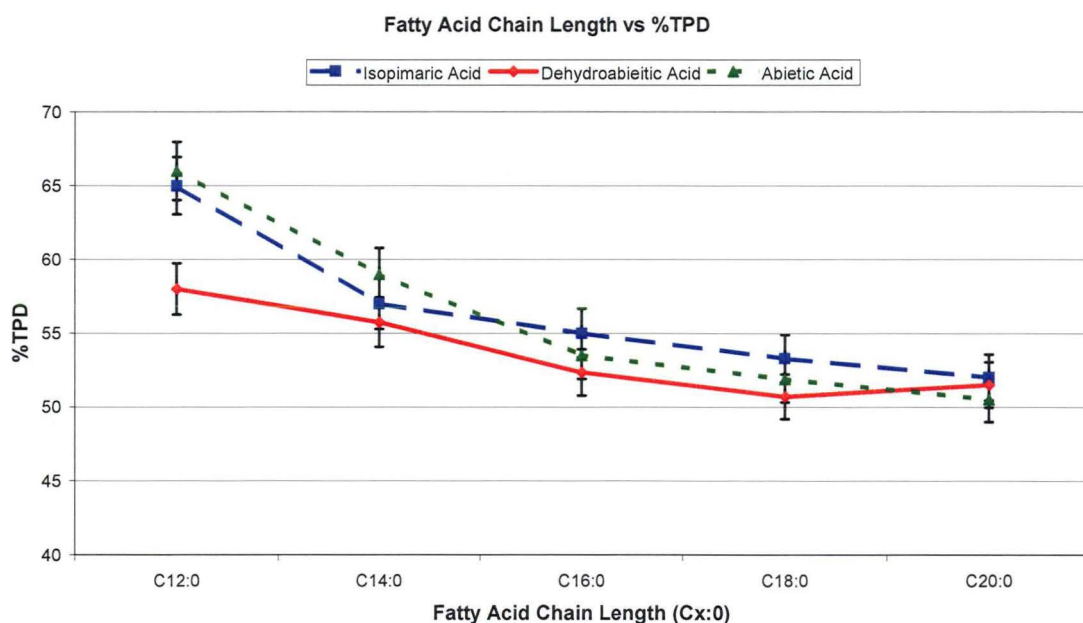
Figure 6.5. Effect of fatty acid chain length on total pitch deposited. Initial concentration of extractives equal to approximately 70mg/L

The effect, on pitch deposition, of the saturation of the fatty acid was also investigated (Figure 6.6). Mono-, di-, and tri-unsaturated fatty acids with 18 carbon atoms were chosen as they dominate the types of fatty acids found in woody plants[22]. These deposition results also indicated that an interaction was occurring between the resin acid and the fatty acid and that an increase in the number of double bonds in the fatty acid resulted in greater deposition. The results also show that, as with the fatty acid chain

length deposition study, the aromatic resin acid behaved differently to the non-aromatic resin acids.

Degrees of Unsaturation vs %TPD
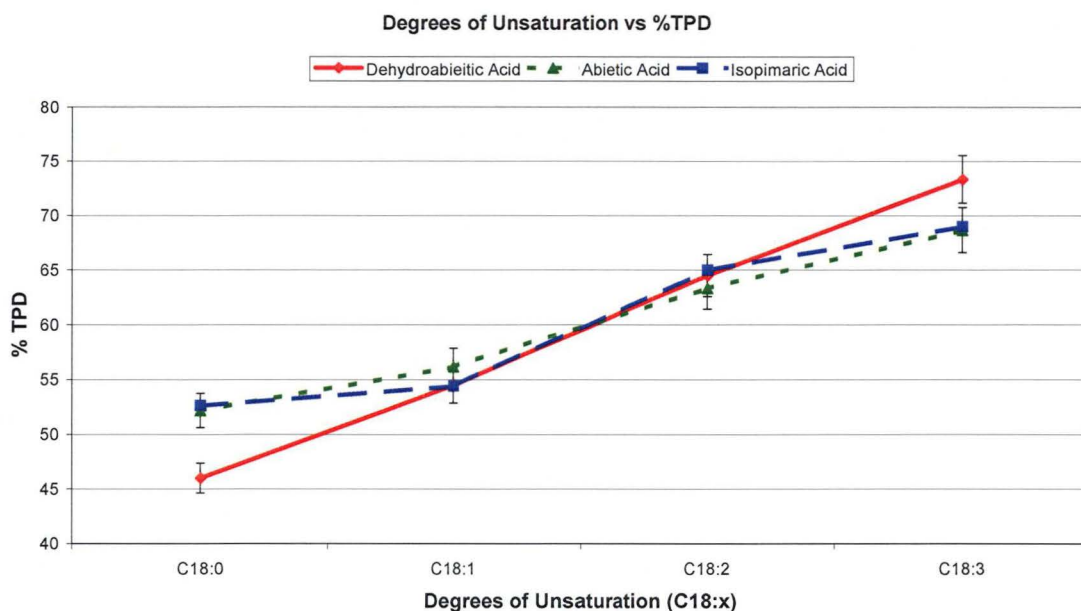
Figure 6.6. Effect of fatty acid saturation on total pitch deposited. Initial concentration of extractives equal to approximately 70mg/L

Although these results do indicate that an interaction is occurring between the resin acid and fatty acid it does not give any insight into how or where these interactions occur. To gain a better insight into the nature of the interactions occurring, computer molecular modelling was employed. Before we could model the interaction the molar ratio of the components in the deposit was required. By observing from the GC analysis results (Table 6.3) the amount of each individual component deposited it could be seen that the molar ratio of the pitch components deposited was 1:1. It can also be noted that this molar ratio of 1:1 was observed for all the fatty acids and resin acids investigated. This meant that when the deposits were modelled one molecule of each of the fatty acids and resin acids was required.

Table 6.3. Typical deposition results (varying fatty acids with dehydroabietic acid) indicating a 1:1 molar ratio.

Fatty Acid	Fatty Acid Deposited (mg)	Molecular Weight (g/mol)	Number of Moles (mmol)	Dehydroabietic Acid Deposited (mg)	Molecular Weight (g/mol)	Number of Moles (mmol)	Molar Ratio FA:RA
C12:0	4.2	200.3	0.02	6.5	300.4	0.02	**0.96**
C14:0	5.0	228.4	0.02	6.5	300.4	0.02	**1.01**
C16:0	5.5	256.4	0.02	6.5	300.4	0.02	**1.00**
C18:0	6.2	284.5	0.02	6.7	300.4	0.02	**0.98**
C20:0	6.5	312.5	0.02	6.3	300.4	0.02	**0.99**

As previously mentioned in Chapter 4 molecular mechanics (MM3) and molecular orbital calculations (PM3) were used to study the binding of the two components in the gaseous state. It should be noted that even though these calculations were conducted in the gaseous state they do give us an understanding of the interactions in an aqueous solution as the dielectric constant was used to partially simulate an aqueous environment. An extra parameter was created to increase the strength and probability of hydrogen bonding to occur at the acidic proton of the carboxylic acids as the parameter originally involved in these calculations was not recognising the occurrence of hydrogen bonds. Future work to complete this understanding could include looking at solvation effects and/or modelling the components with water molecules present in the calculation.

The MM3 method is used to calculate the different conformers that could occur and in most cases the lowest energy conformer was chosen and a molecular orbital calculation was performed. The only time that the lowest energy conformer was not chosen was for the homogenous dehydroabietic dimer as the lowest energy did not contain any hydrogen bonding. In this instance the second lowest conformer was chosen and this was accepted as the true dimer as it contained the desired hydrogen bonding and only differed in heat of formation by 2.17 kJ/mol from the lowest conformer.

Through the modelling of the complexes in a 1:1 ratio it was found that the formation of a dimer predominated over any other type of hydrogen bonding in the non-aromatic systems whereas the aromatic system preferred to form their hydrogen bonds over the electron rich aromatic ring (Figure 6.7). This difference in hydrogen bonding could help

to explain the differences in behaviour between the classes of resin acids in the
deposition studies.
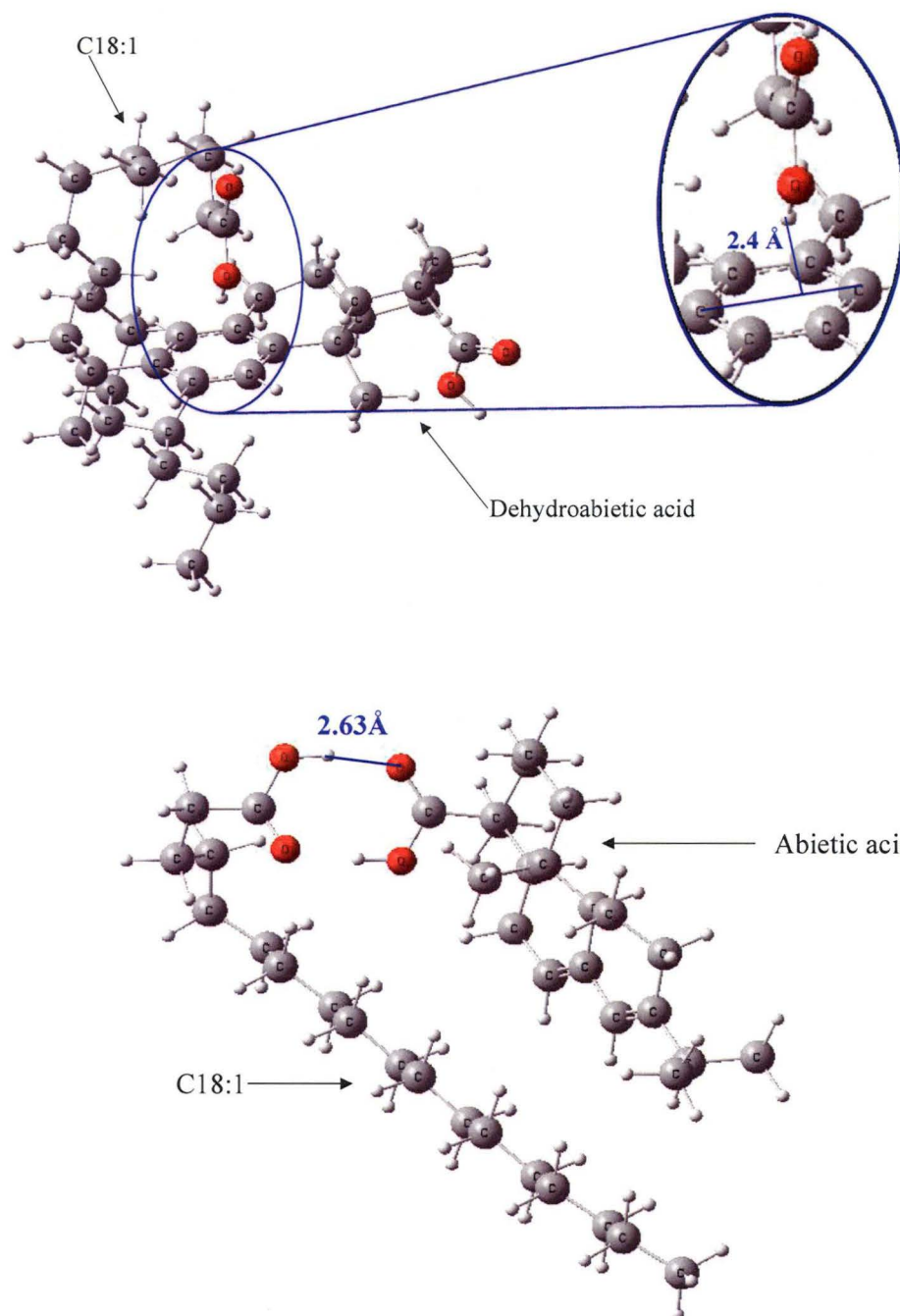
Figure 6.7. Position of hydrogen bonds in aromatic and non-aromatic systems.

The difference in ΔH_f between the MM3 and PM3 calculations was minimal with the
same trends followed for each method. These results can be seen in Table 4.2 with the

ΔH_f values for the single components. It was decided that the MM3 data would be used as it is a more accurate mathematical calculation for calculations we were requiring and more time economical.

Table 6.4a-d shows the ΔH_f values and stabilisation energies for the complex studies where the stabilisation energy is equal to:

$$SE = \left(\Delta H_f A + \Delta H_f B\right) - \Delta H_f Complex \qquad (6.1)$$

where A and B are two components which form a complex.

Table 6.4a. ΔH_f values of individual components.

Component	ΔH_f (kJmol^{-1})
C12:0	-644.6
C14:0	-690.3
C16:0	-750.3
C18:0	-778.6
C18:1	-689.5
C18:2	-577.2
C18:3	-497.4
C20:0	-819.8
Abietic acid	-477.0
Isopimaric acid	-476.4
Dehydroabietic acid	-484.7
Tristearin	-538.1
Trilinolenin	-486.4

Table 6.4b. Sum of ΔH$_f$ values (kJ/mol) for two components (A+B).

	C12:0	C14:0	C16:0	C18:0	C18:1	C18:2	C18:3	C20:0	Abietic	Iso§	Dehydro	TS†	TL‡
C12:0	-1289.2	-1334 9	-1394 9	-1423 2	-1334 1	-1221 7	-1142 0	-1464 4	-1121 6	-1120 9	-1129 3	-1182 7	-1130 9
C14:0	-1334 9	-1380 6	-1440 6	-1469.0	-1379 8	-1267.5	-1187 7	-1510 1	-1167.4	-1166 7	-1175 0	-1228 4	-1176 7
C16:0	-1394 9	-1440.6	-1500 5	-1528 9	-1439 7	-1327 4	-1247.6	-1570 1	-1227 3	-1226 6	-1235 0	-1288 4	-1236 6
C18:0	-1423 2	-1469 0	-1528.9	-1557 3	-1468.1	-1355 8	-1276 0	-1598 4	-1255 7	-1255.0	-1263.4	-1316 8	-1265 0
C18:1	-1334 1	-1379 8	-1439 7	-1468 1	-1378 9	-1266 6	-1186 8	-1509.3	-1166 5	-1165 8	-1174 2	-1227.6	-1175.8
C18:2	-1221 7	-1267 5	-1327 4	-1355.8	-1266 6	-1154.3	-1074 5	-1396 9	-1054.2	-1053 5	-1061 9	-1115 3	-1063 5
C18:3	-1142.0	-1187.7	-1247 6	-1276 0	-1186.8	-1074.5	-994 7	-1317 2	-974.4	-973 7	-982 1	-1035 5	-983 7
C20:0	-1464 4	-1510 1	-1570 1	-1598 4	-1509.3	-1396 9	-1317.2	-1639 6	-1296 8	-1296.1	-1304 5	-1357 9	-1306.2
Abietic	-1121.6	-1167 4	-1227.3	-1255 7	-1166 5	-1054 2	-974.4	-1296.8	-954 1	-953 4	-961 8	-1015.2	-963 4
Iso§	-1120.9	-1166 7	-1226 6	-1255.0	-1165 8	-1053 5	-973 7	-1296 1	-953 4	-952 7	-961 1	-1014 5	-962.7
Dehydro	-1129 3	-1175.0	-1235 0	-1263 4	-1174 2	-1061.9	-982 1	-1304 5	-961 8	-961 1	-969 5	-1022 8	-971.1
TS†	-1182 7	-1228 4	-1288.4	-1316 8	-1227.6	-1115 3	-1035 5	-1357.9	-1015 2	-1014 5	-1022.8	-1076.2	-1024 5
TL‡	-1130.9	-1176 7	-1236.6	-1265 0	-1175 8	-1063 5	-983.7	-1306.2	-963 4	-962.7	-971 1	-1024.5	-972 7

§ isopimaric acid
† tristearin
‡ trilinolenin

Table 6.4c. ΔH_f values (kJ/mol) for the complexes formed from the two components

	C12:0	C14:0	C16:0	C18:0	C18:1	C18:2	C18:3	C20:0	Abietic	Iso§	Dehydro	TS†	TL‡
C12:0	-1237 3	-	-	-	-	-	-	-	-1225 4	-1226 2	-1220 7	-1219 2	-1173 7
C14:0	-	-1265 4	-	-	-	-	-	-	-1256 4	-1256 6	-1248 7	-1262 7	-1224 3
C16:0	-	-	-1289 8	-	-	-	-	-	-1307 3	-1305.4	-1302 9	-1326 2	-1285 5
C18:0	-	-	-	-1302 4	-	-	-	-	-1321 6	-1309 1	-1316 5	-1359 8	-1318 6
C18:1	-	-	-	-	-1273 1	-	-	-	-1245 0	-1250 4	-1259 3	-1268 3	-1227 2
C18:2	-	-	-	-	-	-1126 2	-	-	-1137 2	-1142 4	-1149 3	-1155 5	-1117 7
C18:3	-	-	-	-	-	-	-1016 5	-	-1067 4	-1070 9	-1076 5	-1077 5	-1038 6
C20:0	-	-	-	-	-	-	-	-1316 5	-1344 2	-1342 5	-1343 3	-1398 3	-1362 4
Abietic	-1225 4	-1256 4	-1307 3	-1321 6	-1245 0	-1137 2	-1067 4	-1344 2	-1001 8	-	-	-1056 7	-999 6
Iso§	-1226 2	-1256 6	-1305 4	-1309 1	-1250 4	-1142 4	-1070 9	-1342 5	-	-1006 7	-	-1058 2	-1000 7
Dehydro	-1220 7	-1248 7	-1302 9	-1316 5	-1259 3	-1149 3	-1076 5	-1343 3	-	-	-1010 7	-1064 2	-1009 6
TS†	-1219 2	-1262 7	-1326 2	-1359 8	-1268 3	-1155 5	-1077 5	-1398 3	-1056 7	-1058 2	-1064 2	-	-
TL‡	-1173 7	-1224 3	-1285.5	-1318.6	-1227.2	-1117 7	-1038.6	-1362.4	-999.6	-1000 7	-1009 6	-	-

§ isopimaric acid
† tristearin
‡ trilinolenin

Table 6.4d. Stabilisation energies (kJ/mol) of the two component systems $SE = (\Delta H_f A + \Delta H_f B) - \Delta H_f Complex$.

	C12:0	C14:0	C16:0	C18:0	C18:1	C18:2	C18:3	C20:0	Abietic	Iso§	Dehydro	TS†	TL‡
C12:0	-51 9	-	-	-	-	-	-	-	103 8	105 3	91 4	36 5	42 7
C14:0	-	-115 3	-	-	-	-	-	-	89 0	90 0	73 6	34 3	47 7
C16:0	-	-	-210 7	-	-	-	-	-	80 0	78 7	68 0	37 8	48 9
C18:0	-	-	-	-254 9	-	-	-	-	66 0	54 1	53 2	43 0	53 6
C18:1	-	-	-	-	-105 8	-	-	-	80 5	84 6	85 1	40 8	51 4
C18:2	-	-	-	-	-	-28 1	-	-	83 0	88 9	87 4	40 2	54 2
C18:3	-	-	-	-	-	-	21.7	-	92 9	97 2	94 4	42 0	54 9
C20:0	-	-	-	-	-	-	-	19 7	47 3	46 4	38 7	40 4	56 2
Abietic	103 8	89 0	80 0	66 0	80 5	83 0	92 9	47 3	47 7	-	-	41 5	36 2
Iso§	105 3	89 0	78 7	54 1	84 6	88 9	97 2	46 4	-	54 0	-	43 7	38 0
Dehydro	91 4	73 6	68 0	53 2	85 1	87 4	94 4	38 7	-	-	41 2	41 4	38 5
TS†	36 5	34 3	37 8	43 0	40 8	40 2	42 0	40 4	41 5	43 7	41 4	-	-
TL‡	42 7	47 7	48 9	53 6	51 4	54 2	54 9	56 2	36.2	38 0	38 5		-

§ isopimaric acid
† tristearin
‡ trilinolenin

The stabilisation energies and %TPD of the 1:1 complexes were plotted as a function of fatty acid chain length (Figure 6.9) and degrees of saturation (Figure 6.10) with different resin acids. Figure 6.9 shows that as the fatty acid chain length increases, deposition decreases and the stabilisation energy of the complex also decreases. Likewise Figure 6.10 shows that as the degree of unsaturation increases, deposition and the stabilisation energy both increase.
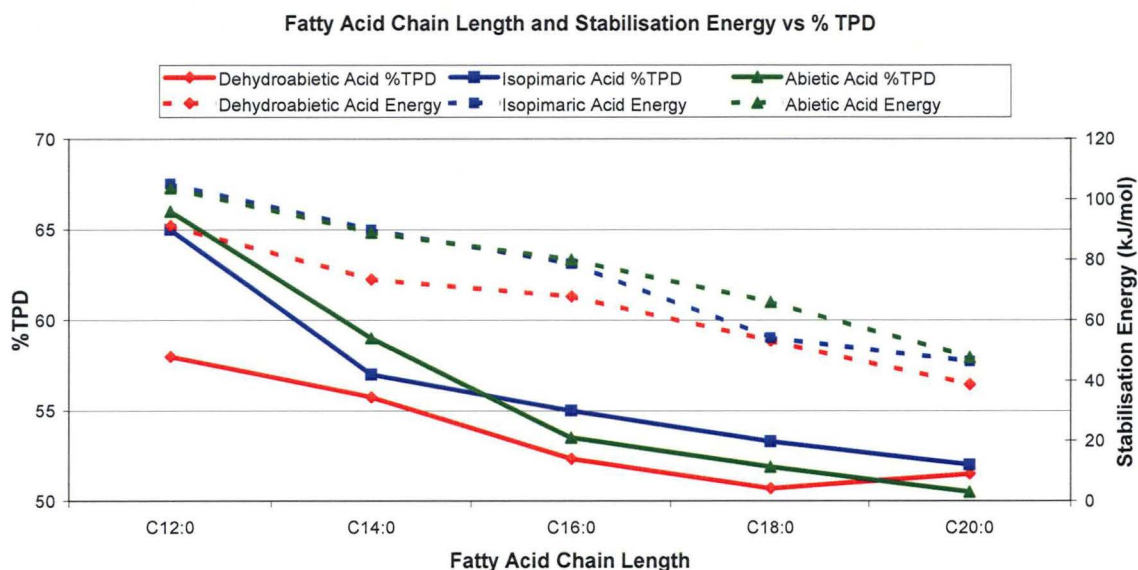
Figure 6.9. Effect of fatty acid chain length on stabilisation energy and deposition. Initial concentration of extractives equal to approximately 70mg/L

%TPD and Stabilisation Energies vs Saturation Levels of C18:x
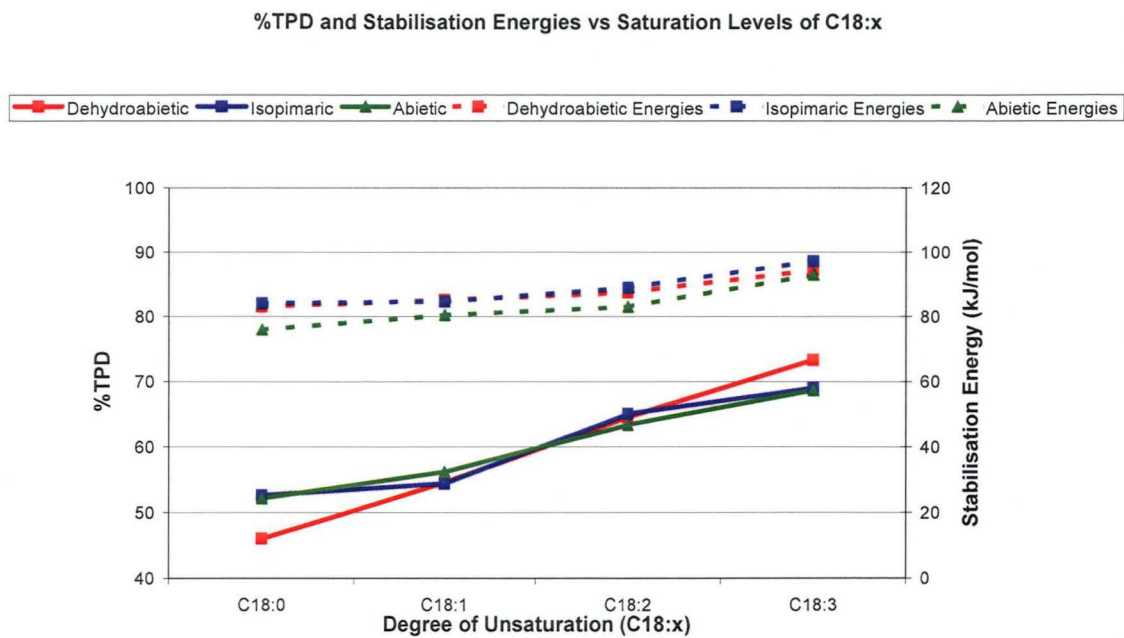
Figure 6.10. Effect of fatty acid saturation on stabilisation energy and deposition.

If the pitch is preferentially depositing in a 1:1 ratio based on the fatty acid and resin acid molar ratios, then the stabilisation energies of the most stable complex must be less than that of the fatty acids and resin acids forming a complex together in a homogenous relationship. This can be seen in Table 6.5 with the stabilisation energies of the heterogenous complexes being higher than that of the homogenous complexes.

Table 6.5. Stabilisation energies for homo-and heterogenous complexes.

Complex	Stabilisation Energy (kJ/mol)
Dehydroabietic acid/Dehydroabietic acid	41.2
C18:0/C18:0	-254.9
Dehydroabietic acid/C18:0	53.2
Abietic acid/Abietic acid	47.7
Abietic acid/C18:0	76.0

The results from both the deposition and modelling studies indicated that there was an interaction occurring between the fatty acid and resin acid. When referring to the molecular modelling results, it must be understood what the stabilisation energy results indicate. A higher stabilisation energy indicates a stronger interaction between the two components and hence, stronger hydrogen bonding between them.

This increase in hydrogen bond strength reduces the component-water interaction which in turn affects the solubility of the complex in water.

If we consider the interaction between the resin acid and the fatty acids of varying chain lengths we notice that as the chain length increases the stabilisation energy of the system decreases. This decrease in energy indicates that the hydrogen bond length is greater between the two components which increases the potential for interaction with water and hence its solubility. In addition, when we increased the number of double bonds in the system, the complex became tighter and the hydrogen bond distance decreased (Table 6.6) causing less interaction with the aqueous environment and lowering its solubility except for C18:2.

Table 6.6. Intermolecular distances for dehydroabietic acid and fatty acid C18:x.

	C18:0	C18:1	C18:2	C18:3
Distance between two molecules at point of unsaturation in fatty acid	4.758Å	4.536Å	4.121Å	3.920Å
Hydrogen bond length	3.276	2.400Å	2.417Å	2.236Å

The deposition results also indicated in both studies that the aromatic resin acid complex had lower deposition showing that it was more soluble in an aqueous environment than the non-aromatic complexes. This is reinforced by observing the computer model of this complex as it has a lower stabilisation energy and therefore weaker hydrogen bonds with more hydrophilic regions exposed to the surrounding environment due to the fact that the interaction between the fatty acid and resin acid is occurring over the aromatic ring.

The modelling results have shown that the hydrophilic and hydrophobic ends of the fatty acid and resin acid molecules could be oriented to assist in solubility with the aromatic systems having an increased amount of hydrophilic regions available due to the position of the hydrogen bond over the aromatic ring. This could also be seen in the modelling results of the dehydroabietic acid dimer (Figure 6.11) and this provides an explanation as to its increased solubility over the non-aromatic resin acids.
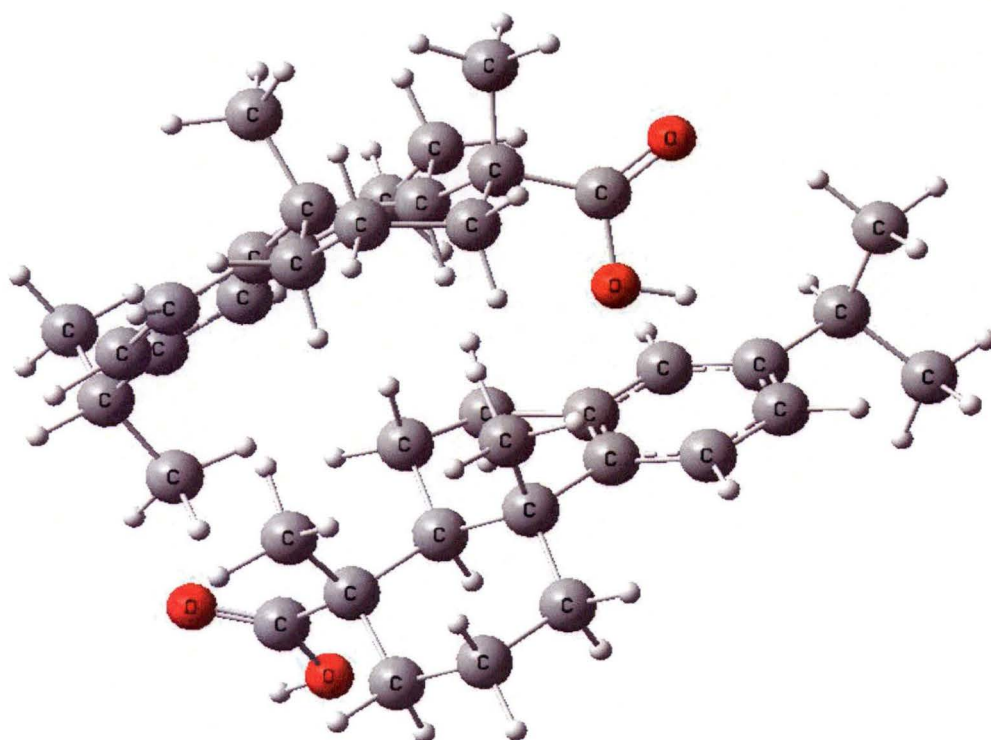
Figure 6.11. Dehydroabietic acid dimer in an aqueous environment.

Resin acid and Triglyceride Interactions

The interesting and promising results indicating that there is an interaction occurring between the fatty acid and resin acid led to an investigation on how the triglycerides behave in a two-component system. Two separate triglycerides were studied. As carbon chains of 18 carbon atoms are the most prevalent in wood plants,[22] two triglycerides with three identical chains of 18 carbons each were chosen. The variable studied was the degree of saturation of the identical chains in each triglyceride, with two being chosen, tristearin with three saturated chains and trilinolenin, which has three chains with three double bonds present. The solubility and physical state of these two triglycerides are quite different in behaviour, with tristearin being more insoluble than trilinolenin, with the former being a solid at room temperature, whereas trilinolenin is a viscous oil.

The first interaction studied was that of the two triglycerides with the three resin acids previously used in the other study. The deposition studies of these results indicated that the structure of the resin acid had very little, or no, effect on the amount of pitch deposited and that the amount of pitch deposited seemed to be affected by the solubility of the triglyceride (Figure 6.12).

%TPD and Stabilisation Energy Comparisons
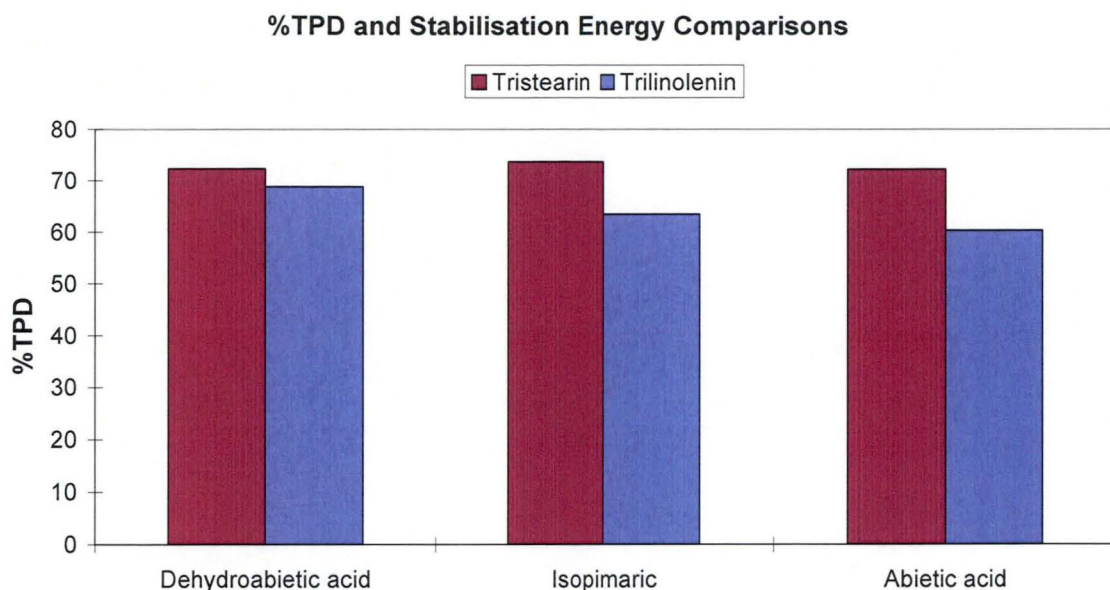
Figure 6.12. Deposition results of interactions between triglycerides and resin acids. Initial concentration of extractives equal to approximately 70mg/L

This fact that the %TPD was related to the solubility of the triglyceride rather than through any interaction is of importance as it indicates that any interaction between the components is not as major an influence on the pitch colloid structure but rather the solubility of the individual components. The molar ratio of the deposit was also observed through the GC analysis (Table 6.7). As expected the molar ratio of triglyceride to resin acid was 1:3. Computer molecular modelling of the resin acid and triglyceride complex was undertaken using a 3:1 ratio of resin acid:triglyceride. The calculations indicated that each resin acid was interacting with the triglyceride via a single hydrogen bond from the acidic proton of the resin acid to the carbonyl oxygen of the triglyceride.

Table 6.7. Typical deposition results (varying resin acids with tristearin) indicating a 3:1 molar ratio.

Resin acid	Resin Acid deposited (mg)	Molecular Weight (g/mol)	Number of moles (mmol)	Tristearin deposited (mg)	Molecular weight (g/mol)	Number of moles (mmol)	Molar ratio RA:Tri
Dehydro	6.6	300.4	0.02	60.9	891.5	0.07	**3.13**
Iso	6.4	302.4	0.02	55.1	891.5	0.06	**2.93**
Abietic	6.4	302.4	0.02	62.1	891.5	0.07	**3.28**

The length of the hydrogen bond was found to be much longer than the hydrogen bond between the resin acid and fatty acid (see Table 6.6). This increase in hydrogen bond length and the fact that there is only a single hydrogen bond indicates that the interaction between the two components is not as strong as the interaction between the fatty acid and resin acid as previously mentioned. Figure 6.13 indicates the stabilisation energies of the complexes formed compared with the deposition results.
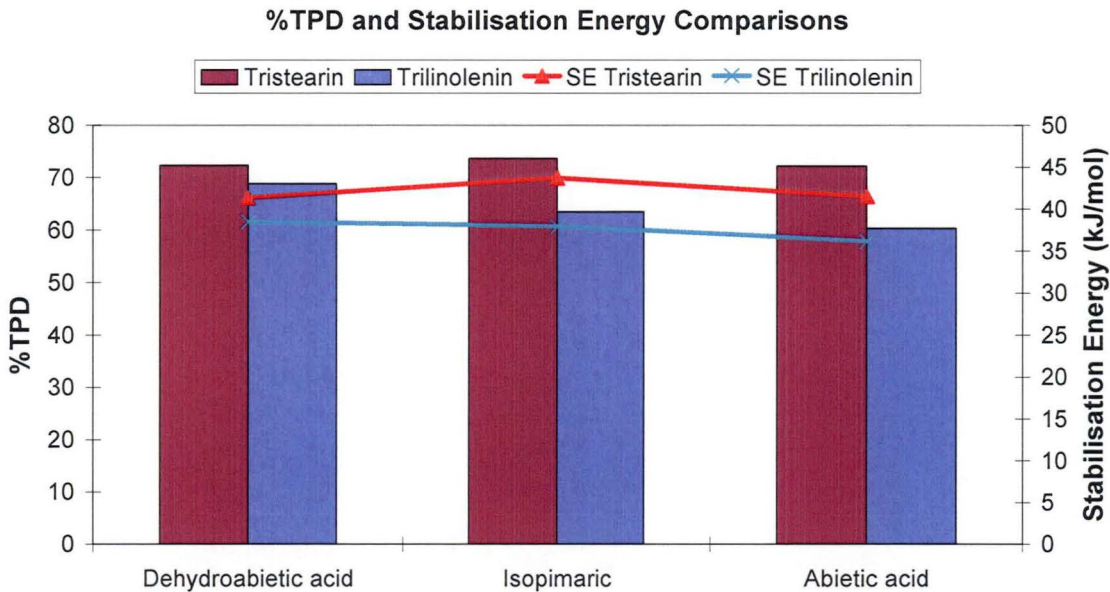
Figure 6.13. Deposition and stabilisation energies of interactions between resin acids and triglycerides. Initial concentration of extractives equal to approximately 70mg/L

Again a correlation could be seen between the %TPD and the SE with an increase in SE leading to an increase in %TPD. It should be noted though that the SE's of the triglyceride complexes are considerably smaller than those of the resin acid:fatty acid complexes. Also the variation in SE between the complexes is significantly smaller than that of previous results indicating that the stability of the colloidal deposit may not be playing a significant role in the deposition of the components.

Fatty Acid and Triglyceride Interactions

With the results of the resin acids and triglycerides indicating that the solubility of the triglyceride may be playing a more important role in the deposition, the interactions of the triglyceride with both saturated and unsaturated fatty acids were also investigated. Figure 6.14 shows both the deposition and the SE results for the two triglycerides and fatty acids with varying chain length.

Average %TPD vs Chain Length for Triglycerides

Figure 6.14. Deposition and stabilisation energies of interactions between fatty acids of varying chain length and triglycerides. Initial concentration of extractives equal to approximately 70mg/L

The varying chain length did not appear to have any affect on the amount of %TPD. Again the deposition was affected by the solubility of the triglyceride with the SE again relatively small compared to those in the resin acid:fatty acid study. The molar ratios were again calculated through the GC analysis and again there was a 3:1 molar

ratio between the fatty acid (both saturated and unsaturated) and triglyceride as seen in Table 6.8.

Table 6.8. Typical deposition results (varying fatty acids with tristearin) indicating a 3:1 molar ratio.

Fatty Acid	Fatty Acid Deposited (mg)	Molecular Weight (g/mol)	Number of Moles (mmol)	Tristearin Deposited (mg)	Molecular Weight (g/mol)	Number of Moles (mmol)	Molar Ratio FA:Tri
C12:0	4.3	200.3	0.022	62.9	981.5	0.071	**3.23**
C14:0	5.1	228.4	0.022	56.9	891.5	0.064	**2.86**
C16:0	5.9	256.4	0.023	65.3	891.5	0.073	**3.20**
C18:0	6.2	284.5	0.022	62.3	891.5	0.070	**3.19**
C18:1	6.4	282.5	0.023	58.5	891.5	0.066	**2.92**
C18:2	6.3	280.5	0.023	55.8	891.5	0.063	**2.78**
C18:3	6.3	278.4	0.023	66.3	891.5	0.074	**3.30**
C20:0	7.0	312.5	0.022	57.6	891.5	0.065	**2.89**

As observed with the resin acid:triglyceride interactions the molecular modelling calculations for the fatty acids and triglycerides showed there was a single hydrogen bond joining each of the fatty acids with the triglycerides through the acidic proton of the fatty acid. Although the hydrogen bond length of the fatty acid:triglyceride interactions is slightly shorter than the resin acid:triglyceride bond length it is still significantly longer than those of the resin acid:fatty acid interactions. Table 6.9 shows these hydrogen bond lengths for interactions between both tristearin and trilinolenin with dehydroabietic acid, abietic acid and both stearic and linoleic acid.

Table 6.9. Hydrogen bond lengths (Å) between examples of all three classes of extractives studied in the two component studies.

	Tristearin	Trilinolenin	Dehydro	Abietic	Stearic	Linoleic
Tristearin	-	-	4.336	4.619	4.216	4.298
Trilinolenin	-	-	4.872	4.976	4.523	4.615
Dehydro	4.336	4.872	-	-	3.276	2.417
Abieitc	4.619	4.976	-	-	2.591	2.467
Stearic	4.216	4.523	3.276	2.591	-	-
Linoleic	4.298	4.615	2.417	2.467	-	-

This significant difference in hydrogen bond length indicates strongly that the interactions between the fatty acids and resin acids are much stronger than those that involve triglycerides.

Figure 6.15 shows both the deposition and SE results of the unsaturated fatty acids. These results support the results from the saturated fatty acids and resin acids and indicate that the solubility of the triglyceride has a major role in the deposition rather than any interaction that occurs between the two components.
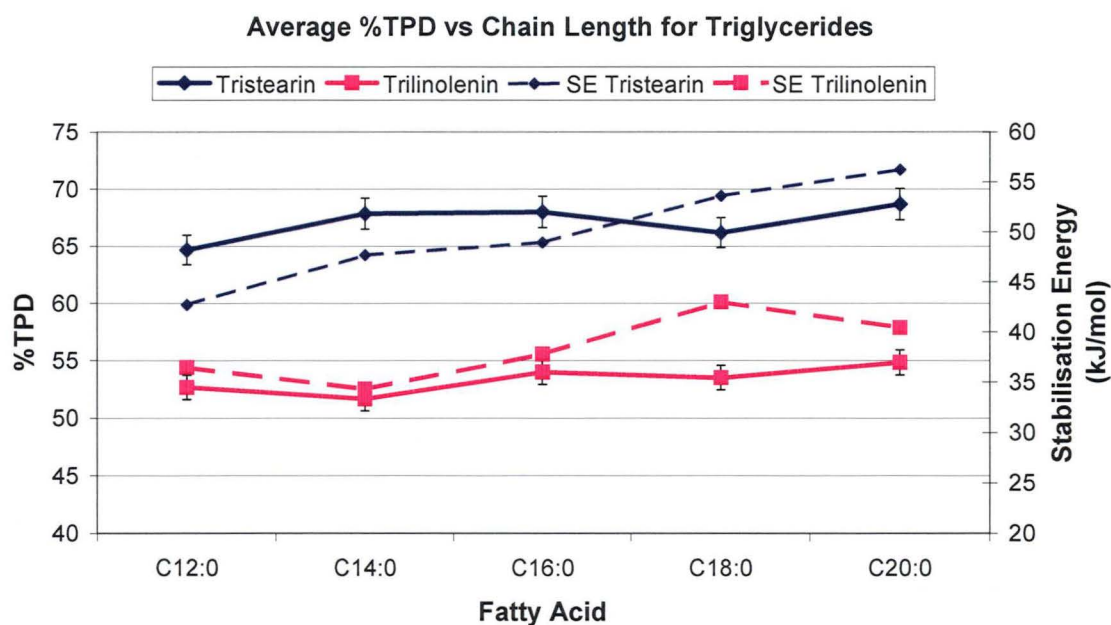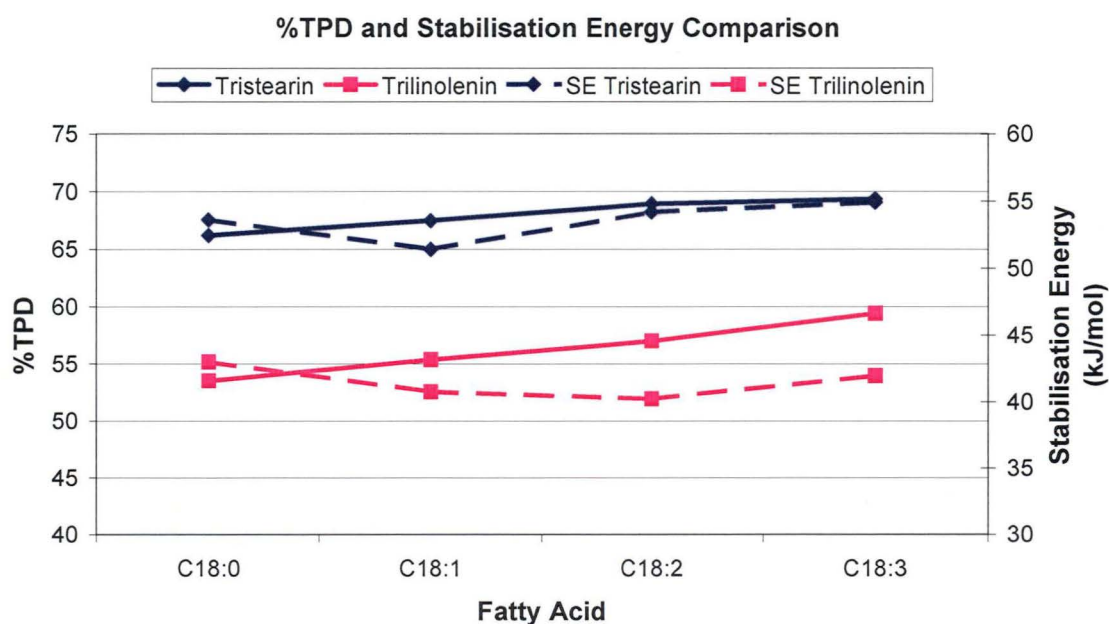

Figure 6.15. Deposition and stabilisation energies of interactions between fatty acids of varying saturation levels and triglycerides. Initial concentration of extractives equal to approximately 70mg/L

Two-component conclusions

The two component studies conducted did convey some conclusive results. It can be seen that the fatty acids and resin acids form very strong complexes between each other and their structure can influence the amount of %TPD. Interactions involving triglycerides however indicated that the solubility of the individual triglyceride had a greater influence on the %TPD than the structure of the individual components. Theoretical calculations also supported the deposition data with larger SE values for the resin acid:fatty acid complexes than those involving a triglyceride. The hydrogen bond lengths could also be used as an indicator of the strength of the interactions between any components. A hypothesis that could be obtained from the two-component studies is that the resin acid and fatty acids have a strong interaction between with each other but the triglycerides have weak interactions with any other component. The solubility of the triglyceride also appears to be the major factor with deposition when it is present.

6.5 Three-Component Results

Following on from the informative results from the two-component system it was decided to investigate the propensity of pitch to deposit in a three-component system. All three components were placed in an aqueous system with equimolar ratios under the same deposition conditions as were carried out for the two-component system. The results of these deposition experiments were surprising but also very informative.

Figure 6.16 shows the deposition results for a three-component system investigating the effect of fatty acid chain length, saturation of triglyceride and class of resin acid. The trends in the graph follow the same trends as the two-component system of a fatty acid and a resin acid with the magnitude of pitch deposited increasing with the decreasing solubility of the individual triglyceride, i.e. a three-component system with tristearin has a higher percentage of total pitch deposited (%TPD) than when no triglyceride is present at all. This data suggests that the fatty acid and resin acid may be interacting with each other where the triglyceride is not interacting but influencing the solubility. This hypothesis can be supported by research conducted by Qin *et al*[1]. Qin *et al* proposed that the most hydrophobic triglycerides form the core and the main part of resin droplets, while the resin acids, fatty acids and sterols, which have a

higher acid-base component of the work of adhesion, are enriched at the outer surface with their carboxyl and hydroxyl groups extending into the water[1].

Deposition of Fatty Acids and Resin Acids with Varying Triglyceride Present
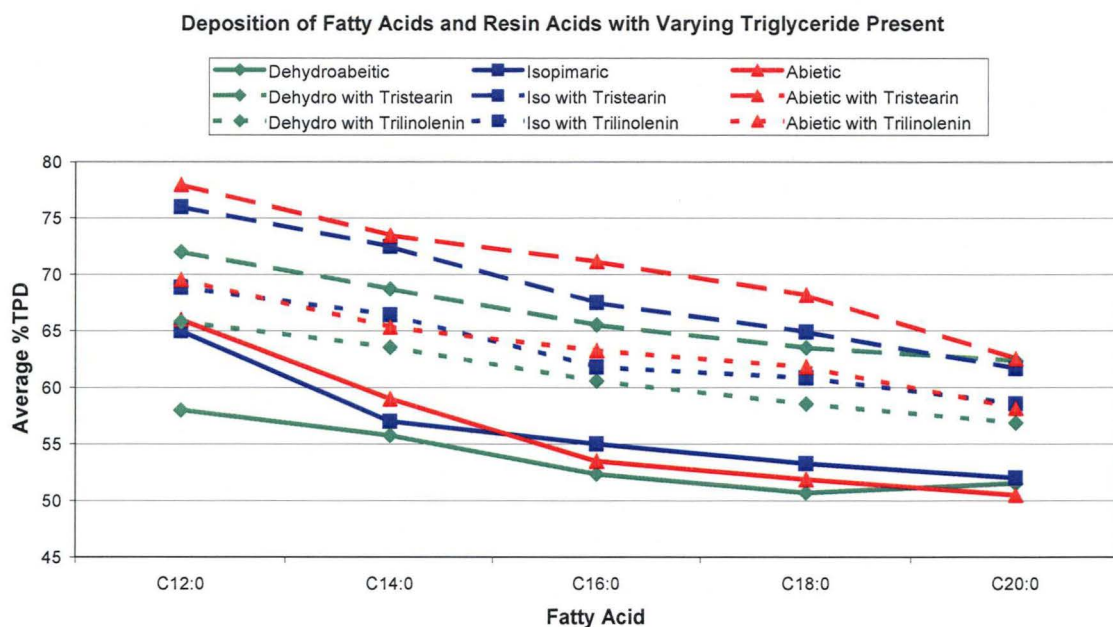
Figure 6.16. Deposition for a three-component system. Initial concentration of extractives equal to approximately 70mg/L

If we consider the results for the three components we can see that the order of magnitude in which the three component pitch deposits is dependent on which triglyceride is present and its solubility. This data therefore tends to agree with the work of Qin *et al*[1] but we can also see in the data that the three components also follow the deposition trends that were seen in the fatty acid/resin acid relationship indicating that there may be an interaction between these two components as well as with the surrounding water molecules. A representation of the three-component pitch colloid can be seen in Figure 6.17. As Qin *et al* proposed, the triglycerides forms a hydrophobic outer core and the fatty acid:resin acid complex forms a hydrophilic outer shell.
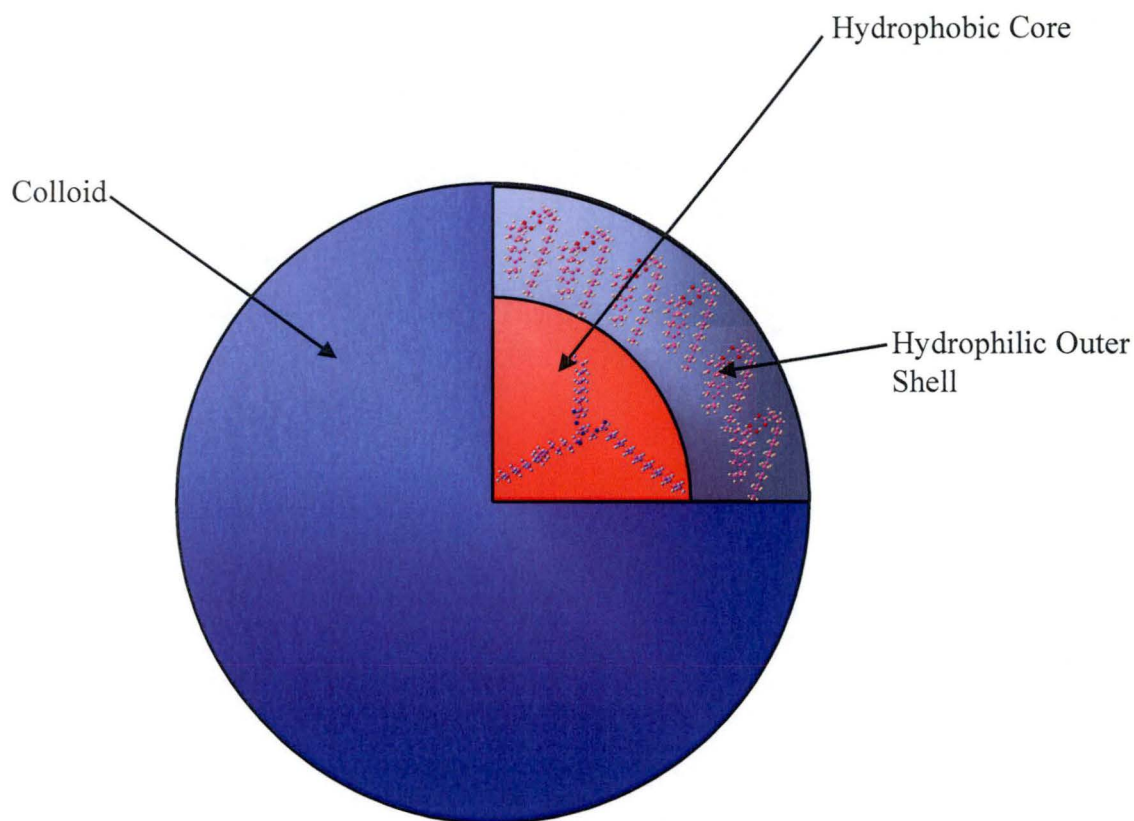
Figure 6.17. Schematic diagram of proposed colloid structure.

The stabilisation energies calculated through molecular modelling also agree with the model of Qin *et al*[1] and the results of this work. It can be reiterated that a higher stabilisation energy indicates a stronger interaction between the two components and hence, stronger hydrogen bonding between them[112-114]. If the deposition seen in Figure 6.16 was purely through interactions between components we would expect an interaction involving tristearin, lauric acid and abietic acid to have a much higher stabilisation energy compared to when lauric acid and abietic acid are interacting together in a two-component system. In Table 6.10 it can be seen that this does not occur and that the stabilisation energies for any system containing a triglyceride is lower and hence less likely to be a stable interaction.

Table 6.10. Stabilisation energies for two and three-component systems.

Interaction	Stabilisation Energy (kJ/mol)
Abietic acid/C12:0	103.8
Abietic Acid/Tristearin	41.5
C12:0/Tristearin	36.5
Abietic acid/C12:0/Tristearin	28.0

The stabilisation energies of the three components were compared to the deposition results in a similar manner to the two component studies. The magnitude of energy is significantly lower than what was seen in the two-component deposition study which reinforces the idea of the colloid depicted in Figure 6.17.

To truly confirm the hypothesis that the three-component pitch colloid did consist of a hydrophobic core surrounded by a hydrophilic outer surface the deposition experiments were repeated with an alkane to mimic the structure of a triglyceride. This alkane is branched similarly to a triglyceride and was synthesised using a Grignard reaction (Scheme 6.1).
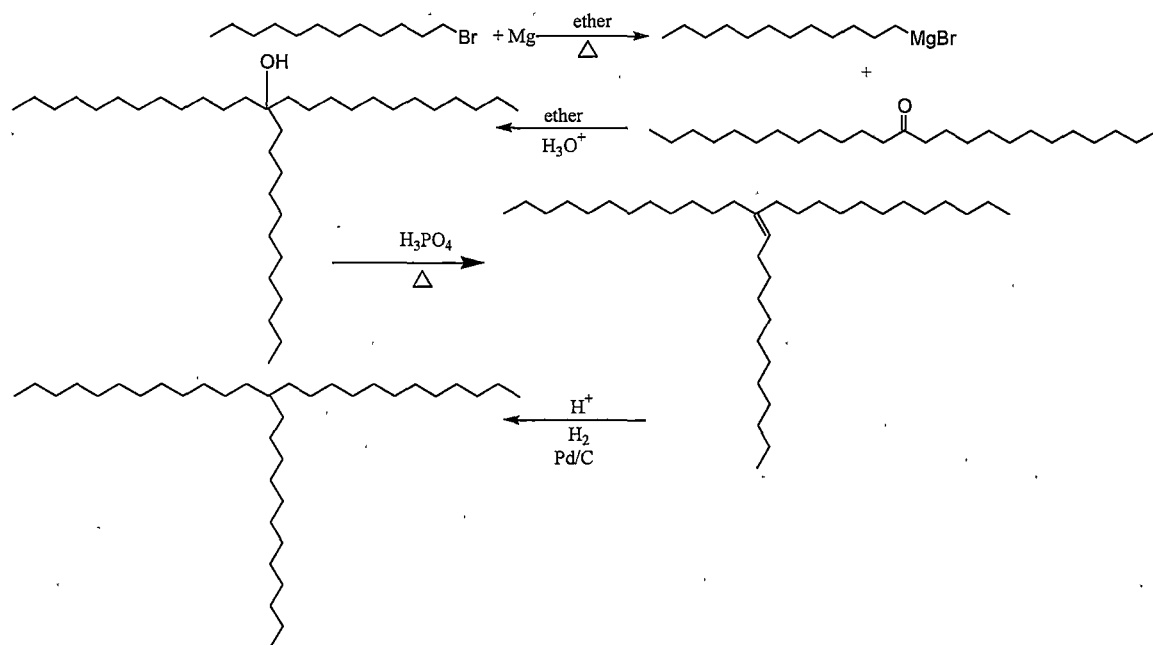
Scheme 6.1. Synthesis of mimic alkane

120

It is designed to mimic the triglyceride in that it is of similar molecular shape but does not contain any active sites, such as the carbonyl group, in which an acid head group can interact. As there are no active sites for interaction it can only behave through solubility whereas the two other components can behave independently. As the alkane is insoluble in water we would expect the %TPD to be higher than the three-component system involving tristearin. Figures 6.18a-c show these results and thus confirm the hypothesis of the colloid structure depicted in Figure 6.17. It can be confirmed that the triglyceride forms a hydrophobic core that is surrounded by a hydrophilic outer shell comprising of a fatty acid:resin acid complex that is bonded through a hydrogen bonded dimer in non-aromatic systems and a single strong hydrogen bond over the aromatic ring with dehydroabietic acid (Figure 6.7).

Deposition of Fatty Acids and Resin Acids with Third Component of Varying Solubility

Dehydroabeitic — Dehydro with Tristearin — Dehydro with Trilinolenin — Dehydro with alkane

As solubility of the third component **DECREASES** the %TPD **INCREASES**
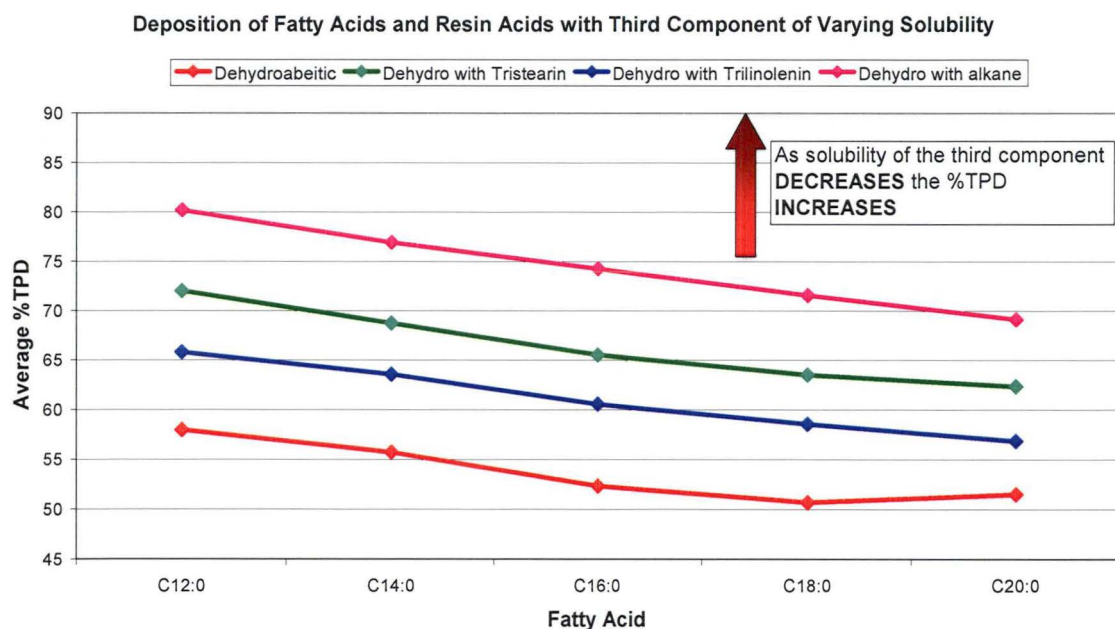
Figure 6.18a. The effect of solubility of the hydrophobic component in concern with the %TPD for dehydroabietic acid. Initial concentration of extractives equal to approximately 70mg/L

Deposition of Fatty Acids and Resin Acids with Third Component of Varying Solubility
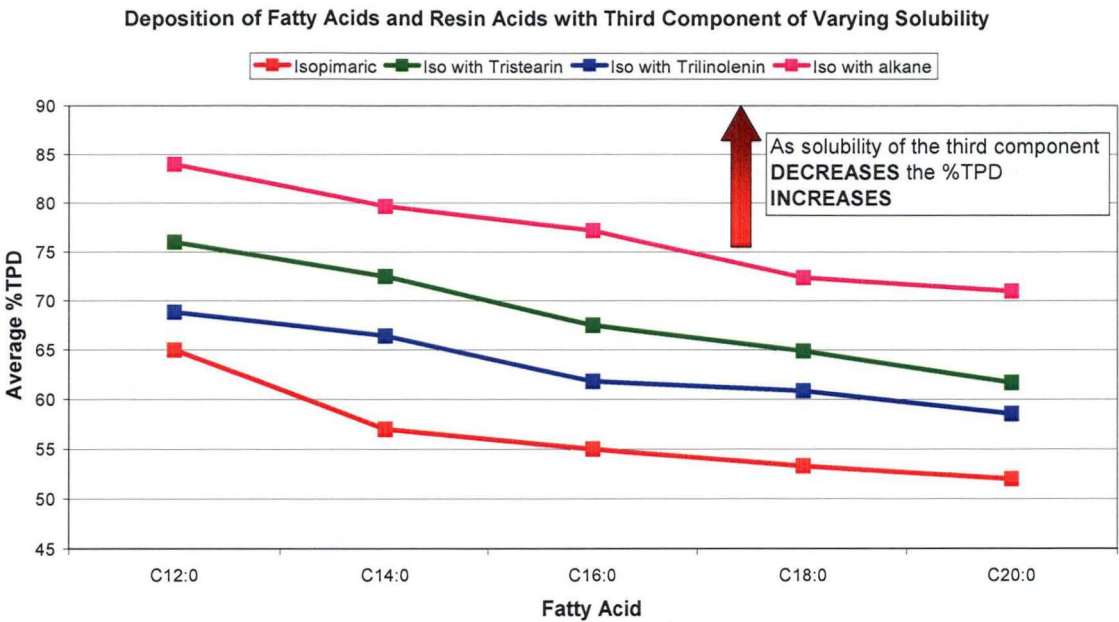
Figure 6.18b. The effect of solubility of the hydrophobic component in concern with the %TPD for isopimaric acid. Initial concentration of extractives equal to approximately 70mg/L

Deposition of Fatty Acids and Resin Acids with Third Component of Varying Solubility
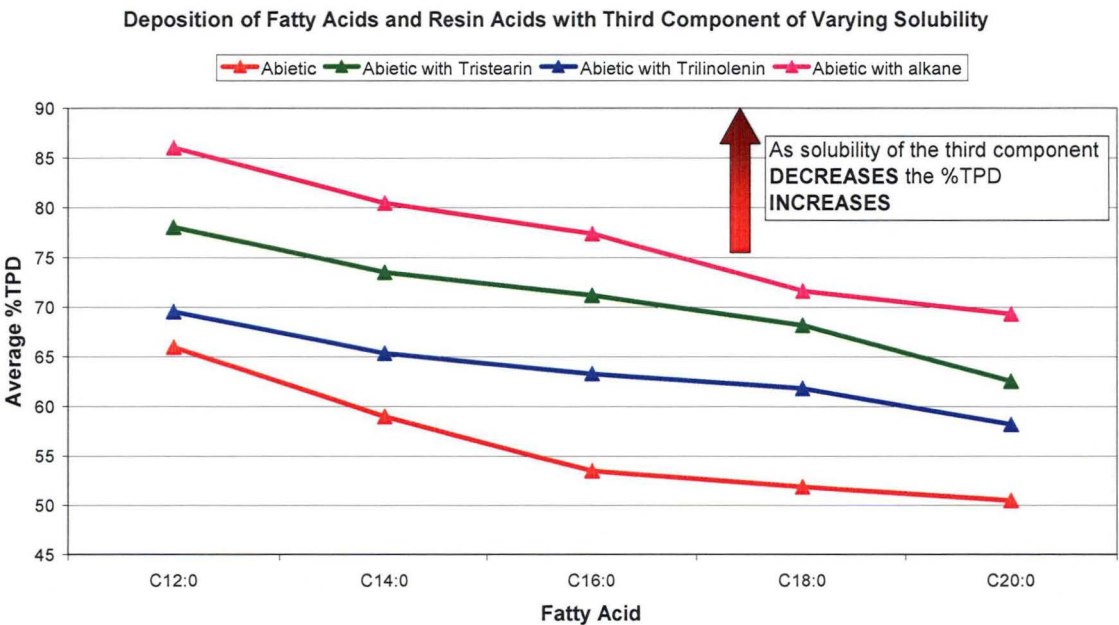
Figure 6.18c. The effect of solubility of the hydrophobic component in concern with the %TPD for abietic acid. Initial concentration of extractives equal to approximately 70mg/L

Conclusions of three-component study

Through both the deposition and modelling data it can be concluded that the structure of a pitch colloid consists of a hydrophobic core of a triglyceride with the fatty acids and resin acids interacting with each other to form a hydrophilic outer shell. This proposed structure has been supported by others[1] who used different methods of analysis but proposed a similar structure. Due to this structure the amount of pitch deposited is related to the solubility of the hydrophobic core and the stabilisation energy of the hydrophilic outer shell.

6.6 Conclusions

From both the two and three component investigations a structure for a pitch colloid could be proposed confidently. The knowledge of this three-component colloid structure can be used to hypothesise what the structure of a pitch colloid would be with other components present. Extractives that are more hydrophobic, such as sterols, would be expected to assist in forming the hydrophobic core whereas more hydrophilic molecules would position there hydrophilic regions towards the outer area of the colloid allowing them to interact with the aqueous atmosphere. It has been shown that different experimental methods can be used to complement each other and to provide insightful, confident results that can be used to investigate colloidal structure.

7. INTERACTIONS BETWEEN HYDROPHOBIC EXTRACTIVES AND HEMICELLULOSE

7.1 Introduction

The major chemical constituents of all wood species are so-called 'structural substances': cellulose, lignin and hemicellulose[115]. Hemicelluloses were originally believed to be intermediates in the biosynthesis of cellulose. Today, however, it is known that hemicelluloses belong to a group of heterogenous polysaccharides which are formed through biosynthetic routes different from that of cellulose. In contrast to cellulose which is a homopolysaccharide, hemicelluloses are heteropolysaccharides and also branched. Like cellulose most hemicelluloses function as supporting material in the cell walls. Hemicelluloses are hydrolysed relatively easily by acids to their monomeric components consisting of hexoses, pentoses, hexuronic acids and deoxyhexoses as depicted in Figure 7.1. Most hemicelluloses have a degree of polymerisation $\left(\overline{DP}_n\right)$ of only 200 compared to the 10 000 of cellulose.

Some wood polysaccharides are extensively branched and are readily soluble in water. Typical of certain tropical trees is a spontaneous formation of exudate gums, which are exuded as viscous fluids at sites of injury and after dehydration give hard, clear nodules rich in polysaccharides. These gums, for example, gum Arabic, consist of highly branched, water-soluble polysaccharides.

The proportion of hemicelluloses in wood (dry weight basis) is usually between 20 and 30% (Table 7.1).

The composition and structure of the hemicelluloses in the softwoods differ in a characteristic way from those in hardwoods. Considerable differences also exist in the hemicellulose content and composition between the stem, branches, roots and bark[115]. Table 7.2 summarises the main structural features of the hemicelluloses appearing in both softwoods and hardwoods.

Hexoses

D-glucose
ß-D-Glc*p*

D-mannose
ß-D-Man*p*

D-galactose
α-D-Gal*p*

Pentoses

D-xylose
ß-D-Xyl*p*

L-arabinose
α-L-Ara*p*

D-arabinose
α-D-Ara*f*

L-arabinose
α-L-Ara*f*

L-arabinose
ß-L-Ara*f*

Hexuronic Acids

D-glucuronic acid
ß-D-Glc*p*A

D-galacturonic acid
α-D-Gal*p*A

4-*O*-methyl-D-glucuronic acid
4-*O*-Me-α,ß-D-Glc*p*A

Deoxyhexoses

L-rhamnose
α-L-Rha*p*

L-fucose
α-L-Fuc*p*
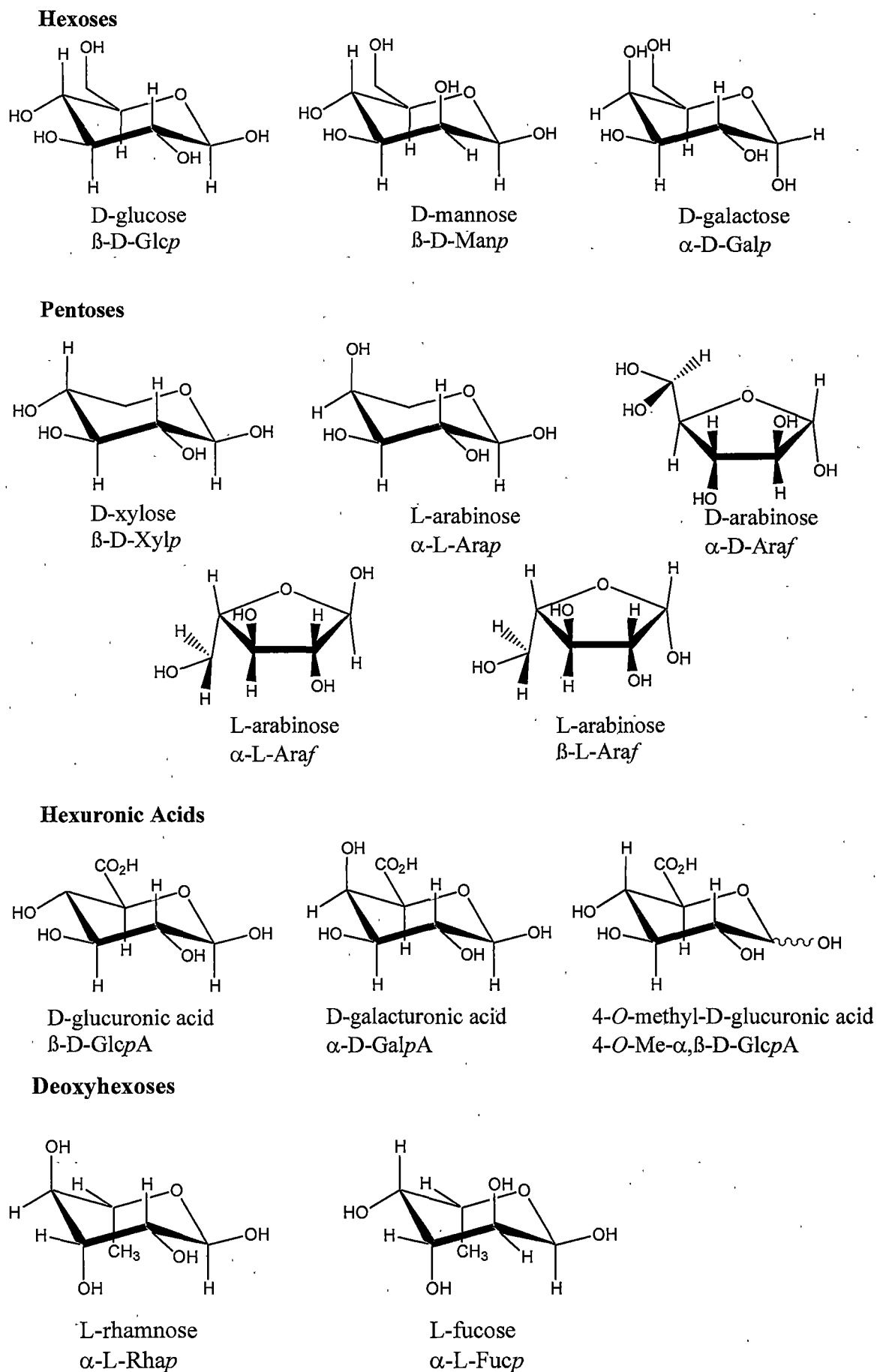
Figure 7.1. The sugar moieties of wood hemicelluloses.[23, 115]

125

Table 7.1. Chemical composition (%w/w) of various wood species[23, 115]

Species	Common name	Total extractives[†]	Lignin	Cellulose	Glucomannan[‡]	Glucuronoxylan[§]	Other polysaccharides	Residual constituents
Softwoods								
Abies balsamea	Balsam fir	2.7	29.1	38.8	17.4	8.4	2.7	0.9
Pseudotsuga menziesii	Douglas fir	5.3	29.3	38.8	17.5	5.4	3.4	0.0
Tsuga canadensis	Eastern hemlock	3.4	30.5	37.7	18.5	6.5	2.9	0.5
Juniperus communis	Common juniper	3.2	32.1	33.0	16.4	10.7	3.2	1.4
Pinus radiata	**Radiata pine**	**1.8**	**27.2**	**37.4**	**20.4**	**8.5**	**4.3**	**0.4**
Pinus sylvestris	Scots pine	3.5	27.7	40.0	16.0	8.9	3.6	0.3
Picea abies	Norway spruce	1.7	27.4	41.7	16.3	8.6	3.4	0.9
Picea glauca	White spruce	2.1	27.5	39.5	17.2	10.4	3.0	0.3
Larix sibirica	Siberian larch	1.8	26.8	41.4	14.1	6.8	8.7	0.4
Hardwoods								
Acer rubrum	Red maple	3.2	25.4	42.0	3.1	22.1	3.7	0.5
Acer saccharum	Sugar maple	2.5	25.2	40.7	3.7	23.6	3.5	0.8
Fagus sylvatica	Common beech	1.2	24.8	39.4	1.3	27.8	4.2	1.3
Betula verrucosa[*]	Silver birch	3.2	22.0	41.0	2.3	27.5	2.6	1.4
Betula papyrifera	Paper birch	2.6	21.4	39.4	1.4	29.7	3.4	2.1
Alnus incana	Gray alder	4.6	24.8	38.3	2.8	25.8	2.3	1.4
Eucalyptus camaldulensis	River red gum	2.8	31.3	45.0	3.1	14.1	2.0	1.7
Eucalyptus globulus	Blue gum	1.3	21.9	51.3	1.4	19.9	3.9	0.3
Gmelina arborea	Yemane	4.6	26.1	47.3	3.2	15.4	2.5	0.9
Acacia mollissima	Black wattle	1.8	20.8	42.9	2.6	28.2	2.8	0.9
Ochroma lagopus	Balsa	2.0	21.5	47.7	3.0	21.7	2.9	1.2

[†] CH$_2$Cl$_2$ followed by C$_2$H$_5$OH
[‡] Including galactose and acetyl in softwood
[§] Including arabinose in softwood and acetyl in hardwood
[*] Also known as *Betula pendula*

Table 7.2 The major hemicellulose Components[115]

Hemicellulose type	Occurrence	Amount (%) of wood	Composition			Solubility[†]	$\overline{(DP_n})$
			Units	Molar Ratios	Linkage		
Galactoglucomannan	Softwood	5-8	β-D-Manp β-D-Glcp α-D-Galp Acetyl	3 1 1 1	1→4 1→4 1→6	Alkali, water[*]	100
(Galacto)glucomannan	Softwood	10-15	β-D-Manp β-D-Glcp α-D-Galp Acetyl	4 1 0.1 1	1→4 1→4 1→6	Alkaline borate	100
Arabinoglucuronoxylan	Softwood	7-10	β-D-Manp 4-*O*-Me-α-D-GlcpA α-L-Araf	10 2 1.3	1→4 1→2 1→3	Alkali, dimethylsulfoxide[*], water[*]	100
Arabinogalactan	Larch wood[‡]	5-35	β-D-Galp α-L-Araf β-D-Arap β-D-GlcpA	6 2/3 1/3 Little	1→3, 1→6 1→6 1→3 1→6	Water	200
Glucuronoxylan	Hardwood	15-30	β-D-Xylp 4-*O*-Me-α-D-GlcpA Acetyl	10 1 7	1→4 1→2	Alkali, dimethylsulfoxide[*]	200
Glucomannan	Hardwood	2-5	β-D-Manp β-D-Glcp	1-2 1	1→4 1→4	Alkaline borate	200

[†] the asterisk represents partial solubility
[‡] larchwood is from a coniferous tree (softwood)

7.2 Softwood Hemicelluloses

As *Pinus radiata* is a softwood only hemicelluloses present in softwoods will be discussed. These differ from hardwood hemicelluloses through structure, polymeric size and the quantity in the wood.

Galactoglucomannans

Galactoglucomannans are the principal hemicelluloses in softwoods (approximately 20%). Their backbone is a linear or possibly slightly branched chain built up of (1→4)-linked β-D-glucopyranose and β-D-mannopyranose units (Figure 7.2).
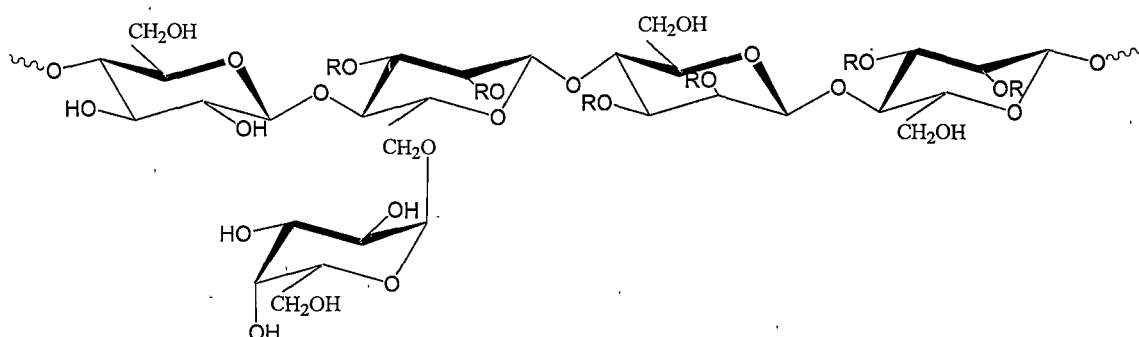
Figure 7.2. Principal structure of galactoglucomannans (R=H, CH₃).

Galactoglucomannans can be roughly divided into two fractions having different galactose contents. In the fraction which has a low galactose content the ratio galactose:glucose:mannose is about 0.1:1:4 whereas in the galactose rich fraction the corresponding ratio is 1:1:3. The former fraction with a low galactose content is often referred to as glucomannan. The α-D-galactopyranose residue is linked as a single-unit side chain to the framework by (1→6)-bonds. An important structural feature is that the hydroxyl groups at C2 and C3 positions in the chain units are partially substituted by *O*-acetyl groups, on average one group per 3-4 hexose units. Galactoglucomannans are easily depolymerised by acids and especially so the bond between galactose and the main chain. The acetyl groups are much more easily cleaved by alkali than acid.

Arabinoglucuronoxylan

In addition to galactoglucomannans, softwoods contain an arabinoglucuronoxylan (5-10%). It is composed of a framework containing (1→4)-linked β-D-xylopyranose units which are partially substituted at C2 by 4-*O*-methyl- α-D-glucuronic acid groups, on the average of two residues per ten xylose units. In addition, the framework contains α-L-arabinofuranose units, on the average of 1.3 residues per ten xylose units (Figure 7.3).
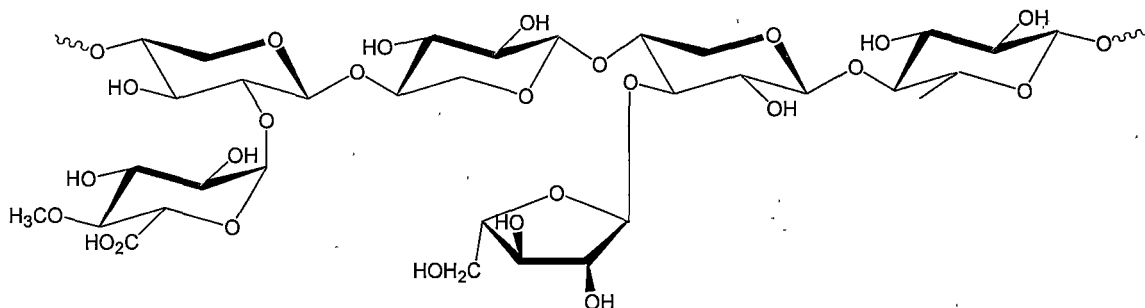
Figure 7.3. Principal structure of arabinoglucuronoxylan

Because of their furansidic structure, the arabinose side chains are easily hydrolysed by acids. Both the arabinose and uronic acid substituents stabilise the xylan chain against alkali-catalysed degradation.

Arabinogalactan

The heartwood of larches contains exceptionally large amounts of water-soluble arabinogalactan, which is only a minor constituent of other softwood species. Its backbone is built up by (1→3)-linked β-D-glucopyranose units. Almost every unit carries a branch attached to position 6, largely (1→6)-linked β-D-glucopyranose residues but also L-arabinose. There are also a few glucuronic acid residues present in the molecule. The highly branched structure is responsible for the low viscosity and high solubility in water of this polysaccharide.

Other polysaccharides

Besides galactoglucomannans, arabinoglucoronoxylan and arabinogalactan, softwoods contain other polysaccharides, usually present in minor quantities. Such polysaccharides include starch (composed of amylose and amylopectin) and pectic substances.

The most common units in pectic polysaccharides consist of D-galactosyluronic acid and, D-galactose, L-arabinose, and L-rhamnose residues. Although the pectic substances are usually not classified as hemicelluloses, the distinction is often difficult and more or less arbitrary. Typical members are galacturonans, rhamnoglacturonans, arabinans, and galactans, mainly located in the primary cell wall and middle lamella.

Galactans occur in minor quantities both in normal wood and tension wood, but high amounts are present in compression wood (about 10% of the wood weight). The backbone of galactans, which is slightly branched, is built up of $(1\rightarrow4)$-linked β-D-glucopyranose units substituted at C6 with α-D-galacturonic acid residues (Figure 7.4).
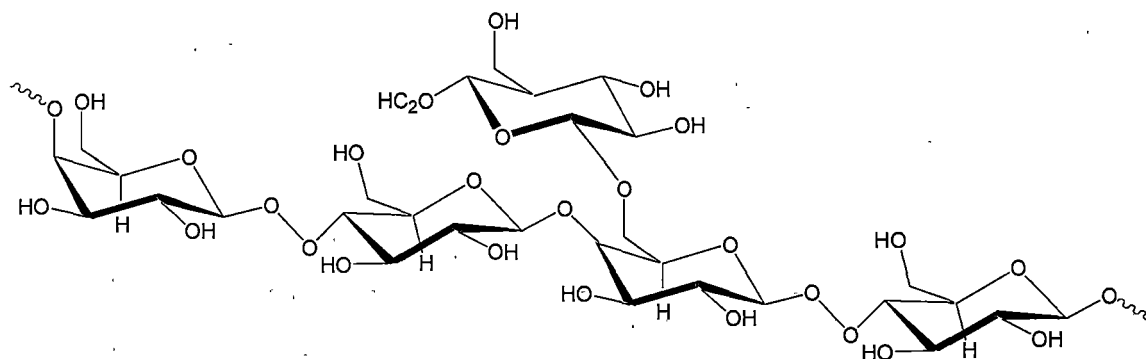
Figure 7.4. Principal structure of galactan in compression wood

The function of galactans in wood is probably more related to hemicelluloses than to pectic substances. In addition, compression wood contains about 2% laricinan, which is a $(1\rightarrow3)$-β-D-glucan and occurs only in trace amounts in normal wood.

7.3 Guar gum

Guar gum is extracted from the seed of the leguminous shrub *Cyamopsis tetragonoloba*, where it acts as a food and water store. Guar gum is a galactomannan similar to locust bean gum consisting of a $(1\rightarrow4)$-linked β-D-mannopyranose backbone with branchpoints from their 6-positions linked to α-D-galactose (*i.e.* $1\rightarrow6$-linked-α-D-galactopyranose). There are between 1.5 - 2 mannose residues for every galactose residue (Figure 7.5).
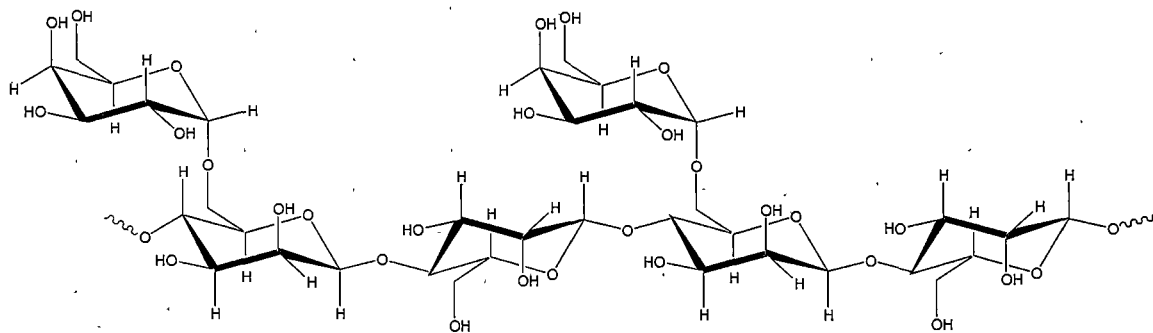
Figure 7.5. Principal structure of guar.

Guar gum is made up of non-ionic polydisperse rod-shaped polymers consisting of molecules (longer than those found in locust bean gum) made up of about 10,000 residues. Higher galactose substitution also increases the stiffness (i.e. decreases the flexibility) but reduces the overall extensibility and radius of gyration of the isolated chains [116]. The galactose residues prevent strong chain interactions as few unsubstituted clear areas have the minimum number (about 6) required for the formation of junction zones. Of the different possible galactose substitution patterns, the extremes of block substitution and alternating substitution give rise to the stiffer, with greater radius of gyration, and more flexible conformations respectively (random substitution being intermediate)[116]. If the galactose residues were perfectly randomized, it is unlikely that molecules would have more than one such area capable of acting as a junction zone, in so disallowing gel formation. A block substitution pattern, for which there is some experimental evidence [116], would allow junction zone formation if the blocks were of sufficient length.

7.4 Aims

Through previously mentioned results the structure of a three component pitch colloid was determined with the hydrophobic extractives, such as triglycerides, forming a hydrophobic core and the more hydrophilic extractives, such as resin acids and fatty acids, interacting with each other to form a hydrophilic outer layer with their hydrophilic groups extending into the aqueous surroundings. This research has not been conducted with any natural hydrophilic extractives of *Pinus radiata* present to act as a natural colloidal stabiliser, which can interact with the colloidal pitch and perhaps decrease its propensity to deposit.

This chapter will discuss the results of both experimental and theoretical methods to explain the interactions that occur between hemicelluloses, a hydrophilic extractive of *Pinus radiata*, and three of the major hydrophobic extractives of *Pinus radiata*, fatty acids, resin acids and triglycerides. Through the theoretical calculations and modelling of the individual sugar groups predictions can also be made as to which hemicellulose structure will have the greatest stabilisation properties against colloidal pitch.

To ensure that only pure hemicellulose with a known molecular structure is interacting with the hydrophobic extractives guar gum will be used for this study. Although guar gum is not a natural hemicellulose found in *Pinus radiata* it is readily available in a pure form and has similar sugar groups present in a similar orientation as galactoglucomannans, the most common hemicellulose of *Pinus radiata*.

7.5   Experimental

Theoretical calculations of polymers

As a hemicellulose is a polymer containing many different sugar groups in different sequences and quantities each sugar group was individually minimised and then their global minimum structure was combined with other minimised sugar groups using Gaussian® and then the lowest energy structure of each hemicellulose monomer was calculated using the same methods as described in previous chapters.

Methanolysis reagent[117]

$$CH_3-C(=O)-Cl \quad + \quad CH_3OH \xrightarrow{N_2} HCl \quad + \quad H_3C-C(=O)-OCH_3$$
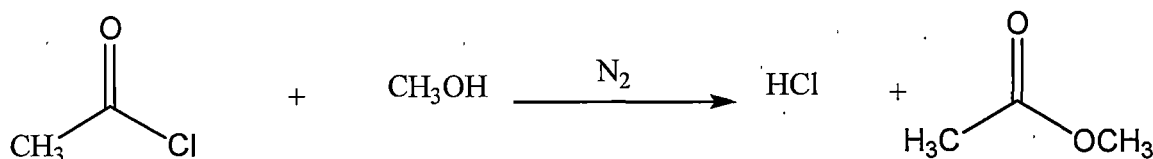
The acid methanolysis reagent was prepared by adding acetyl chloride (14mL, 0.18mol) to dried methanol (86mL, 2.69mol). This operation must be done carefully in an ice bath and under a nitrogen atmosphere. The acid methanolysis reagent can be stored at -24°C for several weeks.

Methanolysis procedure[117, 118]
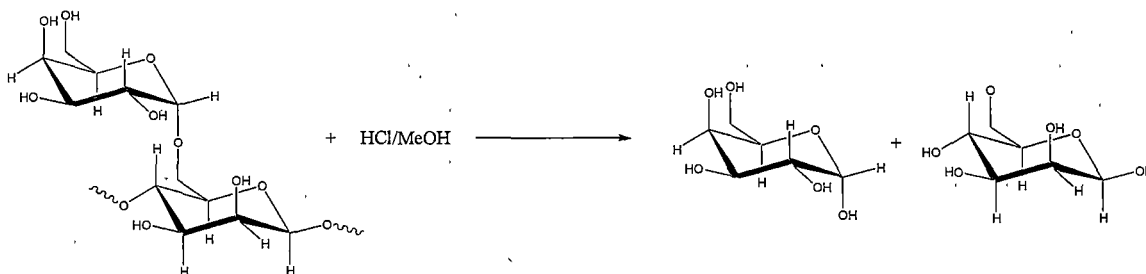
Following the deposition procedure as outlined in Chapter 6 acid methanolysis was performed with 500µL of ~2M anhydrous HCl/methanol at 60°C for 4 hours. Neutralisation, derivitisation and GC analysis were performed according to the procedures outlined in Chapter 6.

Deposition with guar gum present

The guar gum was added to the deposition experiments in a mass ratio of 25:2 (guar gum:total extractives) which is similar to the total concentration of hemicellulose in *Pinus radiata* (Table 7.1). The hydrophobic extractive concentration was kept constant at 100mg/L with the guar gum being added at a concentration of 1125mg/L. These concentrations are similar to work done by others[56].

Charge density determination

The charge density was calculated on a Mütek™ PCD 03 particle charge detector. 10mL of 0.1% w/w solution of guar gum was titrated against 0.001N sodium polyethylene sulfonate.

7.6   Results and Discussion

Guar gum present with a single component

Guar gum was added to the colloidal pitch dispersions as described in the previous chapter with each of the individual hydrophobic extractives studied and the amount of extractive deposited was analysed. The results from this study indicated that the guar gum was stabilising the colloids in solution and preventing them from depositing out of solution. Figures 7.6a-c show the solubility of each of the extractives in their class groups, their deposition tendencies without anything else present and their deposition tendencies with guar gum present.

Fatty Acid Chain Length vs %TPD
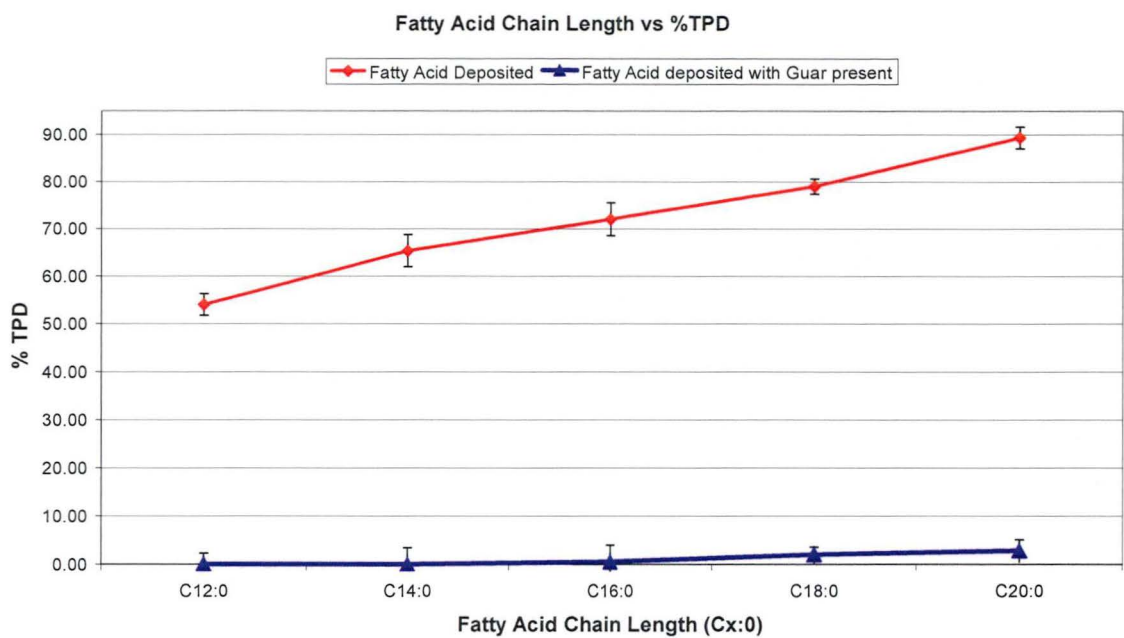
Figure 7.6a. Deposition trends for each fatty acid with and without guar present.

Resin Acid vs %TPD
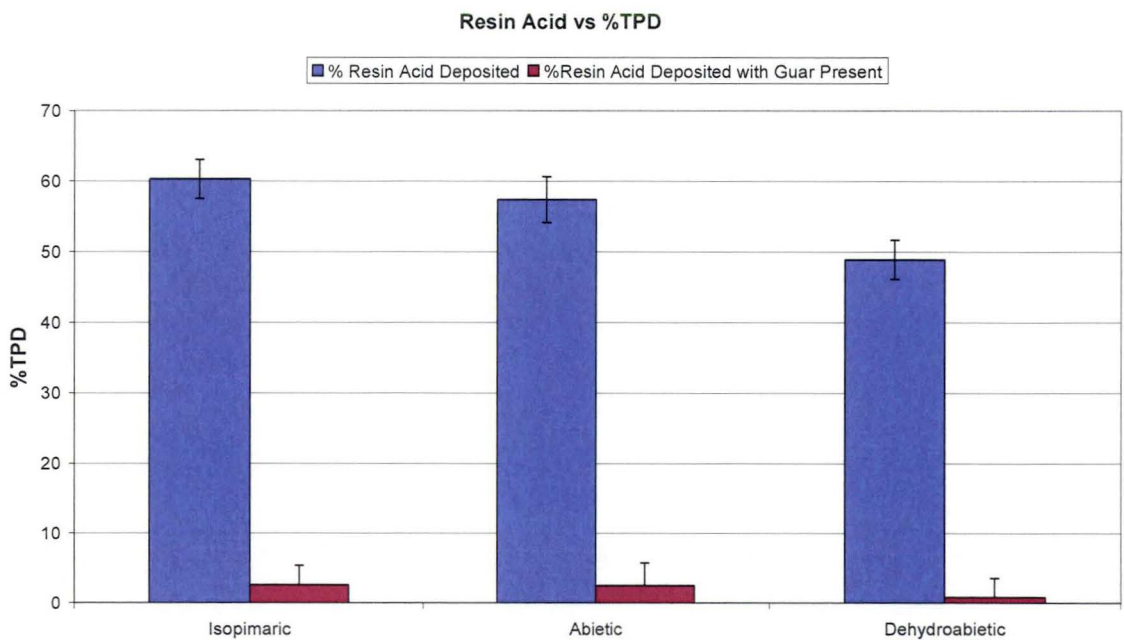
Figure 7.6b. Deposition trends for each resin acid with and without guar present.

Triglyceride vs %TPD
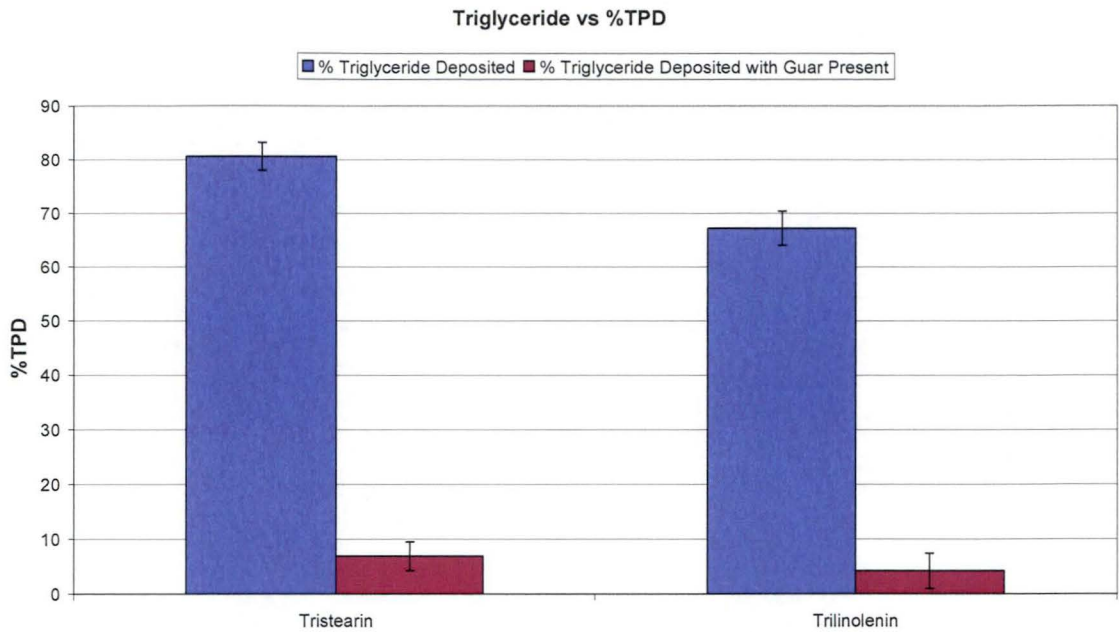
Figure 7.6c. Deposition trends for each triglyceride with and without guar present.

It can be seen that the presence of guar has a significant effect on the deposition of the extractives and in most cases no deposition occurred. This low deposition indicates that the guar may be stabilising the colloids formed from the individual components and preventing them from depositing onto the surface of the deposition jar.

Guar gum present with two different components

Following the deposition study of the individual extractives with guar and the hypothesis that the hemicellulose was acting as a colloidal stabiliser a two-component study was conducted similar to that mentioned in Chapter 6 but with guar gum also present. The results again indicated that the hemicellulose was stabilising the colloid in solution and hindering deposition with it being less than 7% TPD with the most prominent pitch depositing systems. Figures 7.7a-e show the deposition trends for two component systems with and without guar gum present.

Fatty Acid Chain Length vs %TPD
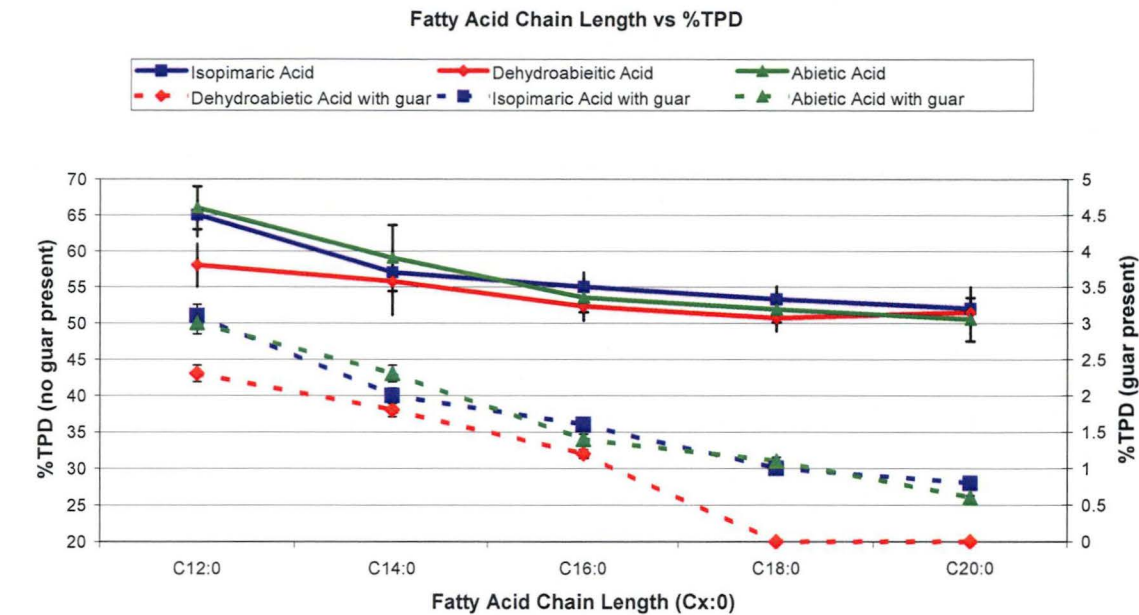
Figure 7.7a. Deposition trends for complexes containing fatty acids of varying chain length and different resin acids with and without guar present.

Degrees of Unsaturation vs %TPD
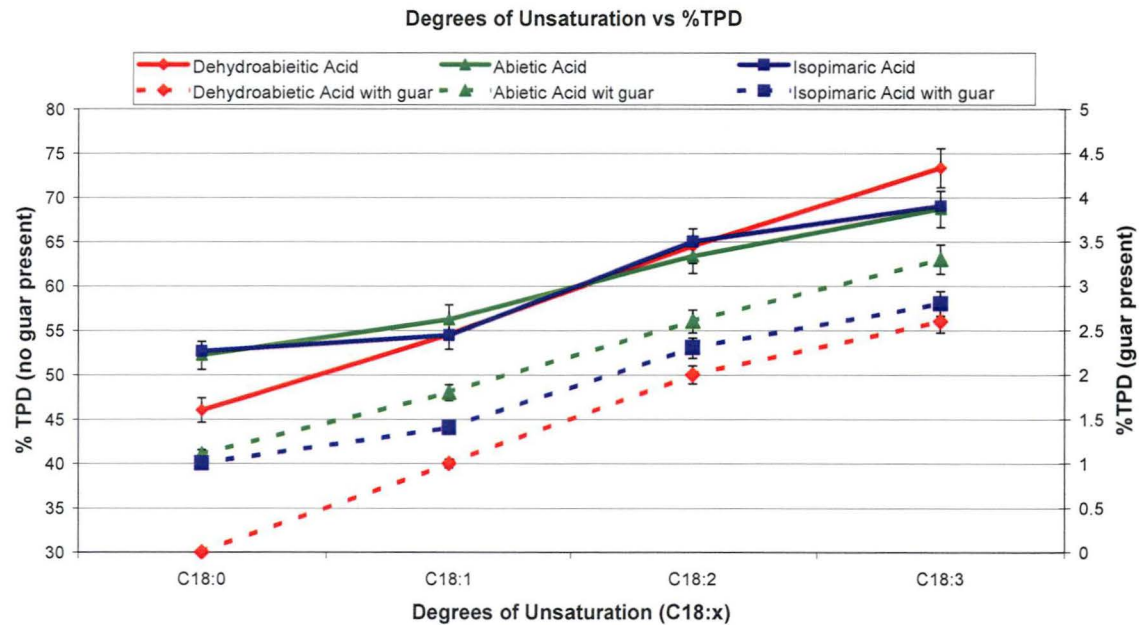
Figure 7.7b. Deposition trends for complexes containing fatty acids of varying degrees of saturation and different resin acids with and without guar present.
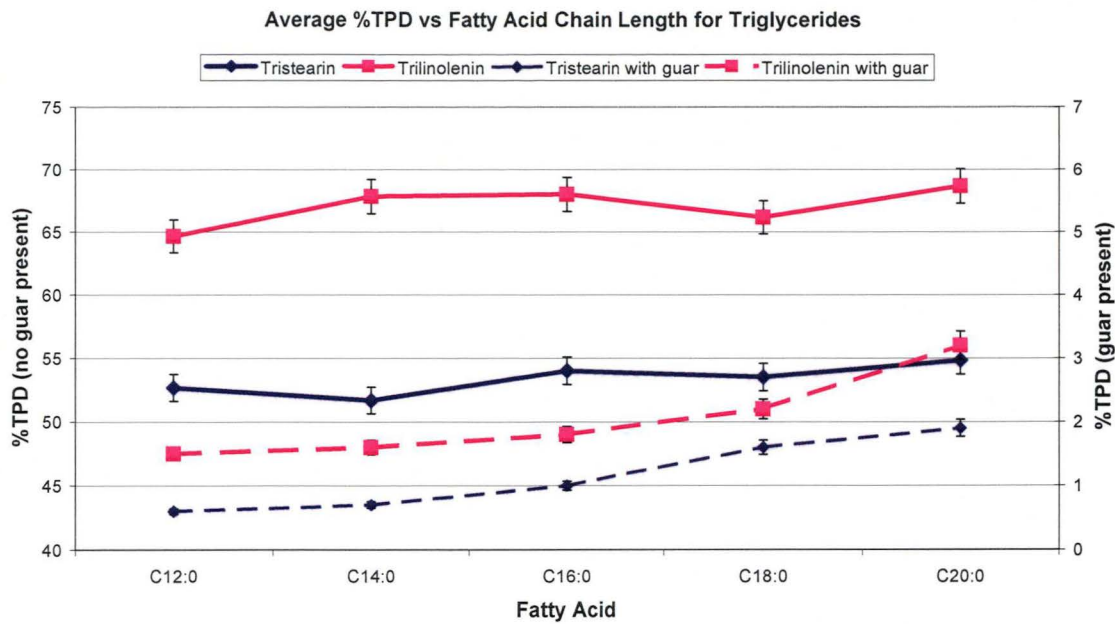
Figure 7.7c. Deposition trends for complexes containing fatty acids of varying chain length two different triglycerides with and without guar present.
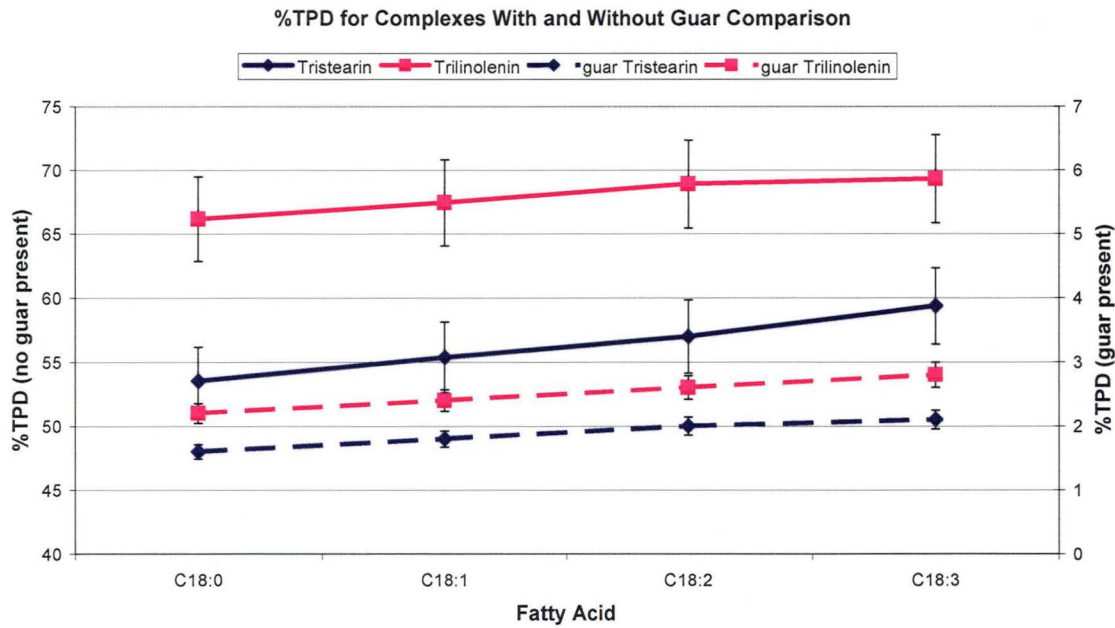
Figure 7.7d. Deposition trends for complexes containing fatty acids of varying degrees of saturation and two different triglycerides with and without guar present.

%TPD and Stabilisation Energy Comparisons
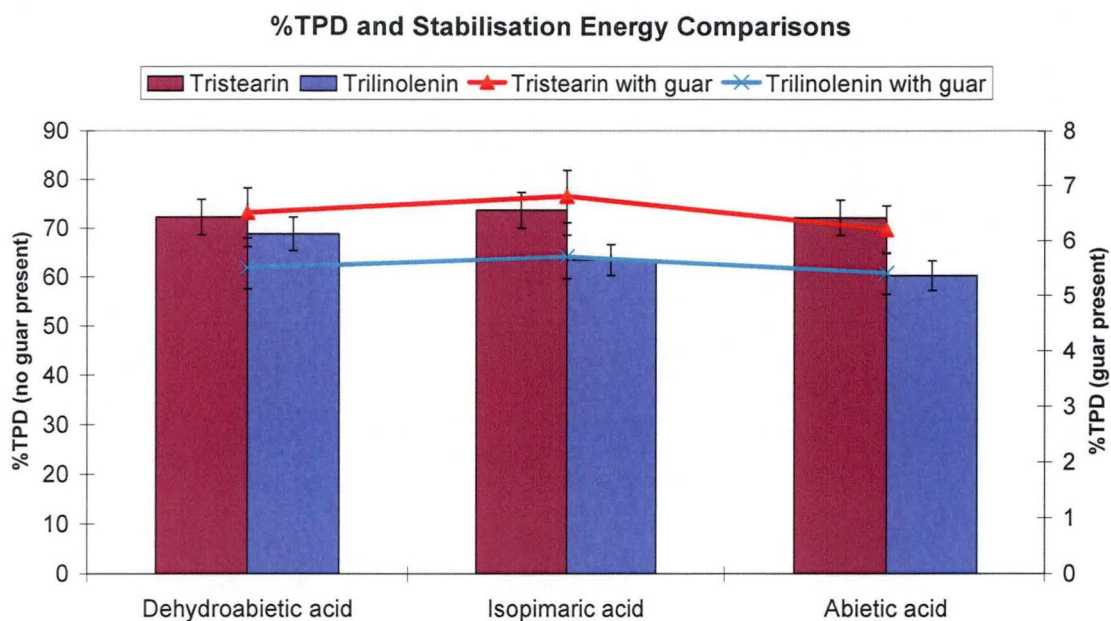
Figure 7.7e. Deposition trends for complexes containing different classes of resin acid and two different triglycerides with and without guar present.

Although the guar gum does not have as great of an affect on the extractive complexes that contain triglycerides the amount of TPD is substantially lower than when guar is not present in the system. This lower affinity of guar gum for triglyceride two-component complexes gives some insight into the interaction mechanism as hydrogen bonding is not as strong with triglycerides as with the other fatty acids and resin acids studied.

Guar gum present with three different components

Guar was also studied for the deposition of a three-component system investigating the effect of fatty acid chain length, saturation of triglyceride and class of resin acid. Figures 7.8a and 7.8b show the deposition results for when both guar gum was present and for when it was not.
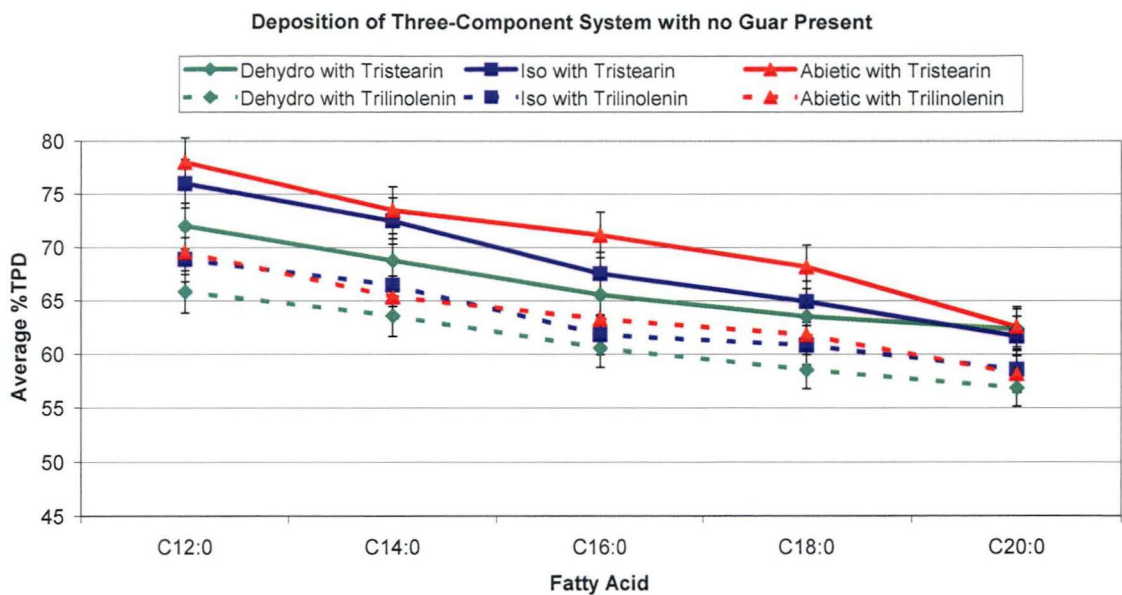
Figure 7.8a. Deposition trends of a three-component system with no guar present.
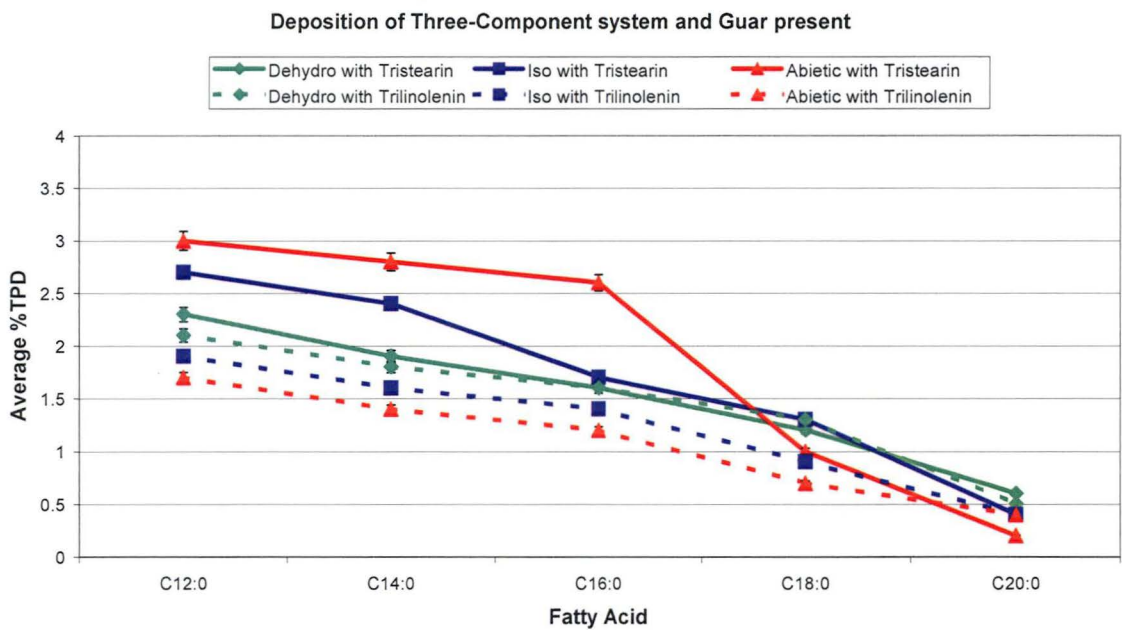
Figure 7.8a. Deposition trends of a three-component system with guar present.

As with both the single and the two-component systems the total amount of pitch deposited was remarkably lower when guar gum was present with no more than 3% (plus 2% experimental error) being deposited. This again supports the hypothesis that the guar is acting as a colloidal stabiliser and with the structure of the colloid being determined in Chapter 6 it can be envisaged that the hydrophilic hemicellulose

may be interacting with the hydrophilic outer shell of the colloid as well as with the surrounding water molecules stabilising the colloid and preventing it from depositing out of solution. As guar gum is composed of sugar groups containing many hydroxyl groups and consists of about 10,000 residues it is possible that there are enough hydrogen bonding sites for both interactions between the colloid and the surrounding water molecules (Figure 7.9). Due to the larger amount of hydrogen bonding sites with the hemicellulose this leads to a stronger interaction with the water than if the colloid was interacting with the water itself.
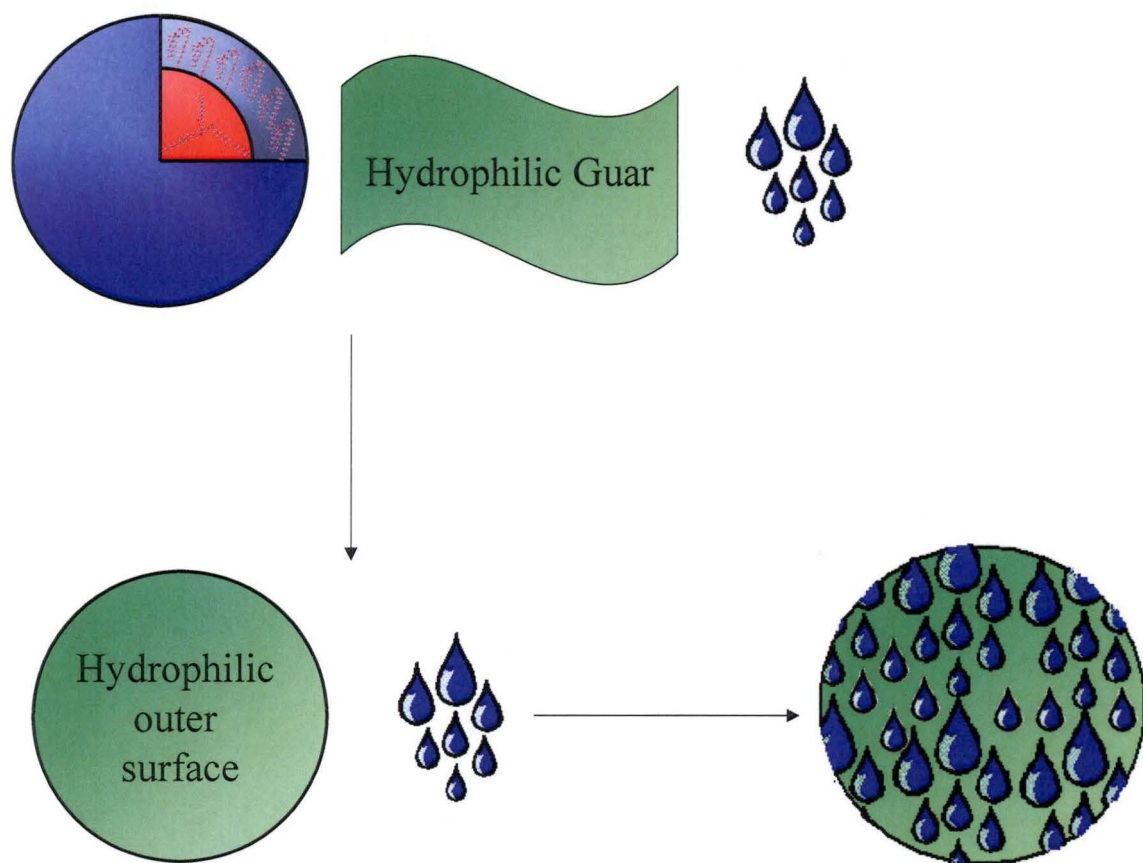
Figure 7.9. Schematic diagram of hemicellulose acting as a colloidal stabiliser.

In effect the surface of a hydrophobic colloidal particle is covered with a hydrophilic material of a polymeric nature. When two such particles approach, the interactions between the absorbed chains cause a repulsion that can be sufficient to induce stability. Its magnitude can be calculated by estimating the effect of the particle separation distance on the free energy of the adsorbed molecules. As they are forced together the number of chain-chain contacts is increased at the expense of chain-

solvent interactions and for a hydrophobic molecule this leads to an increase in free energy (or a repulsive force).

The free energy of mixing of the adsorbed molecular chains as the particles come together can be broken into an enthalpic (ΔH_{mix}) and an entropic part (ΔS_{mix}) part:

$$\Delta G_{mix} = \Delta H_{mix} - T\Delta S_{mix} \tag{7.1}$$

A positive value of ΔG_{mix} (repulsion) can arise from either a positive value of ΔH_{mix} (enthalpic stabilisation) of a negative value of ΔS_{mix} (entropic stabilisation) or both. Enthalpically stabilised systems can be made to coagulate at sufficiently high temperatures (since $\Delta S_{mix}>0$) and the opposite is true of entropically stabilised systems. These remarks apply particularly to systems in which the adsorbed molecules are firmly anchored to the particle surface so that they can neither desorb nor migrate from the encounter region during a collision.

The interaction between the chains on approaching particles will be repulsive if polymer segment-solvent interactions are more favourable than segment-segment interactions. To investigate the relative significance of these effects an important concept in the theory of polymer solutions called the theta point must be considered. It is closely analogous to the Boyle point in the theory of real gases and represents a situation in which the polymer chains exhibit very little or no interaction as they approach and interpenetrate. It is not that there are no intermolecular forces but rather it represents the point at which segment-segment interactions exactly balance segment-solvent interactions. This is most easily illustrated by considering the osmotic pressure, Π of the polymer solution which is given by:

$$\Pi / c = RT / \langle M_n \rangle \tag{7.2}$$

where c is the polymer concentration (kg/m^3) and $\langle M_n \rangle$ is the number average molecular weight. Just as for gas molecules, an attractive interaction between the polymer chains causes negative deviations from this 'ideal' equation and repulsive interactions cause positive deviations. In a 'good' solvent the polymer chains will tend to repel one another (favouring interaction between the polymer segments and the solvent) whilst in a poor solvent the chains will be mutually attractive. When

attractions and repulsions are balanced, the solvent is said to be in the theta condition or at the θ-point. The θ-point may occur at a certain temperature or be produced by a certain (usually rather high) salt concentration or by mixing two differently mutually soluble solvents with different affinities for the polymer. For the θ-point solvent the osmotic behaviour is ideal, at least for dilute polymer solutions. Flory[119] observes that the θ-point polymer molecules of higher molecular weight behave like ideal small molecules. If the dispersion medium is a good solvent for the polymer, the chains will be well extended and will provide a good stabilising barrier. The chains will be interacting strongly with the solvent and will repel one another on approach. At the θ-point the polymer chains cannot see one another as they interpenetrate and the barrier loses its effectiveness entirely.

Guar purity and concentration affects

The guar used for this experiment was purchased at 95+% purity so to confirm that the stabilisation of guar was more of a steric/hydrogen bonding interaction rather than a charge interaction, acid methanolysis was performed and the sugar groups characterised (Figure 7.10).
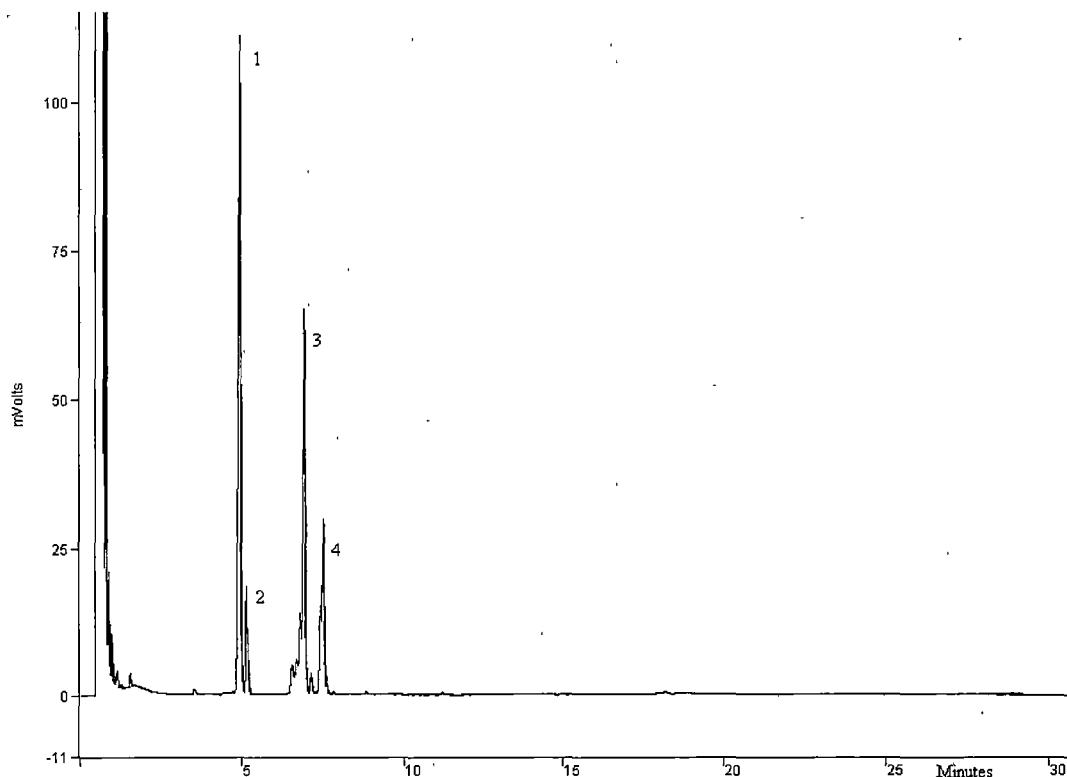
Figure 7.10. Gas chromatogram of acid methanolysis product of guar gum. Peaks indicate the individual sugar groups present (1. β-D-mannose, 2. β-D-glucose (impurity), 3. α-D-galactose, 4. β-D-pyranose)

It can be seen in Figure 7.10 that β-D-glucose was present as an impurity and that some other sugar groups may be present in small quantities eluting at a similar time to α-D-galactose. To confirm that these other small impurities were not charged species, such as hexuronic acids, the charge density was measured at both pH 5.5 and 7. At both these pH values the charge density was found to be 4.14×10^{-7} eq/L indicating that no charged species were present and ruling out any charge/charge interactions that may be occurring between the hemicellulose and the three-component pitch colloid.

The guar gum was added to the deposition experiments in a mass ratio of 25:2 (guar gum:total extractives) which is similar to the total concentration of hemicellulose in *Pinus radiata* (Table 7.1). Figures 7.6-7.8 show that this mass ratio had a substantial effect to the total amount of pitch deposited, more specifically that no pitch deposited as the colloidal pitch was stabilised. To gain a better understanding of the effect of the concentration of guar gum on pitch deposition experiments were designed for a three-component system containing C18:0, abietic acid and tristearin with varying mass ratios of guar gum:total extractives present (Figure 7.11). It should be noted that the x axis of Figure 7.11 represents the %w/w of guar gum with 2%w/w of total extractives being present as this is approximately the concentration of total extractives in *Pinus radiata*[115, 120].

Effect of Guar Gum Concentration of %TPD
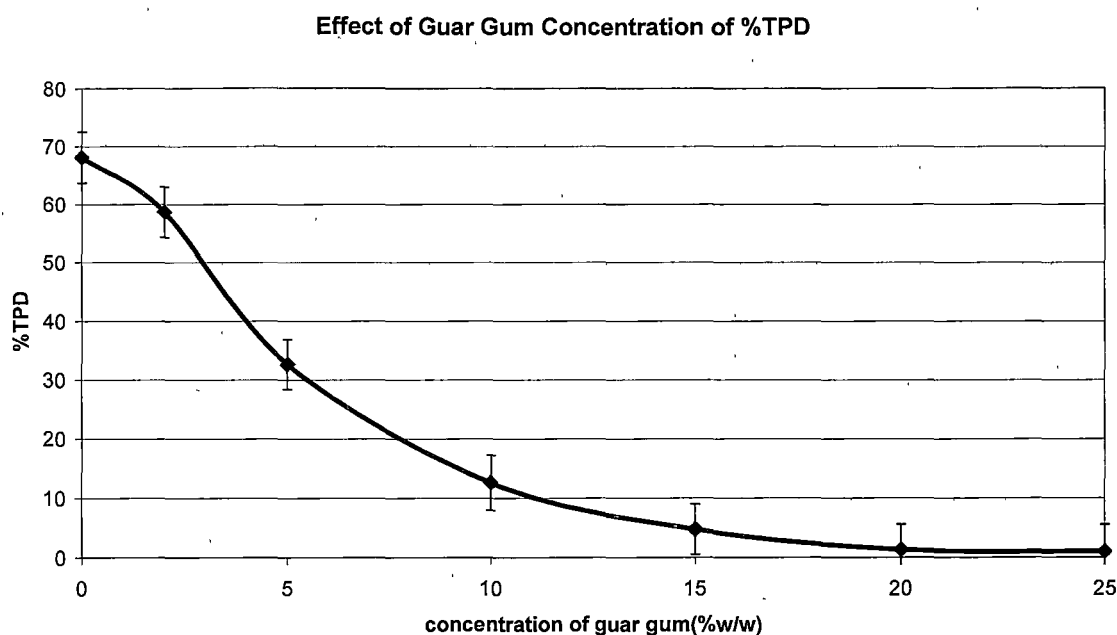
Figure 7.11. Deposition trends for three-component system with varying concentrations of guar present.

As the concentration of guar gum decreases there is still a significant effect on pitch deposition with a concentration of 10%w/w or higher leading to the %TPD being less than 15%. This is significant as it helps to gain an understanding of how much of the extractives are possibly removed during the washing of the pulp and help prevent pitch deposition[121, 122]. The primary reason for washing pulp is to obtain a pulp free of soluble impurities assisting in the prevention of pitch deposition. The hemicellulose can help stabilise the pitch colloids in this washing stage and help in the removal of hydrophobic extractives. However, the hemicellulose that is removed in the washing is no longer available for colloidal stabilisation in the paper machine process water. With environmental standards[123] on water usage reducing the amount of available water to paper machines, they are becoming more closed systems[124]. This closing of the system leads to recycling of water and the reintroduction of hemicellulose into the whitewater which may lead to increased pitch stability.

Theoretical calculations and hemicelluloses

As hemicellulose is a polymer consisting of approximately 10,000 sugar residues it can be difficult to theoretically model with hydrophobic extractives due to the size of calculation and the time it takes for each calculation. Table 7.3 presents the ΔH_f value of the individual sugar groups while Table 7.4a presents the complex energies of the individual components and each sugar group theoretically calculated from computer modelling. The stabilisation energies of each sugar group with each individual hydrophobic extractive is shown in Table 7.4b.

Table 7.3. ΔH_f values for sugar groups

Sugars	ΔH_f (kJ/mol)
Hexoses	
D-glucose	-1274.2
D-mannose	-1248.5
D-galactose	-1248.5
Pentoses	
D-xylose	-1276.2
L-arabinose	-1297.2
D-arabinose	-1278.2
Hexuronic acids	
D-glucuronic acid	-1247.2
D-galacturonic acid	-1267.2
4-*O*-methyl-D-glucuronic acid	-1276.5
Deoxyhexoses	
L-rhamnose	-1278.2
L-fucose	-1234.2

Table 7.4a. Complex energies (kJ/mol) of individual components with each individual sugar group.

	C12:0	C14:0	C16:0	C18:0	C18:1	C18:2	C18:3	C20:0	Abietic	Iso[§]	Dehydro	TS[†]	TL[‡]
β-D-Glcp	-1998.5	-2043 9	-2103.1	-2134 3	-2041 3	-1936 7	-1851.1	-2172.5	-1829 9	-1827.9	-1829 3	-1892 4	-1842 5
β-D-Manp	-1973 3	-2018 5	-2074 4	-2109.6	-2023 6	-1903.8	-1821 1	-2150 1	-1803.0	-1804 7	-1812 0	-1865 0	-1815 0
α-D-Galp	-1974.5	-2017 7	-2074 7	-2112 5	-2013 4	-1905.3	-1826 9	-2146 9	-1807 0	-1807 2	-1811 5	-1864.7	-1815 5
β-D-Xylp	-2000 9	-2048 4	-2105 8	-2141 5	-2048 5	-1942.2	-1850 0	-2170 3	-1837.5	-1847 3	-1852.3	-1895 6	-1842 4
α-L-Arap	-2020.8	-2061 5	-2124 1	-2162 2	-2074 5	-1962.5	-1867.0	-2196 5	-1855 3	-1852 4	-1866 3	-1911.2	-1862.3
α-D-Arap	-2000 0	-2040 2	-2123.7	-2145 2	-2052 4	-1936 0	-1860 5	-2174 3	-1839.1	-1831 8	-1842 5	-1897 6	-1842 6
α-L-Araf	-1993 1	-2038 1	-2095 1	-2121 4	-1842.5	-1917 2	-1836 2	-2159 0	-1816 8	-1813.5	-1822.8	-1876.5	-1825.2
β-L-Araf	-2003 1	-2058 5	-2112 5	-2143 8	-2062.5	-1940 2	-1862 8	-2181 4	-1841.5	-1841.4	-1850.2	-1901 3	-1851 2
β-D-GlcpA	-2029 4	-2061.4	-2118 5	-2157 8	-2062.3	-1956 2	-1870 3	-2189 6	-1850 2	-1850 2	-1862.2	-1921.2	-1865.2
α-D-GalpA	-2001.0	-2053 3	-2115 8	-2143 3	-2055.2	-1932 2	-1855.6	-2179.6	-1834 2	-1836 5	-1845 3	-1892 5	-1846.2
4- β-D-GlcpA[*]	-1956 9	-2003 0	-2063 0	-2090 9	-2002 5	-1889.8	-1810 1	-2132 5	-1789 5	-1788.8	-1797 3	-1850.8	-1798 8
A-L-Rhap	-1998.5	-2043 9	-2103 1	-2134.3	-2041 3	-1936 7	-1851 1	-2172 5	-1829 9	-1827 9	-1829 3	-1892 4	-1842 5
A-L-Rhap	-1973.3	-2018.5	-2074 4	-2109 6	-2023 6	-1903.8	-1821.1	-2150 1	-1803 0	-1804.7	-1812.0	-1865.0	-1815 0

[§] isopimaric acid
[†] tristearin
[‡] trilinolenin
[*]4-O-methyl-D-glucuronic acid

Table 7.4b. Stabilisation energies (kJ/mol) of each sugar group with each hydrophobic extractive.

	C12:0	C14:0	C16:0	C18:0	C18:1	C18:2	C18:3	C20:0	Abietic	Iso[§]	Dehydro	TS[†]	TL[‡]
β-D-Glcp	79.7	79 5	78.6	81.5	77.7	85 4	79.5	78 5	78.7	77 4	70.5	80.1	82.0
β-D-Manp	80.2	79.7	75.6	82.5	85.6	78.2	75.3	81.8	77.5	79.8	78.8	78.4	80.2
α-D-Galp	81 4	78.9	75.9	85.4	75.5	79.7	81 1	78.7	81.5	82.4	78.3	78 1	80 7
β-D-Xylp	80.2	81 9	79.4	86 7	82 9	88.9	76.5	74.3	84.3	94.8	91.4	81.4	79.9
α-L-Arap	79 1	74.0	76 7	86.4	87.9	88.2	72 5	79 5	81.1	78 9	84.5	75.9	78.8
α-D-Arap	77.2	71 7	95.2	88.4	84 7	80 7	84.9	76.3	83.9	77 3	79 6	81.3	78.1
α-L-Araf	101.4	100.7	97.7	95 6	94.1	92.9	91.6	92.0	92 7	90.0	90.9	91.2	91 7
β-L-Araf	91 3	101.0	95.1	98.0	105 9	95 8	98 3	94 5	97.3	97 9	98.4	96.0	97 6
β-D-GlcpA	108.3	94.6	91.7	102.7	96.4	102.6	96.4	93.4	96.7	97.3	101 0	106.6	102.3
α-D-GalpA	78 3	84.8	87.4	86.5	87.5	76.9	80.1	81.7	79 0	82.0	82.4	76 2	81.7
4- β-D-GlcpA*	78.2	78.6	78.6	78 1	78.9	78.5	78.6	78.5	78 3	78.3	78 5	78.5	78.3
A-L-Rhap	79 7	79.5	78.6	81.5	77.7	85.4	79 5	78.5	78.7	77.4	70.5	80.1	82.0
A-L-Rhap	80.2	79.7	75.6	82 5	85 6	78 2	75.3	81.8	77 5	79.8	78.8	78.4	80.2

[§] isopimaric acid
[†] tristearin
[‡] trilinolenin
*4-O-methyl-D-glucuronic acid

There is very little difference in SE between the sugar groups but steric differences do have minor effects. For example, it is expected and observed that the hexuronic acids have the strongest stabilisation energy due to their highly electronegative carboxyl groups.

To observe if the placement of the hydroxyls on the sugar groups have any affect on the stabilisation energies, the repeating unit of several different hemicelluloses was modelled and the stabilisation energy of the monomer with each extractive was also calculated (Table 7.5).

The monomers of these hemicelluloses are quite large, with approximately five sugar groups, each containing different ratios of different sugar groups, (refer to Table 7.2). As a result the steric differences between the hydrophilic hydroxyl groups was quite large and led to more significant differences in stabilisation energies than when the single sugar groups were considered. Table 7.5 can be used to predict that guar gum has the best colloidal stability properties. In respect to hemicelluloses from wood sources used in pulp and paper galactoglucomannans, which are most dominant in softwoods, was found to have the greatest stabilising properties and glucuronoxylan, which are most dominant in hardwoods, has the lowest stabilising properties of the seven different hemicelluloses investigated.

Table 7.5. Stabilisation energies (kJ/mol) of different hemicellulose monomer with each hydrophobic extractive.

	C12:0	C14:0	C16:0	C18:0	C18:1	C18:2	C18:3	C20:0	Abietic	Iso[§]	Dehydro	TS[†]	TL[‡]
Guar	135.9	135 6	134.8	137.6	133.8	141.6	135.7	134.7	134.8	133.6	126.6	136.3	138.1
Galactoglucomannan	122.2	121.7	117.6	124 5	127 6	120 2	117 3	123.8	119.5	121 8	120 8	120.4	122.2
(Galacto)glucomannan	109.6	107 1	104.1	113.6	103.6	107.8	109.3	106 9	109.7	110.5	106.5	106.3	108.9
Arabinoglucuronoxylan	101.4	103.1	100 6	107.9	104.1	110.1	97.7	95 5	105 5	116.0	112.6	102.6	101.1
Arabinogalactan	94.2	89 2	91.9	101.5	103.1	103.3	87.6	94.7	96.3	94.0	99 6	91.1	93.9
Glucuronoxylan	89 4	83.9	107.4	100.5	96.9	92 8	97.1	88.4	96.1	89.5	91.7	93.5	90.3
Glucomannan	131.5	130.8	127.9	125 8	121 9	123 0	121.8	122.2	122 8	120 2	121 0	121.3	121.8

[§] isopimaric acid
[†] tristearin
[‡] trilinolenin

This difference in stabilisation energies with the different forms of hemicellulose helps to predict which form would have a greater stabilisation affect on the pitch colloid in solution. It has been reported that water-soluble wood components could to some extent prevent deposit formation, probably by stabilising the wood resin upon absorption onto the particle surfaces [125,126]. Other authors[125, 127] have also concluded that the stability of colloidal resin is an important factor influencing its deposition. If we can predict which hemicelluloses would have a greater stabilisation affect we may be able to predict the pitch troubles from a certain species of tree through looking at both its hydrophilic and hydrophobic extractive contents. Through our modelling data it can be predicted that tree species with high glucomannan contents, and therefore higher levels of water soluble extractives, will have less pitch troubles than species with high glucuronoxylan contents and similar hydrophobic extractives. It may also be possible for a cheap and affordable hemicellulose, such as guar gum, to be added into the papermaking process to help aid colloidal stability and prevent pitch outbreaks on the papermachine.

7.7 Conclusions

This work has been able to show that hemicelluloses assist in stabilising the pitch colloid in its aqueous environment. Guar gum stabilises the colloid by interacting with the hydrophobic colloid formed by the pitch extractives and with the surrounding water molecules through hydrogen bonds allowing it to stay in solution. The stabilisation energies in Table 7.5 along with the type of hemicellulose and the concentration of hemicellulose allow for an approximation of pitch stability. This is of relevance in a paper mill that uses a variety of wood sources and pulp processes. For example, in a paper mill that uses a hardwood such as *Eucalyptus regnans*, which is high in glucuronoxylan, for CCS pulp as well as a softwood such as *Pinus radiata*, which is high in glucomannan, for TMP pulp to feasibly recycle to the papermachine the TMP process water, or pressate, as the hemicelluloses from this pulp has a greater stabilisation effect on pitch colloids and would inturn help prevent pitch deposition on the papermachine.

8. <u>GENERAL CONCLUSIONS</u>

It can be concluded that the explanation for pitch deposition in paper mills is not a simple one. This is the summary of the conclusions arrived at in the previous chapters.

8.1 Computational Calculations and Experimental Methods

The laboratory and theoretical methods used and developed, throughout this thesis, allowed for reproducible and reliable measurement of interactions between components.

Two methods of computational chemistry were investigated for the study of interactions between the wood extractives of *Pinus radiata*. These two methods were two different levels of theory and molecular mechanics was decided to be the most suitable method for the calculations. The stability of the interactions was calculated through the stabilisation energy and this was proven to be a correct observation through the modelling of some simple known examples. Through this knowledge of stabilisation energies we can successfully model the extractive components and understand the strength and probability of any interactions that occur.

8.2 Computational Calculations of the Hydrogen Bond

It could be concluded from this work that the hydrogen bond can be modelled successfully with a molecular mechanics method. It was observed that there is an aromatic hydrogen bond involving dehydroabietic acid which explains its difference in characteristics and interactive behaviour. It has also been shown that electron density plots are an informative method for observing hydrogen bonding between extractive components as it is visually informative. Non-aromatic resin acids prefer to interact with other components through intermolecular dimer hydrogen bonding.

8.3 Interactions of Components

<u>Two-component conclusions</u>

The two component studies conveyed some conclusive results. It can be seen that the fatty acids and resin acids form very strong complexes between each other and their structure can influence the amount of %TPD. Interactions involving triglycerides however indicated that the solubility of the individual triglyceride had a greater

influence on the %TPD than the structure of the individual components. Theoretical calculations also supported the deposition data with larger SE values for the resin acid:fatty acid complexes than those involving a triglyceride. The hydrogen bond lengths could also be used as an indicator of the strength of the interactions between any components. A hypothesis that could be obtained from the two-component studies is that the resin acid and fatty acids have a strong interaction with each other but the triglycerides have weak interactions with any other component. The solubility of the triglyceride also appears to be the major factor influencing deposition when it is present.

It can also be concluded that there is a strong correlation between theoretical calculations of stabilisation energy and deposition tendency for all systems considered in this study. This correlation between deposition and SE allows for theoretical computer modelling to be used as a tool to predict pitch deposition of known composition. The SE of different complexes and the hydrogen bond length was influenced by the chemical structure of the individual extractives studied.

Conclusions of three-component study

Through both the deposition and modelling data it can be concluded that the structure of a pitch colloid consists of a hydrophobic core consisting of a triglyceride with the fatty acids and resin acids interacting with each other to form a hydrophilic outer shell. This proposed structure has been supported by others[1] who used different methods of analysis but proposed a similar structure. Due to this structure the amount of pitch deposited is related to the solubility of the hydrophobic core and the stabilisation energy of the hydrophilic outer shell. Additional experiments, in which an alkane of similar structure to a triglyceride was prepared and added to both fatty acids and resin acids, conferred that in a three-component system deposition is related to the solubility of the hydrophobic core and little, or no, interaction between the core and outer layer occurs. The structure of this pitch colloid was similar to that of micelles incorporating hydrophobic substances inside themselves whilst in an aqueous environment.

8.4   Interactions Between Hydrophobic Extractives and Hemicellulose

This work has been able to show that hemicelluloses assist in stabilising the pitch colloid in its aqueous environment. Guar gum stabilises the colloid by interacting

with the hydrophobic colloid formed by the pitch extractives and with the surrounding water molecules through hydrogen bonds allowing it to stay in solution. The stabilisation energies in Table 7.5 along with the type of hemicellulose and the concentration of hemicellulose allow for an approximation of pitch stability. Through the theoretical computer modelling it was found that the main softwood hemicellulose, galactoglucomannans, formed more stable complexes than the main hardwood hemicellulose, glucuronoxylan. This is important for those papermills that use both softwoods and hardwoods, for example, in a paper mill that uses a hardwood, such as *Eucalyptus regnans*, for CCS pulp as well as a softwood, such as *Pinus radiata*, for TMP pulp. This mill could feasibly recycle the TMP process water, or pressate, as the hemicelluloses from this pulp has a greater stabilisation effect on pitch colloids and would in turn help prevent pitch deposition provided the other dissolved and colloidal material does not cause other problems with retention on the papermachine.

9. <u>FUTURE WORK</u>

No work, or research, is ever a truly absolute, or complete, and as such the author recommends that the following topics should be further investigated.

9.1 Theoretical Calculations

Theoretical calculations is an area of chemistry which is continually evolving as computers and levels theory are continually being improved. For this work a relatively simple level of theory was used and an improved level of theory may give an even better insight how the interactions between the extractives occur between not just one molecule from each of the two or three components but rather ten or twenty molecules of three components in the one calculation. There is plenty of work being done[128, 129] with theoretical studies of hydrogen bonding and also with larger systems with hundreds of atoms (i.e. proteins) as calculation times decrease with more powerful computers and better calculation methods.

Other future theoretical work may be inclusive of water molecules in the calculations rather than just including the dielectric constant of water. This may show different strengths and orientations of hydrogen bonding between the molecules.

9.2 Deposition Behaviour

The interaction between fatty acids, resin acids, triglycerides, sterols and steryl esters should be explored as others have found sterols and steryl esters to be an important contributor to pitch deposition[130-134].

Due to environmental reasons many paper machines are run at neutral conditions. Due to this fact a more detailed range of deposition pHs and temperatures should be explored in order to better understand their influence on pitch deposition.

Recent work by McLean *et al*[52] showed a common point of deposition under varying pH and temperature conditions where the pre-deposition triglyceride to fatty acid to resin acid molar ratio is 1:4:11. The existence of a point, at any pH and temperature, where deposition is the same and that the components involved are in a set molar ratio suggests that the interaction between the components are stoichiometric in nature. Future work could be done to investigate this ratio in both deposition and theoretical calculations.

9.3 Fixatives and Retention Aids

Fixatives and retention aids are used in the pulp and paper industry to help prevent or decrease the amount of pitch deposition through stabilising the pitch colloid in solution and fixing the dispersed resin onto the fibres, fines, and filler of the papermaking suspension. Through having an understanding of a pitch colloid future work can now be undertaken to gain a better understanding of the mechanism through which fixatives and retention aids work. The strength of the interaction between varying fixatives and retention aids can be calculated through theoretical calculations and approximations be made for the best chemical structure for varying extractive levels at different pulp and paper mills.

10. <u>REFERENCES</u>

1.   Qin, M., Hannuksela, T., and Holmbom, B., *Physico-Chemical Characterisation of TMP Resin and Related Model Mixtures.* Colloids and Surfaces A: Physiochemical and Engineering Aspects, 2003. 221(1-3): 243-254.

2.   Holmbom, B. *Molecular Interactions in the Wet End of Papermaking. International Paper and Coating Chemistry Symposium (CPPA, TAPPI).* 1996. Ottawa, Ontario Canada. 97-104.

3.   Stack, K.R., Stevens, E.A., Richardson, D.E., Parsons, T., and Jenkins, S. *Factors Affecting the Deposition of Pitch in Process Waters and Model Dispersions. 52nd Appita Annual General Conference Proceedings.* 1998. Brisbane, Australia. 59-66.

4.   Gutiérrez, A., del Río, J.C., González-Vila, F.J., and Romero, J., *Variation in the Composition of Wood Extractives from Eucalyptus Globulus During Seasoning.* Journal of Wood Chemistry and Technology, 1998. 18(4): 439-446.

5.   Uprichard, J.M. and Lloyd, J.A., *Influence of Tree Age on the Chemical Composition of Radiata Pine.* New Zealand Journal of Forestry Science, 1980. 10(3): 551-557.

6.   Back, E. and Ekman, R., *The Variability of Wood Resin*, in *Pitch Control, Wood Resin and Deresination*, Back, E. and Allen, L.H., Editors. 2000, TAPPI Press: Atlanta. xii-xiv.

7.   Rao, R. and Kuys, K. *Deinkability of Aged Paper. 48th Appita Annual General Conference Proceedings.* 1995. Hobart Tasmania. 601-608.

8.   Harris, J.M., *Structure of Wood and Bark*, in *Properties and Uses of New Zealand Radiata Pine*, Kininmonth, J.A.K. and Whitehouse, L.J., Editors. 1991, NZ Ministry of Forestry, Forest Research Institute. 2-1 to 2-16.

9.   Sjöström, E., *The Structure of Wood*, in *Wood Chemistry. Fundamentals and Applications.* 1993, Academic Press: San Diego. 1-20.

10.   Back, E.L., *Pattern of Parenchyma and Canal Resin Composition in Softwoods and Hardwoods.* Journal of Wood Science, 2002. 48(3): 167-170.

11.   Holmberg, M., *Pitch and Precipitate Problems*, in *Papermaking Chemistry*, Neimo, L., Editor. 1999, Fapet Oy: Helsinki. 222-240.

12.   Holmbom, B. *Extractives.* 1989. Helsinki University of Technology.

13.   Willför, S., Hemming, J., Reunanen, M., Eckerman, C., and Holmbom, B., *Lignans and Lipophilic Extractives in Norway Spruce Knots and Stemwood.* Holzforschung, 2003. 57(1): 27-36.

14.   Hillis, W.E., *Eucalypts: Chemistry, Uses.* Appita Journal, 1991. 44(4): 239-244.

15.   Back, E.L., *The Locations and Morphology of Resin Components in the Wood*, in *Pitch Control, Wood Resin and Deresination*, Back, E.L. and Allen, L.H., Editors. 2000, TAPPI Press: Atlanta. 1-35.

16.   Dorado, J., van Beek, T.A., Claassen, F.W., and Sierra-Alvarez, R., *Degradation of Lipophilic Wood Extractive Constituents in Pinus Sylvestris by the White-Rot Fungi Bjerkandera Sp. And Trametes Versicolor.* Wood Science and Technology, 2001. 35(1-2): 117-125.

17.   Swan, E.P., Journal of Forestry Production, 1965. 15(7): 272.

18.   Beck, C.W., Naturwissenschaften, 1972. 59(7): 294.

19.   Shaw, G.J., Franich, R.A., Eglinton, G., Allan, J., and Douglas, A.G., Physical Chemistry of the Earth, 1980. 12: 281.

20.   Sjöström, E., *Extractives*, in *Wood Chemistry. Fundamentals and Applications*. 1993, Academic Press: San Diego. 90-108.

21.   Mutton, D.B., *Wood Resins*, in *Wood Extractives*, Hillis, W.E., Editor. 1962, Academic Press: New York. 331-363.

22.   Ekman, R. and Holmbom, B., *The Chemistry of Wood*, in *Pitch Control, Wood Resin and Deresination*, Back, E.L. and Allen, L.H., Editors. 2000, TAPPI Press: Atlanta. 37-76.

23.   Alen, R., *Structure and Chemical Composition of Wood*, in *Forest Products Chemistry*, Stenius, P., Editor. 2000, Fapet Oy: Finland. 12-59.

24.   Uprichard, J.M., *Introduction to Chapter 1*, in *Pulp and Paper from Radiata Pine*. 2002, Appita and Forest Research: Carlton. 2-3.

25.   Neilson, D., *Chapter 2: Resources*, in *The Australian Pine Resource and Solidwood Processing Industry Review 2003*. 2003, DANA Limited: Rotorua. 17-41.

26.   McDonald, I.R.C. and Porter, L.J., *Resin and Fatty Acid Composition of Pinus Radiata Whole Wood, and its Relation to the Yield and Composition of New Zealand Tall Oil.* New Zealand Journal of Science, 1969. 12(2): 352-62.

27.   Wallis, A.F.A. and Wearne, R.H., *Characterization of Resin in Radiata Pine Woods, Bisulfite Pulps and Mill Pitch Samples.* Appita Journal, 1997. 50: 409-414.

28.   Suckling, I.D., Gallagher, S.S., and Ede, R.M., *A New Method for Softwood Extractives Analysis Using High Performance Liquid Chromatography.* Holzforschung, 1990. 44(5): 339-345.

29.   Sim, M., Croucher, M., and Wiseman, N. *A Study of Pitch Deposition in the Newsprint Mill at Tasman Pulp and Paper Company Limited, Kawerau. 44th Appita Annual General Conference Proceedings.* 1990. Rotorua, New Zealand.

30.   Mutton, D.B., in *Wood Extractives and Their Significance to the Pulp and Paper Industries*, Hillis, W.E., Editor. 1962, Academic Press: New York and London.

31.   Arrhenius, D., Svensk Botanisk Tidskrift, 1965. 36: 95.

32.   Swan, B., Svensk Papperstidning, 1965. 71(11): 436.

33.   Pensar, G., Acta Acad. Aboensis, 1969. 29B(3): 1-4.

34.   Pensar, G., Suomen Kemistiseuran, 1970. 79(1): 4-8.

35.   Pensar, G., Acta Acad. Aboemsis, math. Phys., 1970. 30B(3): 5.

36.   Dahn, H.P., Svensk Papperstidning, 1970. 73: 613.

37.   Ekman, R., Peltonen, C., Hirvonen, P., Pensar, G., and von Weisenberg, K., Acta Academiae Aboemsis. Ser. B, 1979. 39(8): 12.

38.   Lloyd, J.A., *Seasonal Variation in the Extractives of Radiata Pine.* 1987, PAPRO: Rotorua. Internal Document, unpublished. 30.

39.   Richardson, D.E., Parsons, T., Bosch, J.v.d., and Harden, P.E. *Factors Affecting the Formation and Control of Pitch Deposits in Newsprint Manufacture from Mechanical Pulp and Recycled Fibre. 50th Appita Annual General Conference Proceedings.* 1996. Auckland, NZ. 499-506.

40.   Allen, L.H., *Pitch Control in Pulp Mills*, in *Pitch Control, Wood Resin and Deresination*, Back, E.L. and Allen, L.H., Editors. 2000, TAPPI Press: Atlanta. 265-287.

41.   Grenz, R., Le, P.C., Weigl, J., and Zeilinger, H., *Erkennung Und Weitgehende Vermeidung Von Polymer-Agglomeraten (White Pitch) Bei Der Wiederverarbeitung Gestrichener Papiere.* Wochenblatt für Papierfabrikation, 1994. 7: 272-279.

42. Allen, L.H., *Mechanisms and Control of Pitch Deposition in Newsprint Mills.* TAPPI Journal, 1980. 63(2): 81-87.

43. Wågberg, L. and Ödberg, L., *The Action of Cationic Polyelectrolytes used for the Fixation of Dissolved and Colloidal Substances.* Nordic Pulp and Paper Research Journal, 1991. 6(3): 127-135.

44. Allen, L.H., *Pitch Particle Concentration. An Important Parameter in Pitch Problems.* Transactions, CPPA, 1977. 3(2): TR32-TR40.

45. Nylund, J., Byman-Fagerholm, H., and Rosenholm, J.B., *Physico-Chemical Characterization of Colloidal Material in Mechanical Pulp.* Nordic Pulp and Paper Research Journal, 1993. 8(2): 280-283.

46. Allen, L.H., *Pitch Control in Paper Mills*, in *Pitch Control, Wood Resin and Deresination*, Back, E.L. and Allen, L.H., Editors. 2000, TAPPI Press: Atlanta. 307-328.

47. Willför, S., Sundberg, A., Sihvonen, A.L., and Holmbom, B., *Interactions between Fillers and Dissolved and Colloidal Substances from Tmp.* Paperi Ja Puu-Paper & Timber, 2000. 82(6): 398-402.

48. Smook, G.A., *Paper Manufacture-Wet End Operations*, in *Handbook for Pulp and Paper Technologisits*. 1992, Angus Wilde Publications: Vancouver. 228-264.

49. Back, E., *The Mechanism of Pulp Resin Accumulation at Solid Surfaces.* Svensk Papperstidning, 1960. 63(17): 556-564.

50. Ohtani, Y. *Utilization of Carbon Fibres for Pitch Quantification and Removal from the Papermaking Systems.* 45th Appita Annual General Conference Proceedings. 1991. Melbourne, Victoria. 109-114.

51. Vincent, D.L., *A Study of the Deposition on Copper from Colloidal Suspensions of Fractions Derived from Sulphite Pitch.* TAPPI Journal, 1956. 39(No. 9): 210A-212A.

52. McLean, D., Stack, K., and Richardson, D. *Wood Pitch Deposition Versus Composition. WPP 2003 Chemical Technology of Wood, Pulp and Paper International Conference.* 2003. Bratislava, Slovak Republic.115-120.

53. Ståhlberg, K., *Pihkavaikeuksista.* Suomen Paperi- Ja Puutavaralehti, 1939. 21(7):124,126-130.

54. McLean, D.S., *The Effect of Wood Extractive Composition on Pitch Deposition.* School of Chemistry. 2003, Hobart: University of Tasmania. pp. 106.

55. Triangular Coordinates; http://www.statsoft.com/textbook/stathome.html (2003)

56. Hannuksela, T. and Holmbom, B., *Stabilization of Wood-Resin Emulsions by Dissolved Galactoglucomannans and Galactomannans.* Journal of Pulp & Paper Science, 2004. 30(6):159-164.

57. McLean, D.S., Vercoe, D., Stack, K.R., and Richardson, D. *The pK$_a$ of Lipophilic Extractives Commonly Found in Pinus Radiata. 58th Appita Annual General Conference Proceedings.* 2004. Canberra, Australia.73-77.

58. Back, E. and Steenberg, B., *Simultaneous Determination of Ionization Constant, Solubility Product and Solubility for Slightly Soluble Acids and Bases. Electrolytic Constants for Abietic Acid.* Acta Chemica Scandinavica, 1950. 4:810-815.

59. Kanicky, J.R. and Shah, D.O., *Effect of Premicellar Aggregation on pK$_a$ of Fatty Acid Soap Solutions.* Langmuir, 2003. 19(6):2034-2038.

60. Spriggs, D., *Cleaning pH Sensors in Pulp and Paper Processes.* TAPPI Journal, 2002. 85(6):73.

61. Orion, *Triode™ pH Electrode Instruction Manual.* 1991: Boston.16.

62. Hunter, R., *Association Colloids*, in *Foundations of Colloid Science.* 2001, Oxford University Press: New York.

63. Atkins, P.W., *Macromolecules and Colloids*, in *Physical Chemistry.* 1998, Oxford University Press: Oxford.679-712.

64. Nyrén, V. and Back, E., *The Ionization Constant, Solubility Product and Solubility of Lauric and Myristic Acid.* Acta Chemica Scandinavica, 1958. 12(6):1305-1311.

65. Kanicky, J.R., Poniatowski, A.F., Mehta, N.R., and Shah, D.O., *Cooperativity among Molecules at Interfaces in Relation to Various Technological Processes: Effect of Chain Length on pK$_a$ of Fatty Acid Salt Solutions.* Langmuir, 2000. 16(1):172-177.

66. Heikkila, R.E., Deamer, D.W., and Cornell, D.G., *Solution of Fatty Acids from Monolayers Spread at the Air-Water Interface: Identification of Phase Transformations and the Estimation of Surface Charge.* Journal of Lipid Research, 1970. 11(3):195-200.

67. White, J.R., *Dissociation Constants of Higher Alkyl Phosphate Esters, Phosphonic Acids, Phosphonous Acids, Phosphinic Acids and Carboxylic Acids.* Journal of the American Chemical Society, 1950. 72:1859-1860.

68.   Kanicky, J.R. and Shah, D.O., *Effect of Degree, Type, and Position of Unsaturation on the pK(a) of Long-Chain Fatty Acids*. Journal of Colloid and Interface Science, 2002. 256(1):201-207.

69.   Christodoulou, A.P. and Rosano, H.L., *Effect of pH and Nature of Monovalent Cations on Surface Isotherms of Saturated C_{16} to C_{22} Soap Monolayers*. Advances in Chemistry Series, 1968. 84:210-234.

70.   Nyrén, V. and Back, E., *The Ionization Constant, Solubility Product and Solubility of Abietic and Dehydroabietic Acid*. Acta Chemica Scandinavica, 1958. 12(7):1516-1520.

71.   Tolstikov, G.A., Irismetov, M.P., Andrusenko, A.A., and Goryaev, M.I., *Synthetic Transformation of Resin Acids iii. The Effect of the Conformation Transfer and Dissociation Constants of Diterpene Acids*. Izvestiya Natsional'noi Akademii Nauk Respubliki Kazakhstan, Seriya Khimicheskaya, 1968. 18:71-76.

72.   Bruun, H., *An Interpretation of the Effect of Ionization Upon Monolayer Properties of Rosin Acids*. Acta Chemica Scandinavica, 1952. 6:955-957.

73.   Lide, D.R., ed. *CRC Handbook of Chemistry and Physics*. 79 ed. 1999, CRC Press: New York.

74.   Daintith, J., ed. *Oxford Dictionary of Chemistry*. 4th ed. 2000, Oxford University Press: New York.

75.   Peng, G.M. and Roberts, J.C., *Solubility and Toxicity of Resin Acids*. Water Research, 2000. 34(10):2779-2785.

76.   Grant, G. and Richards, G., *Molecular Mechanics*, in *Computational Chemistry*, Compton, R., Editor. 1998, Oxford University Press: New York.

77.   Solomons, T.W., *Lipids*, in *Organic Chemistry*, Rose, N., Editor. 1996, John Wiley & Sons: Canada.

78.   March, J., *Bonding Weaker Than Covalent*, in *Advanced Organic Chemistry*. 1992, John Wiley & Sons: New York.

79.   Goodman, J.M., *What Is the Longest Unbranched Alkane with a Linear Global Minimum Conformation?* Journal of Chemical Information and Computer Sciences, 1997. 37(5):876-878.

80.   Young, D., *Molecular Mechanics*, in *Computational Chemistry: A Practical Guide for Applying Techniques to Real World Problems*. 2001, John Wiley & Sons: New York.

81.   Hehre, W., *Theoretical Methods*, in *A Guide to Molecular Mechanics and Quantum Chemical Calculations*. 2003, Wavefuncton Inc.: New York.

82.   Hinchliffe, A., *Molecular Mechanics*, in *Molecular Modelling for Beginners*. 2003, John Wiley & Sons: New York.

83.   Grant, G. and Richards, G., *Quantum Mechanics*, in *Computational Chemistry*, Compton, R., Editor. 1998, Oxford University Press: New York.

84.   Young, D., *Semiempirical Methods*, in *Computational Chemistry: A Practical Guide for Applying Techniques to Real World Problems*. 2001, John Wiley & Sons: New York.

85.   Pimental, G.C. and McClellan, A.L., *The Hydrogen Bond*, ed. Pauling, L. 1960, New York: W. H. Freeman and Company.

86.   Solomons, T.W., *Physical Properties and Molecular Structure*, in *Organic Chemistry*, Rose, N., Editor. 1996, John Wiley & Sons: South Florida.

87.   Green, R.D., *Hydrogen Bonding by C-H Groups*. 1974, New York: Macmillan Press.

88.   Beyer, T. and Price, S., *Dimer or Catemer? Low-Energy Crystal Packings for Small Carboxylic Acids*. Journal of Physical Chemistry B, 2000. 104:2647-2655.

89.   Tamres, M., *H of Solution, IR: Aromatics, Hydrogen Bonding with $CHCl_3$, CH_3OD*. Journal of American Chemical Society, 1952. 74:3375-3378.

90.   Josien, M. and Sourisseau, *IR: v_s for HCl in Many Solvents, Ethers, Aromatics, etc.* Bull. soc. chim. France, 1955:178-183.

91.   Huggins, C.M. and Pimental, G.C., *IR: v_s, $v_{1/2}$, Intensity of Acid-Base Pairs*. Journal of Physical Chemistry, 1956. 60:1615-1619.

92.   Josien, M. and Fuson, N., *IR: Solvent Effect on v_s of Pyrrole, Effect of Solvents*. Journal of Physical Chemistry, 1954. 22:1169-1177.

93.   Fuson, N., Josien, M., Powell, R., and Utterback, E., *IR: v_s and N-H ...N Bonds, Pyrrole, Amines, in CCl_4, CS_2, $CHCl_3$*. Journal of Physical Chemistry, 1952. 20:145-152.

94.   Gordy, W., *IR: v_s of D_2O, HCl, CH_3OD in Many Solvents*. Journal of Physical Chemistry, 1941. 9:215-223.

95.   Searles, S. and Tamres, M., *ΔH_f of Solution, IR: Esters and Lactones. Hydrogen Bonding with $CHCl_3$, CH_3OD*. Journal of American Chemical Society, 1953. 75:71-73.

96.   Gordy, W. and Martin, P., *IR: v_s of HCl in Several Solvents.* Journal of Physical Chemistry, 1939. 7:99.

97.   Gordy, W. and Stanford, S., *IR: v_s of CH₃OD in Many Solvents.* Journal of Physical Chemistry, 1941. 9:204-214.

98.   Buswell, A.M. and Roy, M., *IR: v_s and Hydrogen Bonding of HCl, CHCl₃ in Ether, Anisole, Acetone, Quinoline.* Journal of American Chemical Society, 1938. 60:2528-2531.

99.   Searles, S. and Tamres, M., *H of Solution, IR: Cyclic Ethers Hydrogen Bonding with CH₃Cl₃, CH₃OD.* Journal of American Chemical Society, 1951. 73:3704-3706.

100.   Gordy, W. and Stanford, S., *IR Evidence for Hydrogen Bonds: S-H, N-H Groups, Mercaptans, Amines.* Journal of American Chemical Society, 1940. 62:497-505.

101.   Gordy, W. and Stanford, S., *IR: v_s of CH₃OD in Many Solvents, Effect of Dipole Moment.* Journal of Physical Chemistry, 1940. 8:170-177.

102.   Tamres, M., Searles, S., Leighly, E., and Mohrman, D., *Heat of Mixing and Shift of OD Stretch in CH₃OD Related to K_a.* Journal of American Chemical Society, 1954. 76:3983-3985.

103.   Linnell, R., *IR: Hydrogen Bonding of Pyridine-Pyrrole Mixtures.* Journal of Physical Chemistry, 1953. 21:179-180.

104.   Buswell, A.M., Downing, J., and Rodebush, W.H., *IR: N-H...N and N-H...O Bonds.* Journal of American Chemical Society, 1940. 62:2759-2765.

105.   Huggins, C.M. and Pimental, G.C., *v_s, $v_{1/2}$, Intensity C-D Stretch, CDCl₃ in Various Solvents, Heat of Solution.* Journal of Physical Chemistry, 1955. 23:896-898.

106.   Reeves, L. and Schneider, W., *NMR: Complexes of CHCl₃ with Aromatics, Olefins.* Canadian Journal of Chemistry, 1957. 35:251-261.

107.   Klemperer, W., Cronyn, W., Maki, A., and Pimental, G.C., *IR: Solvent Effect and Association of Amides, Ethylacetamide, N-Butylacetamide, Buterolactam.* Journal of American Chemical Society, 1954. 76:5846-5848.

108.   Tuomikoski, P., *Dielectric Constant: v_s and Dipole Moment for Pyrrole in Acetone, Pyridine, Diethylamine, CH₃Cl₃, Etc.* Mikrochim. Acta, 1955:505-511.

109.   Grant, G. and Richards, G., *Statistical Mechanics,* in *Computational Chemistry,* Compton, R., Editor. 1998, Oxford University Press: New York.

110.   Sundberg, K., Pettersson, C., Eckerman, C., and Holmbom, B., *Preparation and Properties of a Model Dispersion of Colloidal Wood Resin from Norway Spruce.* Journal of Pulp & Paper Science, 1996. 22(7):J 248-J 252.

111.   Holmbom, B., *Extractives*, in *Analytical Methods in Wood Chemistry, Pulping, and Papermaking*, Sjöström, E. and Alén, R., Editors. 1999, Springer: New York.125-148.

112.   Vercoe, D., Stack, K., Blackman, A., and Richardson, D. *Interaction of Pitch Components at a Molecular Level. WPP 2003 Chemical Technology of Wood, Pulp and Paper International Conference.* 2003. Bratislava, Slovak Republic.127-133.

113.   Vercoe, D., Stack, K., Blackman, A., Yates, B., and Richardson, D., *An Innovative Approach to Characterising the Interactions Leading to Wood Pitch Deposition.* Journal of Wood Chemistry and Technology, 2004. 24(2):115-137.

114.   Vercoe, D., Stack, K., Blackman, A., and Richardson, D. *A Multi-Component Insight into the Interactions Leading to Wood Pitch Deposition. 58th Appita Annual General Conference Proceedings.* 2004. Canberra, Australia.65-71.

115.   Sjöström, E., *Wood Polysaccharides*, in *Wood Chemistry. Fundamentals and Applications.* 1993, Academic Press: California.51-70.

116.   Guar Gum; http://www.lsbu.ac.uk/water/hygua.html (2004)

117.   Bertaud, F., Sundberg, A., and Holmbom, B., *Evaluaton of Acid Methanolysis for Analysis of Wood Hemicelluloses and Pectins.* Carbohydrate Polymers, 2002. 48:319-324.

118.   Sundberg, A., Sundberg, K., Lillandt, C., and Holmbom, B., *Determination of Hemicelluloses and Pectins in Wood and Pulp Fibres by Acid Methanolysis and Gas Chromatography.* Nordic Pulp and Paper Research Journal, 1996. 11(4):216-220.

119.   Flory, P.J., *Principles of Polymer Chemistry.* 1st ed. 1953, Ithaca: Cornell University Press.

120.   Jansson, B., Alvarado, F., Bergqvist, A.-K., and Dahlman, O. *Analysis of Pulp Extractives with Off-Line Supercritical Fluid Extraction (SFE) and Supercritical Fluid Chromatography (SFC). Seventh International Symposium on Wood and Pulping Chemistry.* 1993. Beijing, P.R. China.795-801.

121. Crotogino, R., Poirier, N., and Trinh, D. *The Principles of Pulp Washing. 1986 Kraft Recovery Operations Seminar.* 1986.73-83.

122. Dunlop-Jones, N. and Allen, L., *The Influences of Washing, Defoamers and Dispersants on Pitch Deposition from Unbleached Kraft Pulps.* Journal of Pulp and Paper Science, 1989. 15(6):235-241.

123. Ali, M. and Sreekrishnan, T.R., *Aquatic Toxicity from Pulp and Paper Mill Effluents: A Review [Review].* Advances in Environmental Research, 2001. 5(2):175-196.

124. Zhang, X., Beatson, R.P., Cai, Y.J., and Saddler, J.N., *Accumulation of Specific Dissolved and Colloidal Substances During White Water Recycling Affects Paper Properties.* Journal of Pulp and Paper Science, 1999. 25(6):206-210.

125. Sundberg, K., Thornton, J., Holmbom, B., and Ekman, R., *Effects of Wood Polysaccharides on the Stability of Colloidal Wood Resin.* Journal of Pulp & Paper Science, 1996. 22(7):J226-J230.

126. Welkener, U., Hassler, T., and McDermott, M., *The Effect of Furnish Components on Depositability of Pitch and Stickies.* Nordic Pulp and Paper Research Journal, 1993. 8(1):223-5,232.

127. Dreisbach, D.D. and Michalopoulos, D.L., *Understanding the Behavior of Pitch in Pulp and Paper Mills.* Tappi Journal, 1989. 72(6):129-34.

128. Schmuck, C. and Geiger, L., *Dipeptide Binding in Water by a De Novo Designed Guanidiniocarbonylpyrrole Receptor.* Journal of American Chemical Society, 2004. 126:8898-8899.

129. Chandra, A. and Zeegers-Huyskens, T., *Theoretical Study of the Symmetry of the (OH-O)- Hydrogen Bonds in Vinyl Alcohol-Vinyl Alcoholate Systems.* Journal of Organic Chemistry, 2003. 68:3618-3625.

130. Ståhlberg, K., *Hartsivaikeudet Ja Niiden Tutkiminen.* Suomen Paperi- Ja Puutavaralehti, 1944. 26(12):155-166.

131. Holmberg, B., *Sulfitcellulosaindustriens Hartssvårigheter.* Svensk Papperstidning, 1937. 40(8):180-182.

132. Ståhlberg, K., *Om Hartssvårigheter.* Svensk Papperstidning, 1939. 42:408-412.

133. del Río, J.C., Gutiérrez, A., González-Vila, F.J., Martin, F., and Romero, J., *Characterization of Organic Deposits Produced in the Kraft Pulping of*

Eucalyptus Globulus Wood. Journal of Chromatography A, 1998. 823(1-2):457-465.

134. Speranza, M., Martinez, M.J., Gutiérrez, A., del Río, J.C., and Martinez, A.T., *Eucalypt Wood and Pulp Localization of Sterols Involved in Pitch Deposition Using Filipin Fluorescent Staining.* Journal of Pulp and Paper Science, 2002. 28(9):292-297.

APPENDIX A – VARIAN 3800 GC METHOD

Star Chromatography Workstation - Method Listing   Fri Mar 21 09:45:59 2003

Method Boyer15m

```
*************************************************************************

**********************
    3800 GC
**********************
Module Address: 44

8400 Autosampler
----------------
                        Syringe Size  10 uL
                      Injection Mode  Std On Column
           Solvent Penetration Depth  90 %
            Sample Penetration Depth  90 %

                   Default Clean Vial  I
                 Default Clean Volume  5.0 uL
                 Default Clean Strokes 1
           Default Clean Drawup Speed  5.0 uL/sec

   Clean Mode Pre-Inj Solvent Flushes  3
  Clean Mode Post-Inj Solvent Flushes  1
    Clean Mode Pre-Inj Sample Flushes  0
            Clean Mode Solvent Source  I

Valve Table
-----------

 Front Injector Type 1079
 ------------------------
             Oven Power: On
                Coolant: On
      Enable Coolant at: 167 C
        Coolant Timeout: 20.00 min

    Temp     Rate      Hold     Total
    (C)     (C/min)   (min)     (min)
    -------------------------------------
     90        0       0.50      0.50
    325      200      20.00     21.68

     Time    Split     Split
    (min)    State     Ratio
    -----   -------   ------
    Initial   Off       Off

 Front Injector EFC Type 1
 -------------------------
 Pressure    Rate      Hold      Total
    (psi)  (psi/min)   (min)     (min)
 --------------------------
     3.0     0.00      32.67     32.67

Column Oven
-----------
                 Coolant  Off
       Enable Coolant at  50 C
         Coolant Timeout  20.00 min
       Stabilization Time  2.00 min

    Temp     Rate      Hold     Total
    (C)     (C/min)   (min)     (min)
    ------------------------
     90      0.0       1.50      1.50
    320     12.0      12.00     32.67

 Front FID Detector
 ------------------
      Oven Power: On
      Temperature: 360 C
      Electronics: On
    Time Constant: Fast
```

```
      Time   Range  Autozero
      (min)
      -----------------------
    Initial   11     yes
```

Output Port A

```
      Time    Signal   Attenuation
      (min)   Source
      ---------------------------
    Initial   Front        1
```

Output Port B

```
      Time    Signal   Attenuation
      (min)   Source
      ---------------------------
    Initial   Front        1
```

Output Port C

```
      Time    Signal   Attenuation
      (min)   Source
      ---------------------------
    Initial   Front        1
```

Data Acquisition

```
      Detector Bunch Rate : 4 points (10.0 Hz)
          Monitor Length : 64 bunched points (6.4 sec)
       Front FID/TSD Scale: 10 Volts
      Middle FID/TSD Scale: 1 Volts
        Rear FID/TSD Scale: 1 Volts
```

Integration Parameters Address 44   Channel Front

```
Subtract Blank Baseline      : No
Initial S/N Ratio            : 3
Initial Peak Width           : 2 sec
Initial Tangent Height %     : 0%
Monitor Noise                : Before every run
Measurement Type             : Peak Area
Initial Peak Reject Value    : 1500     counts
Report Unidentified Peaks    : Yes
Report Missing Peaks         : Yes
Normalize Results            : No
```

Calibration Setup   Address 44   Channel Front

```
Calculation Type               : Internal Standard
Number of Calibration Levels: 10
Curve Origin                   : Force
Curve Fit                      : Linear
Weighted Regression            : (None)
Replicate Treatment            : Keep Replicates Separate
Replicate Tolerance            : Add replicates within tolerance of  10.0%
    Out-of-Tolerance Action : No Action
Calibration Range Tolerance :       10.0%
    Out-of-Tolerance Action : No Action
```

Verification Setup   Address 44   Channel Front

```
Deviation Tolerance            : 100.0%
    Out-of-Tolerance Action : No Action
```

Peak Table Address 44   Channel Front
---------- ------------------------

```
Reference Peaks Time Windows:Width:  0.10 min.  Retention Time 2.0%
Other Peaks Time Windows    :Width:  0.10 min.  Retention Time 2.0%

Peak Name        : C15:0
Attributes       : Ref:N  Std:N  RRT:N  Lock:Y  Group:0  Time:   6.160 min
Uses Standard    : C17:0 INT STD
Level  1 Amount: 1
Level  2 Amount: 1
Level  3 Amount: 1
Level  4 Amount: 1
Level  5 Amount: 1
Level  6 Amount: 1
Level  7 Amount: 1
Level  8 Amount: 1
Level  9 Amount: 1
Level 10 Amount: 1
Coefficients     : +0.0000e+000x^3 +0.0000e+000x^2 +1.0060e+000x +0.0000e+000

Peak Name        : C17:0 INT STD
Attributes       : Ref:Y  Std:Y  RRT:Y  Lock:Y  Group:0  Time:   7.681 min
Level  1 Amount: 1
Level  2 Amount: 1
Level  3 Amount: 1
Level  4 Amount: 1
Level  5 Amount: 1
Level  6 Amount: 1
Level  7 Amount: 1
Level  8 Amount: 1
Level  9 Amount: 1
Level 10 Amount: 1
Coefficients     : +0.0000e+000x^3 +0.0000e+000x^2 +1.0000e+000x +0.0000e+000

Peak Name        : C18x
Attributes       : Ref:N  Std:N  RRT:N  Lock:Y  Group:1  Time:   8.100 min
Uses Standard    : C17:0 INT STD
Level  1 Amount: 1
Level  2 Amount: 1
Level  3 Amount: 1
Level  4 Amount: 1
Level  5 Amount: 1
Level  6 Amount: 1
Level  7 Amount: 1
Level  8 Amount: 1
Level  9 Amount: 1
Level 10 Amount: 1
Coefficients     : +0.0000e+000x^3 +0.0000e+000x^2 +9.9700e-001x +0.0000e+000

Peak Name        : pimaric
Attributes       : Ref:N  Std:N  RRT:N  Lock:Y  Group:2  Time:   8.380 min
Uses Standard    : C17:0 INT STD
Level  1 Amount: 1
Level  2 Amount: 1
Level  3 Amount: 1
Level  4 Amount: 1
Level  5 Amount: 1
Level  6 Amount: 1
Level  7 Amount: 1
Level  8 Amount: 1
Level  9 Amount: 1
Level 10 Amount: 1
Coefficients     : +0.0000e+000x^3 +0.0000e+000x^2 +8.4900e-001x +0.0000e+000

Peak Name        : sandaracopimaric
Attributes       : Ref:N  Std:N  RRT:N  Lock:Y  Group:2  Time:   8.490 min
Uses Standard    : C17:0 INT STD
Level  1 Amount: 1
Level  2 Amount: 1
Level  3 Amount: 1
Level  4 Amount: 1
Level  5 Amount: 1
Level  6 Amount: 1
Level  7 Amount: 1
Level  8 Amount: 1
Level  9 Amount: 1
Level 10 Amount: 1
Coefficients     : +0.0000e+000x^3 +0.0000e+000x^2 +8.4900e-001x +0.0000e+000
```

A3

```
Peak Name        : isopimaric
Attributes       : Ref:N  Std:N  RRT:N  Lock:Y  Group:2  Time:    8.585 min
Uses Standard    : C17:0 INT STD
Level   1 Amount: 1
Level   2 Amount: 1
Level   3 Amount: 1
Level   4 Amount: 1
Level   5 Amount: 1
Level   6 Amount: 1
Level   7 Amount: 1
Level   8 Amount: 1
Level   9 Amount: 1
Level 10 Amount: 1
Coefficients     : +0.0000e+000x^3 +0.0000e+000x^2 +8.4900e-001x +0.0000e+000


Peak Name        : palustric
Attributes       : Ref:N  Std:N  RRT:N  Lock:Y  Group:2  Time:    8.740 min
Uses Standard    : C17:0 INT STD
Level   1 Amount: 1
Level   2 Amount: 1
Level   3 Amount: 1
Level   4 Amount: 1
Level   5 Amount: 1
Level   6 Amount: 1
Level   7 Amount: 1
Level   8 Amount: 1
Level   9 Amount: 1
Level 10 Amount: 1
Coefficients     : +0.0000e+000x^3 +0.0000e+000x^2 +8.4900e-001x +0.0000e+000


Peak Name        : dehydroabiet
Attributes       : Ref:N  Std:N  RRT:N  Lock:Y  Group:2  Time:    8.960 min
Uses Standard    : C17:0 INT STD
Level   1 Amount: 1
Level   2 Amount: 1
Level   3 Amount: 1
Level   4 Amount: 1
Level   5 Amount: 1
Level   6 Amount: 1
Level   7 Amount: 1
Level   8 Amount: 1
Level   9 Amount: 1
Level 10 Amount: 1
Coefficients     : +0.0000e+000x^3 +0.0000e+000x^2 +8.4900e-001x +0.0000e+000


Peak Name        : abietic acid
Attributes       : Ref:N  Std:N  RRT:N  Lock:Y  Group:2  Time:    9.060 min
Uses Standard    : C17:0 INT STD
Level   1 Amount  1
Level   2 Amount  1
Level   3 Amount  1
Level   4 Amount  1
Level   5 Amount  1
Level   6 Amount  1
Level   7 Amount  1
Level   8 Amount  1
Level   9 Amount  1
Level 10 Amount  1
Coefficients     : +0.0000e+000x^3 +0.0000e+000x^2 +8.4900e-001x +0.0000e+000


Peak Name        : neoabietic
Attributes       : Ref:N  Std:N  RRT:N  Lock:Y  Group:2  Time:   10.020 min
Uses Standard    : C17:0 INT STD
Level   1 Amount: 1
Level   2 Amount: 1
Level   3 Amount: 1
Level   4 Amount: 1
Level   5 Amount: 1
Level   6 Amount: 1
Level   7 Amount: 1
Level   8 Amount: 1
Level   9 Amount: 1
Level 10 Amount: 1
Coefficients     : +0.0000e+000x^3 +0.0000e+000x^2 +8.4900e-001x +0.0000e+000


Peak Name        : Chol. Stear.
Attributes       : Ref:N  Std:N  RRT:N  Lock:Y  Group:0  Time:   20.900 min
```

```
Uses Standard  : C17:0 INT STD
Level   1 Amount: 1
Level   2 Amount: 1
Level   3 Amount: 1
Level   4 Amount: 1
Level   5 Amount: 1
Level   6 Amount: 1
Level   7 Amount: 1
Level   8 Amount: 1
Level   9 Amount: 1
Level 10 Amount: 1
Coefficients    : +0.0000e+000x^3 +0.0000e+000x^2 +8.0800e-001x +0.0000e+000


Peak Name        D.O.G.
Attributes       Ref:N  Std:N  RRT:N  Lock:Y  Group:0  Time:  23.000 min
Uses Standard    C17:0 INT STD
Level   1 Amount  1
Level   2 Amount  1
Level   3 Amount  1
Level   4 Amount  1
Level   5 Amount  1
Level   6 Amount  1
Level   7 Amount  1
Level   8 Amount  1
Level   9 Amount  1
Level 10 Amount  1
Coefficients     +0.0000e+000x^3 +0.0000e+000x^2 +6.7000e-001x +0.0000e+000


Peak Name        : triolene
Attributes       : Ref:N  Std:N  RRT:N  Lock:Y  Group:3  Time:  25.700 min
Uses Standard    : C17:0 INT STD
Level   1 Amount: 1
Level   2 Amount: 1
Level   3 Amount: 1
Level   4 Amount: 1
Level   5 Amount: 1
Level   6 Amount: 1
Level   7 Amount: 1
Level   8 Amount: 1
Level   9 Amount: 1
Level 10 Amount: 1
Coefficients     : +0.0000e+000x^3 +0.0000e+000x^2 +5.0400e-001x +0.0000e+000



Time Events Table   Address 44  Channel Front
---------------------------------------------
Width Event        :     0.0000  4.0    sec
Inhibit Integrate  :     0.0100  until       4.5000
Solvent Reject     :     9.3500  until      12.0000
Inhibit Integrate  :    12.0000  until      20.3000
Width Event        :    22.0000  8.0    sec
Inhibit Integrate  :    30.0000  until      32.6700
```

APPENDIX B – THEORETICAL CALCULATIONS OUTPUT AND GC DATA

Please refer to attached CD. All theoretical files are displayed in .xyz format. GC data is presented in Microsoft Excel format.

Note: A UNIX machine is required to read the data.

<u>APPENDIX C – LIST OF PUBLICATIONS</u>

Printed Publications

Vercoe, D.; Stack, K.; Blackman, A.; Richardson, D. *Interactions of Pitch Components at a Molecular Level.* WPP 2003 Chemical Technology of Wood, Pulp and Paper International Conference. 2003. Bratislava, Slovak Republic.

Vercoe, D.; Stack, K.; Blackman, A.; Richardson, D. *An Innovative Approach Characterising the Interactions Leading to Pitch Deposition.* Journal of Wood Chemistry and Technology. 24(2) 115-137 (2004).

Vercoe, D.; Stack, K.; Blackman, A.; Richardson, D. *A Multi-Component Insight Into The Interactions Leading To Wood Pitch Deposition.* Proceedings of 58th APPITA Annual Conference. 2004. Canberra, Australia.65-71

McLean, D.; Vercoe, D.; Richardson D.; Stack, K. *The pK_a of lipophilic extractives commonly found in Pinus radiata.* Proceedings of 58th APPITA Annual Conference and Exhibition. 2004. Canberra, Australia.73-77

Poster Presentations

Vercoe, D.; Stack, K.; Blackman, A.; Richardson, D. *Interactions of Pitch Components at a Molecular Level.* 57th APPITA Annual Conference and Exhibition. 2003. Melbourne, Australia.

Vercoe, D.; Stack, K.; Blackman, A.; Richardson, D. *Interactions of Pitch Components at a Molecular Level.* RACI conference on Physical Chemistry. 2004. Hobart, Australia.

Future Publications

Vercoe, D.; Stack, K.; Blackman, A.; Richardson, D. *A multi-component insight into the interactions leading to wood pitch deposition.* APPITA Journal. Accepted for publication.

McLean, D.; Vercoe, D.; Richardson D.; Stack, K. *The colloidal pK$_a$ of lipophilic extractives commonly found in Pinus radiata.* APPITA Journal. Accepted for publication.

Vercoe, D.; Stack, K.; Blackman, A.; Richardson, D. *The interactions between hemicelluloses and colloidal wood pitch and the individual hydrophobic extractives.* To be presented at 13th International Symposium on Wood, Fibre and Pulping Chemistry (in conjunction with 59th APPITA conference).